

Synthesis and Evaluation of Innovative Phosphor and Sulfur Containing Materials with Anti Wear and Extreme Pressure Properties derived from Renewable Feedstock

Dissertation

With the aim of achieving the doctoral degree

At the Faculty of Mathematics, Informatics and Natural Sciences

Department of Chemistry

University of Hamburg

Submitted by

Tim Beermann, born 05.09.1992 in Hamburg

2022 in Hamburg

The experimental work described in this thesis has been carried out between February 2018 and November 2020 at the Institute for Technical and Macromolecular Chemistry, University of Hamburg in the research group of Professor Dr. Gerrit A. Luinstra.

The following evaluators recommend the admission of the dissertation:

1. Evaluator: Professor Dr. Gerrit A. Luinstra
2. Evaluator: Professor Dr. Joachim Thiem

Examination commission:

1. Prof. Dr. G. A. Luinstra
2. Prof. Dr. W. Maison
3. Dr. T. Hackl

Date of thesis defense: 03.02.2023

Date of approval: 13.02.2023

List of Publications in Context of this Thesis

Note: Parts of this thesis are summarized in the following published documents:

Luinstra, G. A.; Kipphardt, H.; Beermann, T. *Verschleißadditive auf Basis von biologischen Alkoholen. Abschlussbericht über ein Entwicklungsprojekt, gefördert unter dem Az : 34486 / 01 von der Deutschen Bundesstiftung Umwelt*; Hamburg, 2021.

Luinstra, G. A.; Kipphardt, H.; Beermann, T. *AW-Additive*. Deutsches Gebrauchsmuster Nr. DE20 2020 107 390. 2021

Luinstra, G. A.; Kipphardt, H.; Beermann, T. *EP-Additive*. Deutsches Gebrauchsmuster Nr. DE20 2021 002 910. 2021

Luinstra, G. A.; Kipphardt, H.; Beermann, T. *Polymer AW Compounds*. WO2021148385 A1 2021.

Luinstra, G. A.; Kipphardt, H.; Beermann, T. *Polymere AW-Verbindungen*. DE102020000344 A1 2021.

Danksagung

Ich möchte mich ganz herzlich bei Prof. Dr. G. A. Luinstra für das mir entgegen gebrachte Vertrauen und die Bereitstellung dieses interessanten Themas bedanken. Weiterhin bedanke ich mich für die Hilfestellungen und Ratschläge, welche erheblich zu dem Gelingen dieser Arbeit beigetragen haben.

Herrn Prof. Dr. J. Thiem danke ich für die Übernahme des Zweitgutachtens und die regelmäßigen konstruktiven Diskussionen.

Mein Dank gilt ebenso Dr. Kipphardt für die erfolgreiche Kooperation sowie den fachlichen Diskussionen.

Für das Anfertigen der vielen EDX Analysen danke ich ganz besonders Frau Walter.

Weiterhin danke ich den Analytischen Abteilungen der Universität Hamburg, insbesondere der NMR-Abteilung, der Massenspektroskopischen Abteilung sowie der Zentralen Elementaranalytik.

Ich danke meinen Büro- und Laborkollegen Niklas Voigt, Lasse Finzel, Yannick Wencke sowie Fabian Ratzke für die tolle Zeit.

Ich danke den Mitgliedern des AK Luinstra für die tolle Gemeinschaft und die Hilfsbereitschaft.

Besonderer Dank gilt meinen Eltern die mir mit stetem Interesse und finanzieller Unterstützung den erfolgreichen Abschluss dieses Studiums ermöglicht haben.

Weiterhin gilt mein herzlichster Dank Isi, welche mir eine große Stütze ist und viel zum Erfolg der Arbeit beigetragen hat.

List of Abbreviations

AES	Auger Electron Spectroscopy
At%	Atom %
ATR IR	Attenuated total reflection infra red spectroscopy
AW	Anti Wear
COF	Coefficient of Friction
CMR	Cancerogenic mutagen toxic for reproduction
EDX	Energy Dispersive X Ray
EP	Extreme Pressure
DTP	Dithiophosphate
EHA	Ethyl hexyl acrylate
HDDA	Hexane diol diacrylate
HOSO	High oleic sunflower oil
ISL	Initial Seizure Load
LNSL	Last non-seizure load
MS	Mass spectroscopy
MWF	Metal working fluid
PBT	Persistent bioaccumulative toxic
POEA	Phenoxy ethyl acrylate
TPP	Triphenyl phosphate
TPPT	Triphenyl phosphorothionate
VKA	Vierkugelapparat (Four-Ball Apparatus)
WSD	Wear scar diameter
ZDDP	Zinc dialkyl dithiophosphate
XANES	X-ray absorption near-edge structure spectroscopy

Table of Content

List of Publications in Context of this Thesis.....	3
Danksagung	4
List of Abbreviations	5
Zusammenfassung	4
Summary	5
1. Introduction.....	7
2 Theory and Background	8
2.1 Friction and Wear.....	8
2.2 Types of Additives.....	10
2.3 Synthesis of Phosphor Additives.....	11
2.4 Structure-response Relationship	13
2.5 Mechanism of Action.....	15
2.6 Harvesting of Renewable Alcohols.....	19
3 Motivation	21
4 Experimental Approach	22
4.1 AW & EP determination with the Four-Ball Apparatus (VKA).....	24
5 Results.....	29
5.1 Novel Structures	29
5.1.1 Alternative Dithiophosphate-Michael-Adducts.....	29
5.1.2 Novel Thiophosphates	38
5.1.3 Renewable Phosphonates	40
5.1.4 Innovative Polysulfides.....	41
5.2 Anti Wear Performance	49
5.2.1 Anti Wear Benchmark	49
5.2.2 Anti Wear Performance of Alcohols	51
5.2.3 Anti Wear Performance of Mercaptanes	53
5.2.4 Anti-Wear Performance of Phosphites	58

5.2.5 Anti Wear Performance of Phosphates	61
5.2.6 Anti Wear Performance of Thiophosphates	63
5.2.7 Anti Wear Performance of Dithiophosphates	67
5.2.8 Anti Wear Performance of Phosphonates	72
5.2.9 Anti Wear Performance of Benchmark on 1.0616 and 1.4034 Steel	75
5.2.10 Anti Wear Performance in Ester Oils.....	81
5.3 Extreme Pressure Performance	82
5.3.1 Concept of a Novel Extreme Pressure Screening Method	82
5.3.2 Validation of the novel Extreme Pressure Screening Method	84
5.3.3 Extreme Pressure Performance of Tudalen 12 ®	89
5.3.4 Extreme Pressure Performance of Phosphites	89
5.3.5 Extreme Pressure Performance of Phosphonates	90
5.3.6 Extreme Pressure Performance of Thiophosphates.....	92
5.3.7 Extreme Pressure Performance of Dithiophosphoric Acids.....	94
5.3.8 Extreme Pressure Performance of Dithiophosphate Acrylate Adducts	95
5.3.9 Extreme Pressure Performance of 1,3,4-Thiadiazol-2,5-dithiol Derivatives .	98
5.3.10 Extreme Pressure Performance of Dialkyl Polysulfides	99
5.3.11 Extreme Pressure Additives in Comparison.....	104
5.3.12 Performance of Combined Anti Wear/Extreme Pressure Additives.....	105
5.3.13 Energy Dispersive X-Ray Analysis of Extreme Pressure Wear Scars.....	108
6. Experimental.....	121
6.1 Chemicals and Safety ¹⁹³	121
6.1.1 Disposal	126
6.2 Scientific Devices	126
6.3 Organic Chemical Nomenclature	128
6.4 Synthesis of Dialkyl Dithiophosphates	128
6.5 Synthesis of Dialkyl Dithiophosphoric-Acid-Michael-Adducts.....	129
6.6 Synthesis of Acylated Diisopropyl Dithiophosphate	132

6.7 Synthesis of Novel Thiophosphates Derived from Phosphor Trichloride.....	133
6.8 Synthesis of Thiophosphates Derived from Trialkyl Phosphites $P(OR)_3$	133
6.9 Synthesis of Renewable Phosphonates.....	134
6.10 Synthesis of Renewable Terpene Polysulfides	135
6.11 Linear Drive Screening Procedure	136
6.12 DIN 51350-2 Procedure	139
6.13 DIN 51350-3 Procedure	139
7. References	140
8. Declaration on Oath.....	154

Zusammenfassung

Das Ziel der vorliegenden Arbeit war die Synthese von schwefel- und phosphorhaltigen Substanzen ausgehend von erneuerbaren Ressourcen mit verschleißmindernden (*anti wear*, AW) sowie Schwerlast-Eigenschaften (*extreme pressure*, EP) als Ersatzstoffe für Triphenylphosphorothionat (TPPT).

Die tribologischen Eigenschaften wurden mit dem Hansa Press Vierkugelapparat (VKA), die mechanische Oberflächenanalyse mit einem Laserscanning Mikroskop und die chemische Oberflächenanalyse mittels energiedispersiver Röntgenstrahlung (EDX) realisiert, um Struktur-Wirkungsprinzipien verschiedener funktioneller Gruppen tiefergehend zu verstehen.

Für dieses Vorhaben wurden die AW-Eigenschaften von Tri- und Dialkylphosphiten, Phosphaten, Thiophosphaten, Dithiophosphorsäuren, Dithiophosphorsäure-Acrylat-Michael-Addukten, Alkoholen, Mercaptanen, Sulfoxiden, Thioethern sowie Thiadiazolen mit jeweils 1, 1,5 und 2 mmol Phosphor oder Schwefel pro 50 g Basisöl bestimmt. Tri- und Dialkylphosphite, Thiophosphate, Dithiophosphorsäure, Dithiophosphorsäure-Acrylat-Michael-Addukte, Thiadiazole und Polysulfide wurden mit Konzentrationen von 1, 1,5 und 2 mmol Phosphor oder Schwefel pro 50 g Basisöl hinsichtlich der EP Eigenschaften untersucht.

Die EP-Eigenschaften der Substanzen wurden mit einem Versuchsaufbau zur Bestimmung dynamischer Lastanstiege ermittelt. Unabhängig vom verwendeten Basisöl, sowie der verwendeten Stahlsorte der Prüfkugeln, haben die Experimente Dialkylphosphite (Phosphonate) als hervorragende verschleißmindernde (AW) Substanzen identifiziert, wobei für das aus nachwachsenden Alkoholen zugängliche Oleyl-stearylphosphonat mit 70 mol% Oleylalkohol ein Gebrauchsmuster (Deutsches Gebrauchsmuster Nr. 20 2020 107 390) beantragt wurde.

Die EP-Versuche haben gezeigt, dass Phosphor kaum Einfluss auf die Schwerlast-Eigenschaften hat, und bestätigt, dass für effizienten Schutz bei Schwerlastanwendungen Schwefel unabdingbar ist. Die aus D-Limonen, einem Abfallstoff der Saftproduktion, hergestellten Polysulfide zeigten hervorragende Schwerlasteigenschaften sowie die erfolgreiche Umsetzung von nachwachsendem D-Limonen und elementarem Schwefel, zu Schmierstoffadditiven.

EDX Analysen der AW-Kalotten nach 15 kg Belastung und 60 min Testzeit belegten, dass Phosphor das dominierende Element in den Kalottenoberflächen ist und effektiven Schutz vor Verschleiß bei niedrigen und mittleren Lasten bietet. Mit zunehmenden Lasten stagniert oder sinkt der Phosphoranteil und Schwefel dominiert die resultierenden Kalottenoberflächen. Die elektronenmikroskopischen Analysen legten die Bildung von leicht abtragbaren schwefelhaltigen Schichten nahe, welche in den Grenzbereichen der Verschleißkalotten als aufgeschichteter Abrieb erkennbar waren.

Kombinationen von biobasierten Oleyl-stearylphosphonaten und D-Limonen-polysulfiden zeigten überragenden Verschleißschutz bei gleichzeitig sehr gutem Schwerlastverhalten. Ferner ergab sich, dass keine Reaktion von Phosphonat mit Polysulfid auftrat, was einen negativen Einfluss auf die Eigenschaften hätte.

Das Ziel, nachwachsende Rohstoffe für die Synthese von Schmierstoffadditiven einzusetzen und damit im Vergleich zu kommerziellen Produkten vergleichbare oder bessere AW/EP Eigenschaften zu erzielen, konnte erfolgreich erreicht werden.

Summary

Main objectives of this thesis were syntheses and characterizations of novel phosphor and sulfur containing anti wear (AW) and extreme pressure (EP) additives derived from renewables as substitute for oil-based components such as triphenyl phosphorothionate (TPPT).

Therefore, essentially three major types of analyses were established: four-ball apparatus experiments in combination with laser scanning microscope to determine the AW and EP properties, as well as EDX analysis to gain information about the surface chemistry of different additive groups.

The AW performances of phosphites, phosphonates, phosphates, thiophosphates, dithiophosphoric acids, dithiophosphate acrylate adducts, alcohols, mercaptanes, sulfoxides, thioethers and thiadiazoles were determined for concentrations of 1, 1.5 and 2 mmol phosphor or sulfur per 50 g of base stock.

The EP analyses were conducted for dialkyl phosphonates, trialkyl phosphites, trialkyl thiophosphates, dialkyl dithiophosphates, thiadiazoles, as well as polysulfides at concentrations of 1, 1.5 and 2 mmol P or S per 50 g of base stock.

With regard to the EP properties, a novel and efficient method to determine EP performances was successfully developed and validated. In conclusion it was shown, that phosphor(III) derivatives lacking sulfur exhibit predominant AW properties independent of the used steel as well as the base oil. Especially dialkyl phosphonates were identified as superior AW additives, and for oleyl stearyl phosphonate with 70 mol% oleyl alcohol a utility model application was filed (Deutsches Gebrauchsmuster Nr. 20 2020 107 390).

Screening experiments revealed, that phosphor had minor impact on the EP properties, whereas sulfur containing structures were identified as potent EP additives.

EDX analysis performed on the wear scars derived from the AW experiments at low loads of 15 kg maintained for 1 h indicated, that phosphor likely builds-up tribolayers preventing debris and failure at low loads. The sulfur containing additives did not show sulfur in the tribolayers. The EDX analysis of the wear scars derived from EP experiments revealed a different situation. Exclusively phosphor containing additives yield phosphor in the tribolayer, but not show any EP performance. The main indicators were severe vibration effects accompanied by tremendous wear scar diameters. Phosphor and sulfur containing additives revealed phosphor at low to medium loads within the wear scar, which decreased with increasing loads; simultaneously the detection of sulfur increased within the tribolayer. In addition, the distribution of phosphor and sulfur within the wear scar changed in dependence of the load: while at low to medium loads the elements are evenly distributed throughout the wear scar, high loads led to detection of phosphor and sulfur in piled-up debris at the edges of the wear scars. The EDX analysis of pure sulfur additives revealed an increasing sulfur content with increasing loads at comparable distribution behaviors. This indicated the formation of sulfur containing layers, which prevent direct contacts of bulk materials.

Furthermore, it could be shown that phosphonate based on renewable oleyl and stearyl components as well as polysulfides derived from limonene exhibited superior AW and EP properties. In addition, synergistic effects of dialkyl phosphonates and limonene

polysulfide were recognized. Thus, use of renewable feedstocks for the synthesis of AW and EP additives as substitute for TPPT was successfully accomplished.

1. Introduction

Parts of this chapter are summarized elsewhere.^{1–5}

Lubricants are known to human kind since thousands of years. Ancient civilizations like the Egyptians and Greeks used water to reduce the friction between stone brick surfaces for construction of pyramids and temples. The first complex compounds used as lubricants were based on vegetable or animal fat and their reaction products with burned wood ash.^{6–8} The resulting metal soaps are still known and used for different applications until today.⁹ These lubricants were used in wooden axles and joints until the industrial age. Nowadays, the use of lubricating fluids is inevitable for industrialized applications and tremendous monetary and energy losses go along with failure due to poor lubrication.¹⁰ Over the centuries, the demand for lubricants increased, accompanied by the foundation of a novel science: the tribology. Tribology is the art of investigation of physical phenomena occurring between two surfaces with different relative motions and first experiments were performed by Leonardo da Vinci.¹¹

Accompanied by the development of iron based machines like steam engines and later combustion engines, the requirements to the lubricants with regard to performance and temperature stability increased significantly.¹⁰ Finally, the invention of the first general accepted concept of an automobile by Carl Benz in 1886 sealed the need of vast amounts of lubricating oil and initiated the ascending era of automotive mobility.¹² To serve the increasing demands for lubricating fluids, further additives were developed.¹³ Thiophosphates are common anti-wear additives and are synthesized by the reaction of phenol or alkylated phenols like tertiary butylated phenol with phosphor trichloride and sulfur.^{14,15} The necessity of lubricants and the role of additives will be explained in the following chapters.

2 Theory and Background

Parts of this chapter are summarized elsewhere.^{1–5}

2.1 Friction and Wear

Microscopic views reveal metal surfaces to show no smooth but rather rough constitutions. Grinding or polishing metal surfaces can reduce the asperities, however, they cannot be eliminated. If two surfaces come into contact these asperities are the limiting factor for their closest proximity.¹⁶ A schematic model of two contacting surfaces is given in Figure 1.

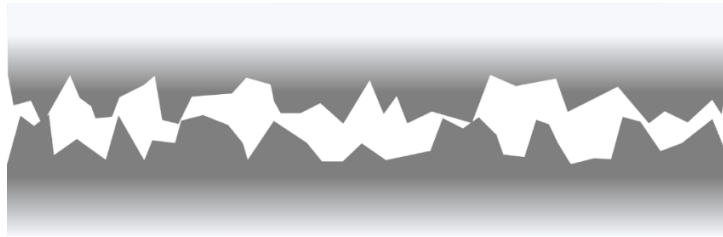


Figure 1. Schematic proximity of two contacting surfaces. Adapted from Vakis et al.¹⁷

Under the influence of different relative motions of the two surfaces, the asperities contact each other and friction, respectively wear occurs. By friction and wear, the asperities flatten until the resulting contact area is able to support the load.¹⁸ Nevertheless, wear and the formation of debris continues due to friction.¹⁹ Those phenomena are ubiquitous in moving systems, thus it is necessary to minimize the contact between the metal surfaces. To address this challenge, viscous films generated by fluids, e.g. oils, can be applied to the surfaces.²⁰

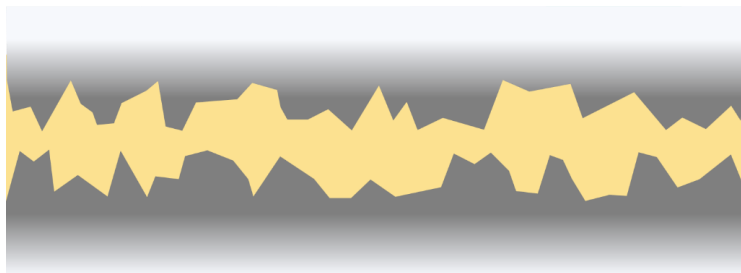


Figure 2. Surface separation by a viscous liquid (yellow).

Figure 2 depicts the schematic separation of the asperities by a lubricating film. The formation of lubricating films is dependent on the relative motion of the surfaces, the load as well as the viscosity of the lubricant. Richard Stribeck was the first to investigate the dependence of the coefficient of friction (COF) with regard to the applied load (P),

the viscosity (η) and the speed of motion (N) in different bearings which is now known as the Stribeck curve.^{21,22} A schematic Stribeck curve is depicted in Figure 3.²³

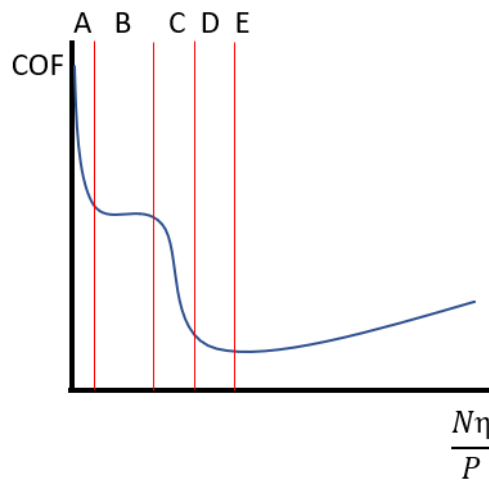


Figure 3: Schematic depiction of the Stribeck curve in dependence of the Hersey number.

The curve is divided into 5 sections of lubrication regimes. Direct contact friction between dry and clean surfaces is characterized by high COFs and wear, designated as region A. As the lubricant thickness increases and is slightly larger or equal to the median asperity height, for example by increasing load, slower motions or decreasing viscosity, boundary lubrication is observed (B). Boundary lubrication exhibit lower COFs compared to dry contact. The transition of boundary lubrication to elastohydrodynamic or hydrodynamic lubrication is titled as mixed lubrication regime (C). The lubricant film is thicker compared to the boundary lubrication, but still contact of asperities is possible. Typically, those contacts are noncritical, due to already build up layers which prevent serious damage. The transition of the mixed lubrication to the hydrodynamic lubrication (E) is characterized by the so called elastohydrodynamic lubrication regime (D). Both are characterized by a complete separation of the surfaces by a lubricant layer which is capable of sustaining the load. The difference is given by the height of the films.^{23,24}

The AW properties of the novel substances were determined in a four-ball apparatus, operated according to DIN 51350-3.²⁵ The determination of the extreme pressure (EP) properties is realized by a newly developed screening method derived from DIN 51350-2.^{25–27} The trigonal-pyramidal geometry of the four-ball set-up generally leads to a pin point contact on the resting balls which prevents hydrodynamic lubrication between the balls. In addition, the resulting velocities of 0.55 m/s of the running ball (@1450 rpm) are too low to build up hydrodynamic lubricating films between the balls. Thus, the four-

ball apparatus provides a method to measure the lubricating effects of additives independent of the viscosity of the base oil. Dependent on the load (EP or AW), boundary or mixed lubrication is considered.²⁸ Boundary lubrication is dominant at the start of the measurements.

2.2 Types of Additives

Based on the commercial and industrial fractions of functional lubricating fluids, engine applications make up more than 60% of the market.²⁹ Other industries consuming lubricating fluids are metal working fluids (MWF), turbine oils, hydraulic oils, process oils (e.g. rubber/tire production) etc. Lubricating oils are complex formulations consisting of multiple chemicals, which improve the performance dependent from the application. This is reflected in the amount of 5.000 to 10.000 different lubricant formulations covering 90% of the applications.³⁰ The constant development of high performance engines and expanding lubricant applications was accompanied by design of additives due to the insufficiency of crude base oils to deliver the required performance.²⁹ In addition to other additives, anti-wear and extreme pressure additives are part of such additive packages and will be focused in this thesis.

Henning Brand of Hamburg discovered phosphor by distillation of urine in 1669.³¹ Substantial steps in the development of the organic phosphor chemistry were made by Wilhelm Hofmann, August Michaelis and Alexander Arbusov in the beginning of the 20th century.³² Later, Schrader continued the gathering of knowledge and synthesized a broad range of phosphor derivatives including the most toxic chemicals on earth such as Sarin and Tabun.³³ The industrial use and significance of phosphor chemicals gathered tremendous importance after 1945 for a broad range of applications including pesticides, fertilizers, metal fluids etc. Later in the 20th century, the field of application for phosphor chemicals extended by usage as catalysts, flame retardants and resulted in the known applications of phosphor today.^{34,35} Nevertheless the societal use of those derivatives enabled the adequate supply of modern civilizations with food, drugs, fuel and increasing mobility but the dual use potential of phosphor chemicals requires awareness.³⁶ In fact, phosphor enables³⁷ and disables³⁸ living.

Triaryl phosphorothionates (TPPT) and **zinc dialkyl dithiophosphates (ZDDP)** are the dominating additives for wear reduction and registered in the European Union with

4.000 t/a and 340.000 t/a, respectively.^{39–50} Furthermore, ashless dialkyl dithiophosphates and sulfur rich compounds are used as all-round additives, respectively EP additives with registered volumes of approx. 3.000 t/a and 110.000 t/a.^{51–55}

As the registered volumes indicate, phenolic thiophosphates have significant commercial values, but recently received major criticism on account toxicological issues resulting from the phenolic derivatives released after hydrolysis.^{56,57} Phenol and alkylated phenols are classified as CMR substances and their application in lubricant additives might be prohibited in the future.^{58,59} Especially the use of those systems in contact with food needs to be reconsidered. Zinc dialkyl dithiophosphates are the most common used additives with regard to wear reduction, but they also exhibit antioxidative, anticorrosive and limited extreme pressure properties.^{27,60,61} Furthermore, ZDDPs show major disadvantage in poisoning of automotive exhaust gas catalysts, accompanied with a very effective deactivation of the catalytic conversion of unburned fuel and nitroxides.^{62–65} Both ashless as well as zinc dialkyl dithiophosphates exhibit unpleasant esthetics (e.g. strong odor), especially in the context of decomposition.⁶⁶

In addition to aforementioned additive types, phosphor (III) and (IV) derived species are known as lubricating additives, such as trialkyl phosphates, acidic phosphates, trialkyl phosphites, dialkyl phosphites (dialkyl phosphonates), acid phosphites etc. These compounds were extensively reviewed by Papay and Spikes.^{67–69} Their industrial relevance is far smaller than the afore described thiophosphates and dithiophosphates.

2.3 Synthesis of Phosphor Additives

The synthesis of phosphorothionates can be realized by reaction of alcohol (3 mol equivalents) with phosphor trichloride followed by oxidation with elemental sulfur. Alternatively, reaction of alcohol with thio-phosphoryl chloride in presence of base is also a possible route.^{14,15}

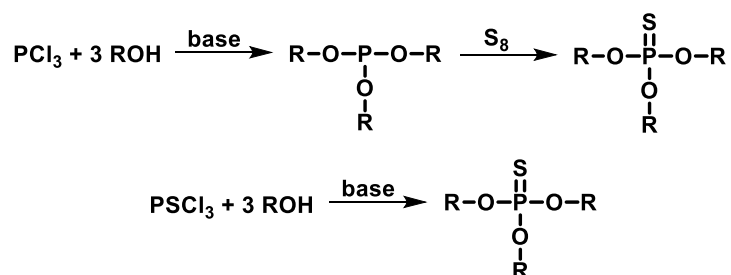


Figure 4. Reaction scheme for the synthesis of thiophosphates.

Reaction of excess alcohol with phosphor trichloride without base yields dialkyl phosphites, respectively dialkyl phosphonates and one equivalent chloro alkane (Figure 5).⁷⁰

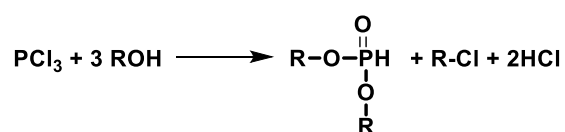


Figure 5. Reaction of phosphor trichloride with excess alcohol without presence of base.

In addition, transesterification reactions of dialkyl phosphonates with alcohols are known to give access to a broad range of dialkyl phosphonates.^{71,72}

Dialkyl dithiophosphoric acids are easily synthesized by alcoholysis of phosphor pentasulfide. Therefore, alcohol in excess is reacted with phosphor pentasulfide.^{14,73}

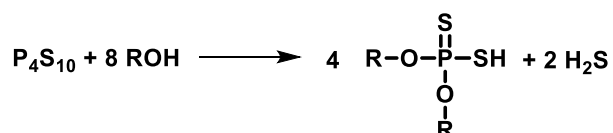


Figure 6. Schematic synthesis of dialkyl dithiophosphoric acids.

Depending on the type of alcohol, either alkyl or aryl, the reaction temperatures are in the range of 60 to 80 °C or 80 to 120 °C. The resulting dithiophosphoric acids can be either neutralized with zinc oxide or transformed through a reaction with compounds having an activated double bonds (e.g. Michael-Systems) to yield the mentioned AW additives.^{73–75}

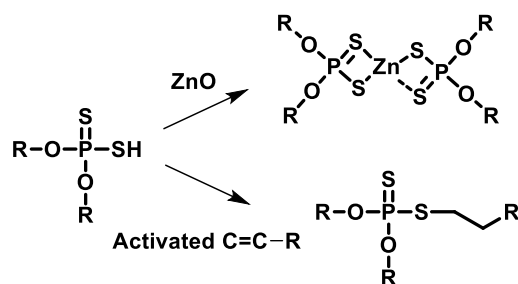


Figure 7. Reaction scheme for synthesis of neutralized dithiophosphates.

As these reaction schemes imply, phosphor trichloride as well as phosphor pentasulfide are platform chemicals for the synthesis of highly active AW/EP additives.

2.4 Structure-response Relationship

The wear reducing properties of neutralized dithiophosphoric acid derivatives revealed a correlation between the resulting wear, the temperature and the chain length of the alcoholic entities. The results for neutralized i-propyl, i-butyl, i-pentyl and 2-ethylhexyl dithiophosphoric acid with acrylate *Michael* products exhibited comparable wear reducing properties at 100 °C, but indicated long alkyl chains to be superior at temperatures of 150 °C. Experiments with esters of ethyl, n-butyl, i-decyl and i-tridecyl of the corresponding acrylic acid at 100 °C showed no differences with regard to the chain length. The experiments at 150 °C again revealed significant dependence of the wear reducing properties, with longer chain acrylic acid esters yielding better wear reducing properties. The lower effectiveness of the short chain derivatives was pinpointed to their lower degradation temperature, determined by TGA.⁷⁶

The examination of metal dithiophosphates in form of Zn, Ni, Cu, Co, Cd, Pb, Bi or Sn lead to the conclusion that the AW/EP performance can be correlated with the metal ion radius, thus Cd and Pb exhibited best the performance. The examination of different alcohols reacted to dithiophosphate and their characterization by the four-ball apparatus indicated no significant dependence of the load wear index (LWI). The results for the weld loads indicate, that secondary alcohols have enhanced EP properties while primary alcohols with up to 6 carbon atoms exhibit good AW properties.⁷⁷⁻⁷⁹

Anti-wear studies were performed for addition products derived from dimethyl-, diethyl- and dibutyl phosphite with high oleic sunflower oil (HOSO) and compared to ZDDP. The results indicated increasing wear scar diameters (WSDs) of 0.274, 0.410 and

0.619 mm with increasing length of the alkyl chain (WSD of HOSO = 0.507 mm). The obtained results were comparable to ZDDP performance.⁸⁰ Corresponding commercial products as lubricant additives are available as Dapraphos® or Doverphos®.^{81,82}

Polymeric trialkyl phosphites as well as polymeric thiophosphates and polymeric phosphates are also known as wear reducing lubricant additives.⁸³

Comprehensive studies with different chain length (ethyl-, butyl-, ethylhexyl-, dodecyl-, lauryl-, stearyl-) on the acidic phosphate revealed, that the wear scar diameter are higher than tricresyl phosphate (TCP, 0.28 mm against 0.32 to 0.76 mm) but exhibit better EP properties with regard to the initial seizure load (ISL). The ISL is with values ranging from 80 to 160 kg at least twice as high as tricresyl phosphate (40 kg, same for base stock) for both di-alkyl as well as mono-alkyl phosphates. The weld loads were 110 kg for TCP which is same for the base stock and weld loads (WL) ranging from 130 kg to 160 kg for the examined acidic phosphates, indicating no significant improvement in EP properties. Neutralized phosphate esters are also used. Experiments with amine salts of dibutyl phosphate and diethylhexyl phosphate were performed with regard to the WSD, ISL as well as WL behavior. The WSD for the acidic dibutyl phosphate was 0.42 mm after 1h, 15 kg load and 1500 rpm. The corresponding salts with different mono alkyl amines yielded lower WSDs ranging from 0.26 mm to 0.33 mm. The ISL for dibutyl phosphate was 85 kg and the weld load 140 kg. The ISLs for the corresponding amine salts are slightly increased and in the range of 85 kg to 105 kg but still within the same magnitude, indicating no dependence of the used amine. The results were obtained at 4 mmol Phosphorous/100g base stock.⁸⁴

The results for the diethylhexyl phosphate with different amines yielded better AW and EP properties with decreasing chain length of the amine as well as better AW and EP performance with increasing bulkiness of the amine. Varying the chain length of the phosphate indicated that long chain amines and short chain phosphates yield best results. This was explained by the better coordination ability of the polar phosphorous entity.⁸⁴ These findings were confirmed by additional examinations.⁸⁵ Mixed salts of amine phosphates (typically C11-C14 branched alkylamines and mono- or dihexyl phosphates) are still in use and commercially available for example as Irgalube 349 or chinese clones Runlube 349 and Sungate Lube 349.^{86–88}

A comparative study of the AW and EP properties of triphenyl phosphorothionate (TPPT) and tricresyl phosphate (TCP) gave comparable AW behavior but better EP performance for TPPT. This was assigned to the role of sulfur in TPPT.⁸⁹

Nowadays, a broad range of acidic or neutral phosphate esters are available. The available products and their properties differ in dependence of the rests, and can be individually tuned for different applications. In general, phosphates exhibit good AW properties but weak EP properties. This results in the application as additives for low load applications.^{90–92}

With regard to the EP properties, disulfides and polysulfides yield higher weld loads compared to monosulfides. In addition, di tert. butyl and dibenzyl disulfides exhibited better EP properties and lower WSDs compared to diethyl disulfide. Thus, bulky and relatively large rests at sulfides yield better EP results.⁹³

Early EP additives were based on chlorinated alkanes with high chlorine contents. These additives received concerns due to toxicological issues and are nowadays nearly extinct in industrial use due to persistent, bio accumulative and carcinogenic properties.⁹⁴ Sulfur carriers (e.g. polysulfides) are the additive of choice for EP situations and replaced chlorinated alkanes.^{95,96}

2.5 Mechanism of Action

Since extensive research was performed on the coherence of additives and wear, theories regarding the mechanism of action of wear reducing additives evolved within the years. Early studies revealed phosphor containing additives to yield iron phosphide formation which polishes the surface due to its hardness.⁹⁷ In general, following adsorption to the metal surface, a reaction of additives with the metal under influence of friction is assumed, called tribofragmentation.^{76,98}

Comparative Auger Electron Spectroscopy (AES) examinations of tricresyl phosphate (TCP) and TPPT over a concentration range of 1 to 5 wt% revealed the presence of 4 % phosphor in the resulting wear scars of TCP and 6 % sulfur respectively 4 % phosphor in the wear scar of TPPT. In addition, the determined weld loads and last non seizure loads were higher for the sulfur containing TPPT, while the resulting WSDs of the AW tests are comparable. This finding was attributed to the presence of sulfur in TPPT.⁸⁹

Examination of wear scars of an acidic ashless dithiophosphate, a neutral ashless dithiophosphate and an thiophosphate by X-ray absorption near-edge structure (XANES) spectroscopy gave insight into the tribochemistry. All additives yielded iron (II) polyphosphate films and iron (II) sulfate after a short running-in period of 5 min. While the acidic DTP exhibited a thicker film than the other additives, the WSD was larger; this was contributed to the presence of acidic species, which would give initial corrosive wear. After 1 h and 6 h of wear, the chemical composition of the tribolayer, e.g. the iron(II)phosphate, did not show changes, but the thickness of all resulting tribolayers aligned to those yielded by the acidic DTP. After completion of the test, the acidic DTP gave significant lower WSD and thus better wear protection than the thiophosphate and the neutral DTP. The depletion mechanism for the additives was assumed to occur by adsorption of the additive to the metal surface followed by cleavage of the P=S bond, resulting in the formation of iron phosphates as well as iron sulfate by further oxidation of the sulfur with iron oxides from the passive layer.⁹⁹

Wear experiments with tributyl phosphite and tributyl phosphate on stainless steel in ultra-high vacuum were monitored by mass spectroscopy. The reactions of those additives with the iron substrate comprised adsorption to the metal surface with activation energies of approx. 110 kJ/mol for tributyl phosphite and 120 kJ/mol for tributyl phosphate accompanied with cleavage of either the P-O or C-O bonds resulting in the formation of hard polyphosphate glasses covered by a graphitic layer. In addition, the evolution of hydrogen was observed and attributed to the decomposition of either the phosphate/phosphite or the butoxy rests on the metal surface yielding butene or carbon and adsorbed hydrogen. The resulting hydrogen then reduced the oxide layer to react with the butoxy species to form butanol. The adsorbed carbon undergoes temperature-dependent reactions above 800 K to reduce the oxide layer. In any case, small amounts of carbon remained in the surface and were identified as graphitic carbon, which exhibits low shear deformation properties. The experiments with tributyl phosphate yielded analogous results, which indicate, reduction of phosphate to phosphite and a consecutive reaction cascade leading to polyphosphates.^{100,101}

Comparable observations were made by the ATR IR examinations of the tribochemistry of TPPT on a metal coated ATR crystal. In addition, XPS spectroscopy was performed. Following adsorption to the metal surface with coordination of sulfur and oxygen atoms, the thiophosphate was reduced to phosphite. The resulting

adsorbed phosphor ester was attacked by the oxygen nucleophile of a solvated triphenyl phosphate (TPP) molecule. As a result pyrophosphates were formed and served as protective layer. In addition, formation of sulfides was observed, which are further oxidized to sulfates.¹⁰²

The analysis of different dialkyl dithiophosphates with several acrylates indicated the formation of a phosphor rich layer which reduced wear and friction and thus maintained lubrication.⁷⁶

The EDX analysis of wear scars after seizure experiments with two ZDDPs and two unspecified phosphor and sulfur compounds (P-S compound) revealed phosphor contents ranging from 1 % to 2.5 % at 3 wt% additive concentration and sulfur concentrations ranging from 1 to 2 % at 3 wt% additive concentration for the ZDDPs. The examination of the phosphor and sulfur content within the wear scar for the two P-S compounds gave values from 1 to 1.5 % phosphor at 1 wt% additive concentration respectively 9 to 3 % phosphor at 10 wt% additive concentration. The results of the sulfur content exhibited less variation at higher level of 9 to 13.5 % for the studied additive concentrations.²⁷ The Auger Electron Analysis (AES) of the resulting wear scars of ZDDP gave insight into the depth profile of the resulting tribolayers. It was concluded, that at higher additive concentrations, a deeper penetration or diffusion of sulfur and phosphor results. Experiments with 0.2 wt% and 3 wt% additives yielded penetration depth of 0.2 or 2 μm .²⁷

The XPS analysis of tribofilms generated by ZDDP after various times of rubbing and temperatures indicated that some time is needed to build up effective tribolayers. After initial rubbing of 25 min, long chain polyphosphates were the dominating structures in the resulting tribolayer, which turned into pyrophosphates within 3 h of rubbing. The thickness of the resulting tribolayers is dependent of the applied load as well as the temperature. It ranges from 0.055 to 0.09 μm .¹⁰³ The formation of a thin layer of iron sulfide (5-10 nm) was further found to build up between the phosphate layer and the substrate.¹⁰⁴

The mass spectroscopy (MS) analysis of aged ZDDP oil gave evidence for several types of decomposition products. These include dialkyl thiophosphates, dialkyl phosphates, monoalkyl dithiophosphates, monoalkyl thiophosphates, monoalkyl phosphates, sulfuric acid as well as phosphoric acid.¹⁰⁵ The analysis of the tribolayer

of ashless dithiophosphates revealed comparable results to the composition of ZDDPs, mainly consisting of phosphates and sulfates. Nevertheless, the films generated by ashless DTPs are thinner than those from ZDDP and they build up even slower.⁶⁸

Synergies were recognized in the combination of ZDDPs with phosphor additives. In detail, acidic mono and disubstituted phosphates with long alkyl chains exhibit better AW properties than the corresponding trisubstituted phosphates. Especially dialkyl acid phosphates in combination with ZDDPs in a ratio of 2P:1Zn exhibited good values. IR spectra indicated the formation of a zinc dialkyl phosphate, which is assumed to be an active wear inhibiting species.⁹²

The mechanism of action for sulfur containing compounds acting as EP additives is comparable to the mechanism of action of AW additives. Sulfides are assumed to adsorb on the metal surface accompanied by the formation of an iron sulfide complex. At extreme conditions, (heat, friction etc.) the adsorbed sulfur compounds are depleted and the formation of iron sulfide is general assumed.⁹³ Recent XANES analysis of the wear scars derived from polysulfides indicate the formation of varying fractions of FeS, FeS₂, FeSO₃ and FeSO₄ in dependence of friction, speed and time.¹⁰⁶ Furthermore, these resulting tribolayers are facile dissipated, thus preventing direct contact between the surfaces.¹⁰⁷

A lot of research towards the chemical modification of olefinic compounds for the synthesis of lubricant additives was performed since the end of the last millennium. Early patents describe the conversion of sulfhydrated olefinic structures (in detail those based on pinene and dipentene) with sulfides of phosphor (P₄S₁₀) at elevated temperatures.¹⁰⁸ The reaction of dipentene with sulfur chlorides followed by treatment with P₄S₁₀ to yield EP additives is also disclosed.¹⁰⁹ In addition, low amounts of dipentene (up to 1wt%) are able to stabilize sulfurized fats and oils.¹¹⁰ The reaction products of olefinic compounds (dipentene) with elemental sulfur and a mercaptan are disclosed as lubricant additives with AW properties.¹¹¹ The conversion of mixtures of terpenic (for example pine oil and dipentene) structures and at least one other olefinic compound with elemental sulfur are used as antioxidants, AW and EP additives and compatible with nitrile seals.¹¹²

The reaction product of excess sulfur with olefins (e.g. isobutylene, dipentene/limonene) in a pressurized vessel at elevated temperatures in the presence

of an amine as catalyst yields lubricant additives containing 80 to 90% polysulfides and 10 to 20% low molecular weight compounds (dithiol- or thione type).¹¹³ The reaction of olefins, H₂S, sulfur, water and nitrogen containing polymers are described as multifunctional additives with AW/EP as well as thermal and oxidative stability for lubricants.¹¹⁴ The treatment of the reaction product of dipentene (50:50 mixture of D- and L- limonene) and elemental sulfur with activated alumina at elevated temperatures is described as a further procedure to reach corrosion inhibiting compounds.¹¹⁵ The cited patents describe dipentene (a mixture of D- and L-limonene) as suitable substance for the synthesis of lubricant additives.

2.6 Harvesting of Renewable Alcohols

Novel approaches to platform chemicals aim at valorization of biomass. Lignin, one of the most available sources for functionalized phenols is a by-product of the paper industry. It is crucial for the stability of plant structures.¹¹⁶ Paper is predominantly made of pulp (cellulose), which needs to be separated from lignin and hemicellulose.^{116,117} Various approaches for the purification of pulp were established over the years. The sulfite process introduced by Benjamin Chew Tilghman uses calcium bisulfite lye, while the Kraft process by Carl Ferdinand Dahl consults sulfate lye.^{118,119} The separated lignin is predominantly used in thermal combustion to generate heat for drying the paper pulp.¹²⁰

Lignin is a natural occurring polymer consisting of functionalized propyl phenylidene structures (C₉ building blocks), which can be reformed by depolymerization. A broad range of chemicals are the result of the decomposition process, such as p-coumaryl alcohol, coniferyl alcohol as well as sinapyl alcohol and vanillin.^{117,121,122} Over time, much research towards the use of lignin as source for renewable phenol derivatives was performed and different approaches were established and reviewed by Sun.¹²³

Menthol is also a natural occurring compound. Meanwhile, it is a high volume chemical with manufactured or imported tonnages of 10.000 to 100.000 $\frac{t}{a}$ in the European Economic Area.¹²⁴ Menthol can be isolated from geranial and neral, whereas natural menthol is harvested from *mentha arvensis*. Natural menthol can e.g. be extracted from the leaves using supercritical carbon dioxide or by steam distillation.¹²⁵ The

industrial significant synthesis of menthol from geranial and neral was established by BASF.¹²⁶

Citral, a further natural occurring chemical, is synthesized from isobutylene and formaldehyde, followed by aldol condensations as well as racemization reactions. Hydration of citral leads to geraniol as well as nerol, which are racemized to menthol catalyzed by ruthenium and rhodium catalysts.^{126,127}

Yet another class of starting materials for the synthesis of novel biobased additives are terpenes, e.g. limonene and pinene. Limonene is a by-product of the lemon and orange juice industry. Limonene can be extracted from the peels of citrus fruits either by steam distillation or squeezing.¹²⁸ Nowadays D-limonene is used in the paint industry as renewable solvent and as scent ingredient. Current publications describe limonene as a promising substances for inverse sulfur vulcanization to yield polymers. One application of these polymers may be the extraction of heavy metals from waste water streams.^{128,129} In addition, the chemical conversion of limonene in the context of lubricating additives derived from dithiophosphoric acids is known.¹³⁰ In addition, the reaction of limonene with sulfur was examined in some detail. Volatile sulfur limonene derivatives and polymeric products as non-volatile products are some of the compounds.¹³¹

3 Motivation

Parts of this chapter are summarized elsewhere.¹⁻⁵

The objective of this thesis was the synthesis of phosphor and sulfur containing AW and EP additives with acceptable toxicological, ecological and commercial profiles. Natural occurring feedstocks were considered as precursors to substitute TPPT and TPPT+, which face toxicological and ecological issues.^{57-59,132} Triphenyl phosphorothionate (TPPT) is a common product (Figure 8) and is used as reference substance for determination of the AW/EP performance of novel products. TPPT is on the brink of a potential CMR classification.¹³³

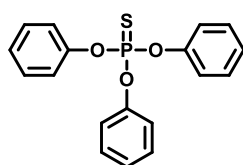


Figure 8. Triphenyl phosphorothionate (TPPT).

Lubricating additives are commodity products. This requires simple and robust syntheses routes and more important, acceptable prices of the used resources. To serve the requested toxicological, ecological and commercial profiles at the same time with superior performance, natural occurring phenols, alcohols and terpenes were to be used to synthesize novel additives. Lignin derived phenols as well as natural alcohols were preferred as potential platform chemicals from renewable biomass.^{121,128,134} Some structures are shown in Figure 9.

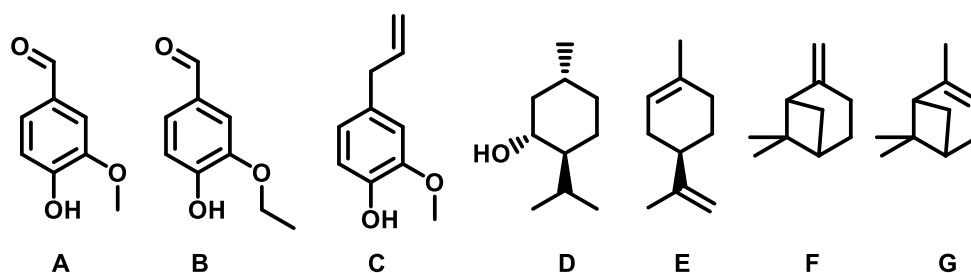


Figure 9. Renewable alcohols used for the synthesis of novel additives. From left to right: A: vanillin, B: ethyl vanillin, C: eugenol, D: (-) menthol, E: D-limonene, F: beta pinene, G: alpha pinene.

The alcohols were to react with phosphor trichloride and sulfur to obtain thiophosphates and with phosphor pentasulfide to yield dithiophosphates.¹⁴ Oleic acid, eugenol, eugenyl acetate and terpineol were reacted with elemental sulfur to yield renewable EP additives.

4 Experimental Approach

Parts of this chapter are summarized elsewhere.^{1–5}

The AW and EP properties of the resulting structures were to be classified by a trinity of analysis: The AW and EP properties should be assessed from measurements in a four-ball apparatus in combination with a laser scanning microscope. In addition, EDX analysis of the wear scars is to be performed to gain information on the mechanism of action. Structure-response relationships are derived and the best substances to be identified.

Natural phenols, which can be derived from lignin, as well as further natural occurring alcohols were used to synthesize sulfur and phosphor containing derivatives as next generation lubricant additives. The equivalent molecular mass of the additives either with regard to the phosphor or sulfur content was used to map the lubricating action. The following formula was the basis:

$$M_{Seq} = \frac{\text{molar mass}}{\frac{\sum \text{sulfur}}{\text{molecule}}}; \quad M_{Peq} = \frac{\text{molar mass}}{\frac{\sum \text{phosphorous}}{\text{molecule}}}$$

Tributyl thiophosphate and dibutyl dithiophosphate are considered as an example to account for the different phosphor to sulfur content within the molecules (Figure 10).

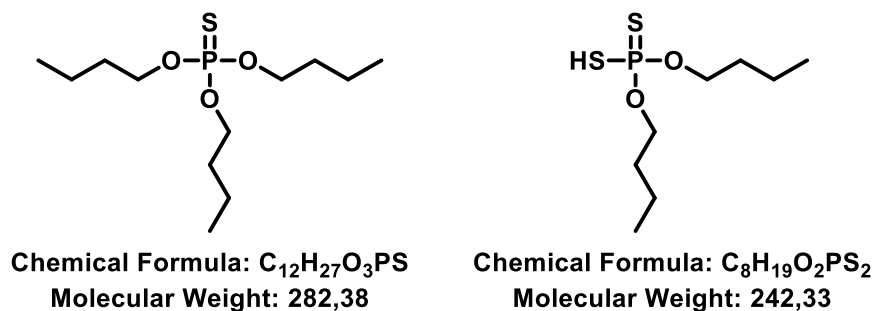


Figure 10. Molecular structures of tributyl thiophosphate (left) and dibutyl dithiophosphoric acid (right).

Tributyl thiophosphate contains one phosphor and one sulfur atom, while dibutyl dithiophosphoric acid contains one phosphor and two sulfur atoms per molecule. As a result, at equal moles based on the standard molecular weight, dibutyl dithiophosphoric acid would exhibit twice the amount of sulfur within the same amount of base stock. The performance in lubrication is here related to the phosphor content or sulfur content. Therefore, in case of additives with phosphor : sulfur ratios different from 1, equivalent molecular masses with regard to either phosphor or sulfur are calculated by above

mentioned formulas and necessary sample masses with both molecular weights calculated and solved in base stock. More detailed, the molecular masses are divided by the amount of sulfur or phosphor per molecule, leading to the resulting equivalent molecular weights:

$$M_{Seq} \text{Tributyl thiophosphate} = \frac{\text{molar mass}}{\frac{\sum \text{sulfur}}{\text{molecule}}} = \frac{282.38 \frac{g}{mol}}{1} = 282.38 \frac{g}{mol}$$

$$M_{Peq} \text{Tributyl thiophosphate} = \frac{\text{molar mass}}{\frac{\sum \text{phosphor}}{\text{molecule}}} = \frac{282.38 \frac{g}{mol}}{1} = 282.38 \frac{g}{mol}$$

$$M_{Seq} \text{Dibutyl dithiophosphate} = \frac{\text{molar mass}}{\frac{\sum \text{sulfur}}{\text{molecule}}} = \frac{242.33 \frac{g}{mol}}{2} = 121.17 \frac{g}{mol}$$

$$M_{Peq} \text{Dibutyl dithiophosphate} = \frac{\text{molar mass}}{\frac{\sum \text{phosphor}}{\text{molecule}}} = \frac{242.33 \frac{g}{mol}}{1} = 242.33 \frac{g}{mol}$$

Using the equivalent molecular weight, 1, 1.5 and 2 mmol with reference to the mentioned elements are thus made comparable and independent of the functional group (in the example thiophosphate : dithiophosphate). In conclusion, the necessary amounts to obtain samples with, 1, 1.5 and 2 mmol sulfur/50g base stock as well as 1, 1.5 and 2 mmol phosphor/50g base stock are given in Table 1.

Table 1. Equivalent molecular weights and the sample masses to obtain concentrations of 1, 1.5 and 2 mmol/50g base stock of sulfur and phosphor.

Substance	Molecular weight / $\frac{g}{mol}$	Sulfur-equivalent molecular weight/ $\frac{g}{mol}$	Phosphor-equivalent molecular weight/ $\frac{g}{mol}$	Sample mass for 1 mmol S/50 g base stock	Sample mass for 1.5 mmol S/50 g base stock	Sample mass for 2 mmol S/50 g base stock
Tributyl thiophosphate	282.38	282.38	282.38	0.28g	0.42g	0.56g
Dibutyl dithiophosphate	242.33	121.17	242.33	0.24g	0.36g	0.48g

The additives were solved in Tudalen 12®, a mineral base oil, and tested with the Hansa Press four-ball apparatus according to DIN 51350-3. The EP properties were determined by an adapted screening method.²⁷ The obtained data is always given with regard to the element.

4.1 AW & EP determination with the Four-Ball Apparatus (VKA)

The AW and EP performance of the substances were determined with a four-ball apparatus (VKA) according to DIN 51350-1¹³⁵ purchased from Hansa Press- und Maschinenbau GmbH located in Hamburg. In Figure 11 a picture of the used VKA is shown.



Figure 11. Picture of the VKA.

The picture shows the engine (top) the casing for the test setup (middle) and the load lever with the 10 kg load. Furthermore, the ball pot with cooling hoses is shown (bottom). The applied force on the four-ball system can be varied by sliding the load over the lever, more precise the load is decreased by sliding the load to the left and increased by sliding the load to the right (Figure 12).¹³⁵

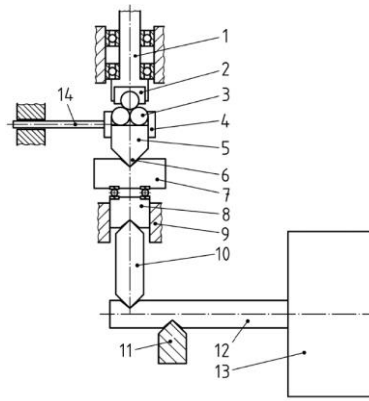


Figure 12. Drawing of the test chamber, including the load variation mechanism.¹³⁵

The engine rotates the spindle (1) which holds the ball chuck (2) with the running ball. The ball holder (parts 14, 4, 5 and 6) contains three resting balls (3) which are locked into position by the clamp (4). The ball holder rests in a conic bearing (6 & 7), resulting in a self-centering of the four-ball system. The lower part of the conic bearing (7) itself is supported on a ball bearing (between 7 & 8) so that rotation is possible. The weight lever (12) is mounted on two edge-bearings (11 & 10 respectively 9), delivering the weight on the four-ball system. By sliding the weight (13) on the weight lever (12) the load on the four-ball system can be controlled.

The four-ball testing apparatus used in this investigation was equipped with a load cell located in the edge bearing (10). The load cell recorded the actual weight on the four-ball system. The handle of the ball holder (14) is also connected to a torque sensor, enabling the measurement of the torque conducted through the friction of the four-ball system in normal direction to the rotation (Figure 13).

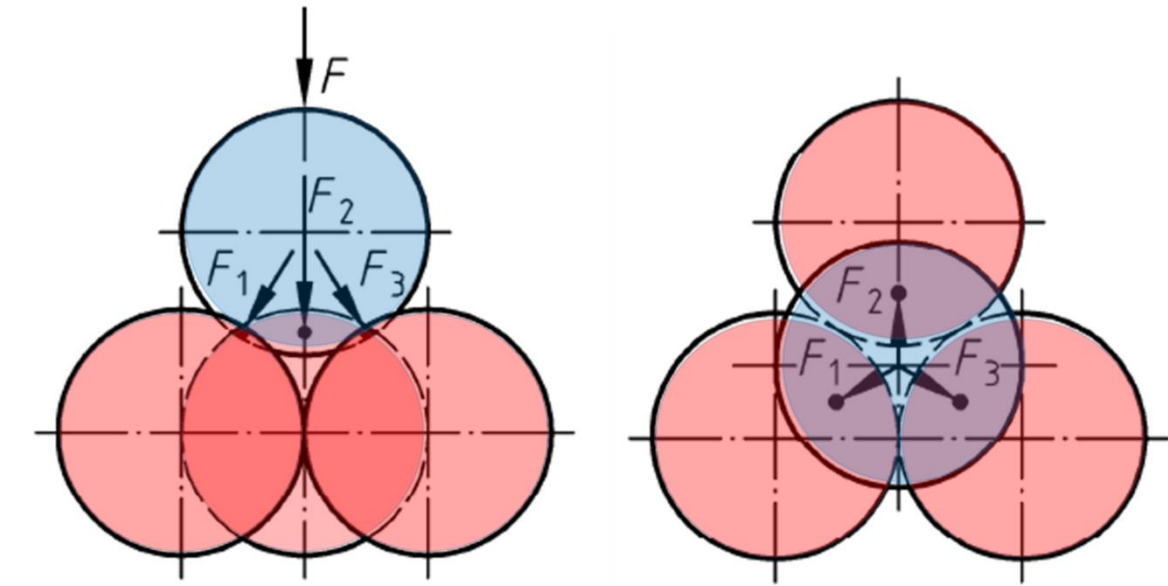


Figure 13. Four-ball system. Side and top view on the left with running ball (blue).¹³⁵

The four-ball system consists of two parts: the resting balls (colored red) and the running ball (colored blue). The running ball is fixed in a rotating chuck, driven by the engine resulting in a line contact. The second part are the three resting balls locked into position by a clamp resulting in a point contact (Figure 12). The load applied on the system divides equal on the 3 resting balls according to the formula $F_1 = F_2 = F_3 = \frac{F}{\sqrt{6}}$.

Two types of wear scars according to the friction are found in the four-ball system: the running ball suffers a line contact, leading to a circular wear scar, and the resting balls suffer a spot wear at the marked positions. In dependence of the applied force the four-ball system suffers slight wear up to welding of the four-ball system at high loads.

The procedures for the determination of anti wear (AW) and extreme pressure (EP) properties are described in 6.13 DIN 51350-3 Procedure & 6.12 DIN 51350-2 Procedure.

The evaluation of the lubricants AW&EP performance was carried out by measuring the diameter of the developed wear scar on the resting balls with a Keyence VK-X200 laser scanning microscope, the surface composition was examined by electron microscopy. The diameter was measured in sliding as well as rectangular to the sliding direction of the running ball. The diameter rectangular to the sliding direction was used to evaluate the AW performance due to sharper edges and therefore smaller statistical scattering of the values. A smaller diameter of the wear scar represents a better AW

performance respectively a large wear scar represents weak AW performance. (Figure 14).

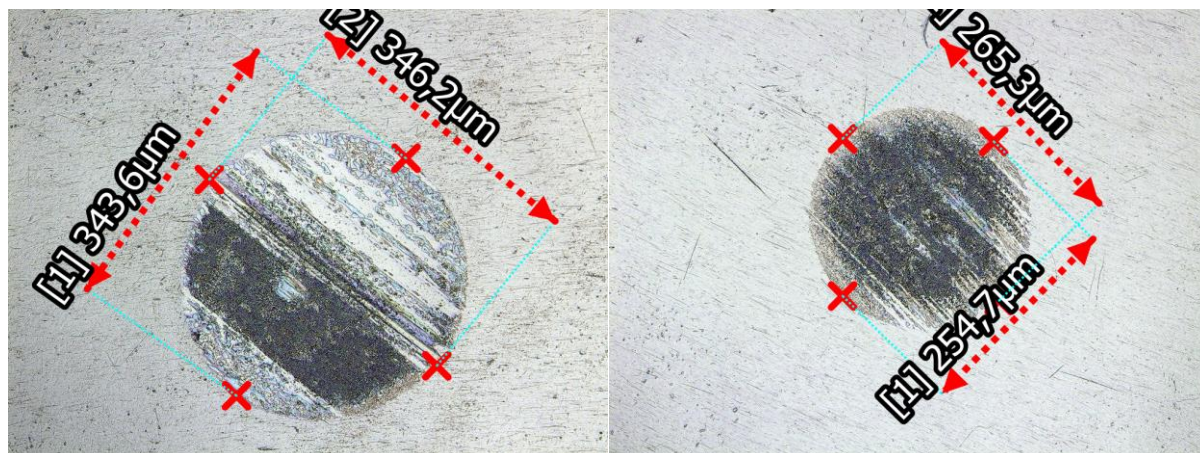


Figure 14. Representative laser scanning microscope pictures of 1 mmol TPPT (left) and 1 mmol Irgalube 63 ® at 20x magnification. Test conditions: 1 mmol/50 g base stock, 100Cr6 Steel, 15 kg load, 60 min, 1450 rpm, 25°C.

The difference between the two additives is clearly visible.

According to the Hertzian contact mechanics 220 μm is the lowest observable mean wear scar diameter of the wear scars at the mentioned test conditions.²⁵ The Hertzian contact formula for the resulting wear scar diameter of static load in the four-ball geometry is given in the following.¹³⁶

$$\text{Wear Scar Diameter} = 2 \left(\frac{3\pi \frac{1}{\sqrt{6}} L (k_1 + k_2) R_1 R_2}{4(R_1 + R_2)} \right)^{1/3}$$

$$k_1 = k_2 = \frac{1 - \nu^2}{\pi E}$$

where L is the load on the four-ball system in kg, R_1 and R_2 are the radii of the steel balls, ν is the Poisson ratio of the used materials and E is the Young modulus of the used materials. The mechanical properties of the materials and the load the resulting radius of the contact area can be calculated using the above mentioned formula. The Hertzian contact radius determines the smallest possible wear scar diameter in a four-ball experiment. Three different materials were used to study the surface chemistry of the examined additives. The additives were examined for their AW properties at low loads and for their EP properties in load screening experiments with a newly developed setup (5.3.1 Concept of a Novel Extreme Pressure Screening Method). The used

materials were 1.3505 (100Cr6) steel¹³⁷, common material for four-ball tests¹³⁵, 1.0616 a standard carbon steel with low resistance for corrosion^{138,139} and 1.4034 a high chromium and nickel steel which is more resistant to corrosion and oxidation.^{139,140}

5 Results

Parts of the following chapters are summarized elsewhere.¹⁻⁵

5.1 Novel Structures

5.1.1 Alternative Dithiophosphate-Michael-Adducts

Irgalube 63 ® is a common AW/EP additive in industrial grade lubricants (Figure 15).¹⁴¹ In addition to triphenyl phosphorothionate (TPPT) it is used as AW/EP reference for determination of the AW/EP performance of novel substances in this study.

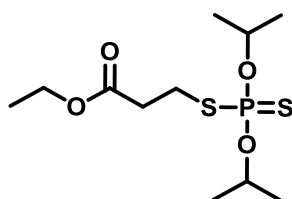


Figure 15. Structure of Irgalube 63 ®.

Irgalube 63 ® is accessible by a Michael addition of diisopropyl dithiophosphoric acid onto ethyl acrylate.^{74,142} The preparation was performed according to the procedure described in chapter 6.5 Synthesis of Dialkyl Dithiophosphoric-Acid-Michael-Adducts. The product has a pungent smell, which is unpleasant especially at higher temperatures.

Thus, one challenge was to synthesize novel dithiophosphate-Michael-adducts with enhanced acceptance. The innovative products should not have the unpleasant odor while sustaining the excellent AW/EP performance. Furthermore, the usage of renewable alcohols to synthesize dithiophosphoric acids should be in focus to gain products with tentatively less harmful decomposition products. Acrylates with higher molecular weights were used to increase the molecular weight leading to less volatile products with corresponding AW/EP performances. Therefore, diisopropyl dithiophosphate was reacted with phenoxyethyl acrylate (POEA, $M_w = 192.21 \frac{g}{mol}$), ethylhexyl acrylate (EHA; $M_w = 184.28 \frac{g}{mol}$) and hexanediol diacrylate (HDDA; $M_w = 226.27 \frac{g}{mol}$) to the corresponding products EHA-DTP; $M_w = 398.56 \frac{g}{mol}$, POEA-DTP; $M_w = 406.49 \frac{g}{mol}$ and HDDA-DTP; $M_w = 654.83 \frac{g}{mol}$ (Figure 16).

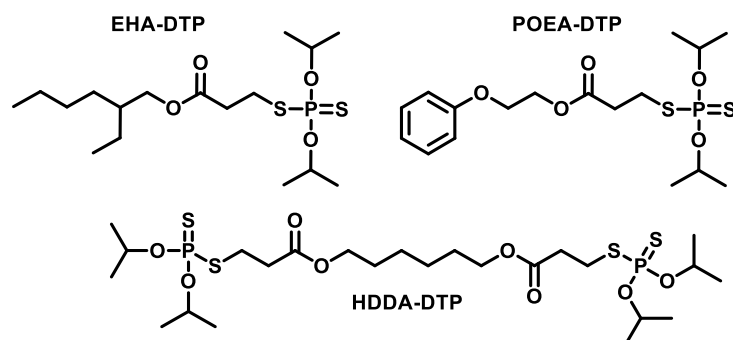


Figure 16. Structures of ethylhexyl acrylate dithiophosphate, phenoxy ethyl acrylate dithiophosphate and hexanediol diacrylate dithiophosphate.

Model reactions involving dibutyl dithiophosphoric acid and ethyl acrylate were performed as explained in the following to gain some experience with the addition reaction, and furthermore to identify occurring impurities. Initially an excess of butanol was therefore reacted with phosphor pentasulfide at 65 °C to give dibutyl dithiophosphoric acid.⁷³ The preparation was performed according to the procedure described in chapter 6.4 Synthesis of Dialkyl Dithiophosphates. After phosphor pentasulfide was dissolved completely, argon gas was led through the reaction mixture for 0.5 h to remove dissolved H₂S. The excess alcohol was removed in vacuum (approx. 10⁻¹ mbar).

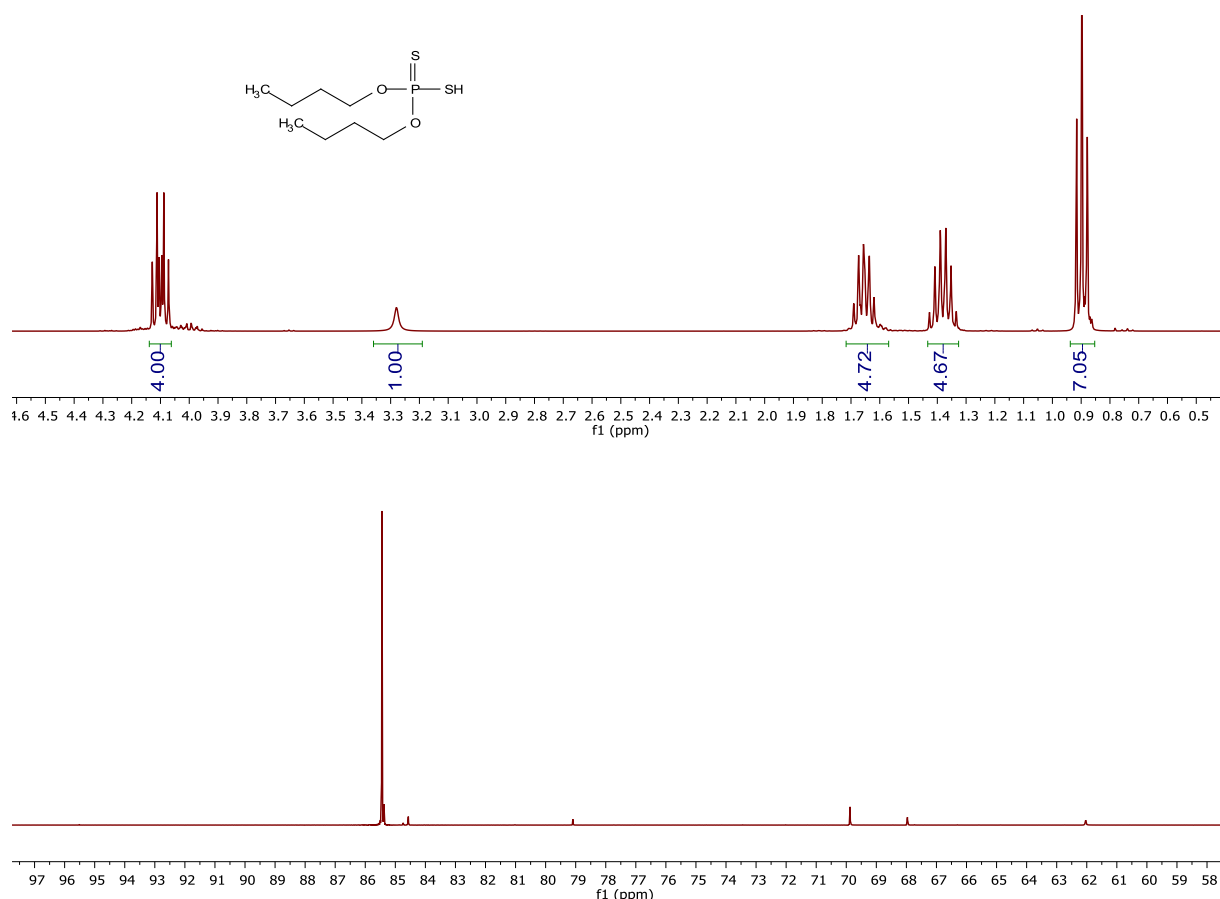


Figure 17. Top: ^1H -NMR of dibutyl dithiophosphoric acid in CDCl_3 . Bottom: ^{31}P -NMR of dibutyl dithiophosphoric acid in CDCl_3 .

The ^1H -NMR shows characteristic signals of the desired product (Figure 17). The signal at 4.1 ppm corresponds to the P-O-CH_2 -group of the butyl adjacent to the phosphor atom. These protons couple with phosphor, resulting in a doublet of a triplet (dt).¹⁴³ The signal at 3.3 ppm corresponds to the SH-proton. The signals at 1.7 ppm and 1.4 ppm are the two CH_2 -groups within the butyl rest, whereas the signal at 0.9 ppm is closer to the phosphor atom, the signal at 0.9 ppm corresponds to the CH_3 -group of the butyl rest. The ^{31}P -NMR spectra reveals several phosphor species in minor amounts. The dominating peak at 85.5 ppm corresponds to the desired product.¹⁴⁴ Calculated from this ^{31}P -NMR, dibutyl dithiophosphoric acid has a purity of approx. 86 %. For a detailed identification of the impurity species, an enlarged ^{31}P -NMR spectra is shown in Figure 18.

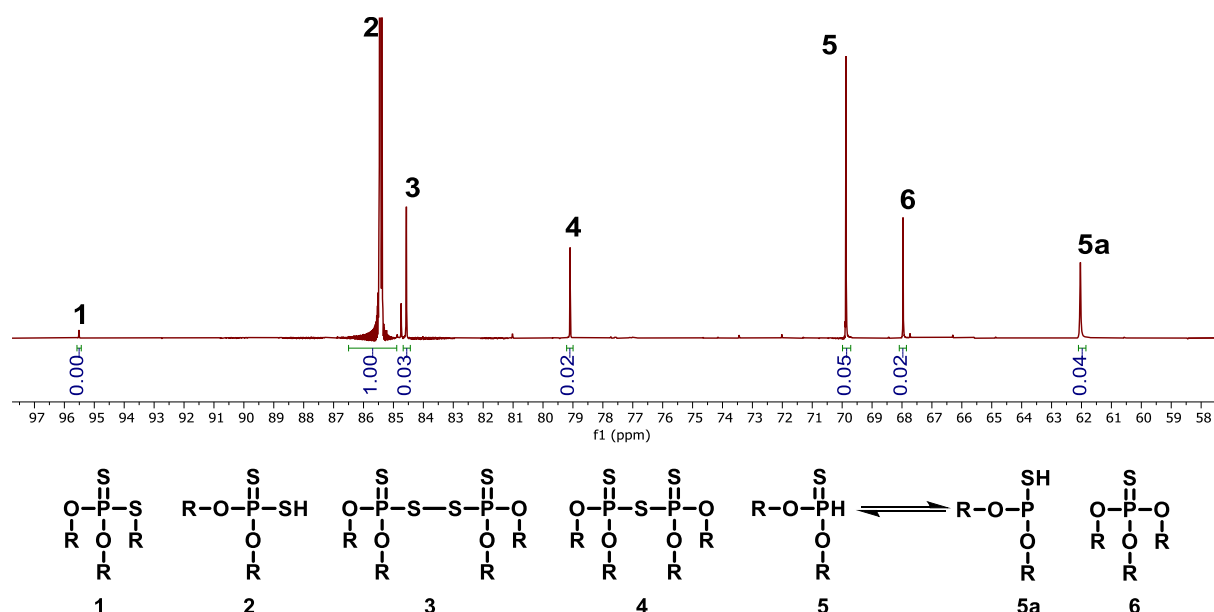


Figure 18. Impurities in the synthesis of dibutyl dithiophosphoric acid identified by their chemical shift (R = butyl).

The impurities were identified from their respective chemical shifts. The ^{31}P spectral shift is very sensitive to the substitution pattern, and model compounds are available to substantiate the assignments. The peak 1 at 95.5 ppm tentatively corresponds to the O,O,S-triester. Peak 2 corresponds to dibutyl dithiophosphoric acid, peak 3 corresponds to the oxidized product of the dibutyl dithiophosphoric acid, a disulfide. Peak 4 corresponds to the SP-S-PS ester. Peak 5 corresponds to the thiophosphonate. Peak 6 corresponds to the common chemical shift of tributyl thiophosphate and peak 5a corresponds to the tautomeric form of structure 5, the acid form of the phosphonate.^{144–146}

The Michael addition of dibutyl dithiophosphoric acid over ethyl acrylate was performed at elevated temperature. The thio acid was heated to 95 °C and an 10 mol% excess of ethyl acrylate was added dropwise using a syringe. The reaction mixture was stirred for an hour after the addition was completed, after which a dynamic vacuum (approx. 10^{-1} mbar) was applied to remove unreacted acrylate. The reaction mixture gave evidence for the formation of the intended product. It appeared as a colorless to slight yellow liquid.

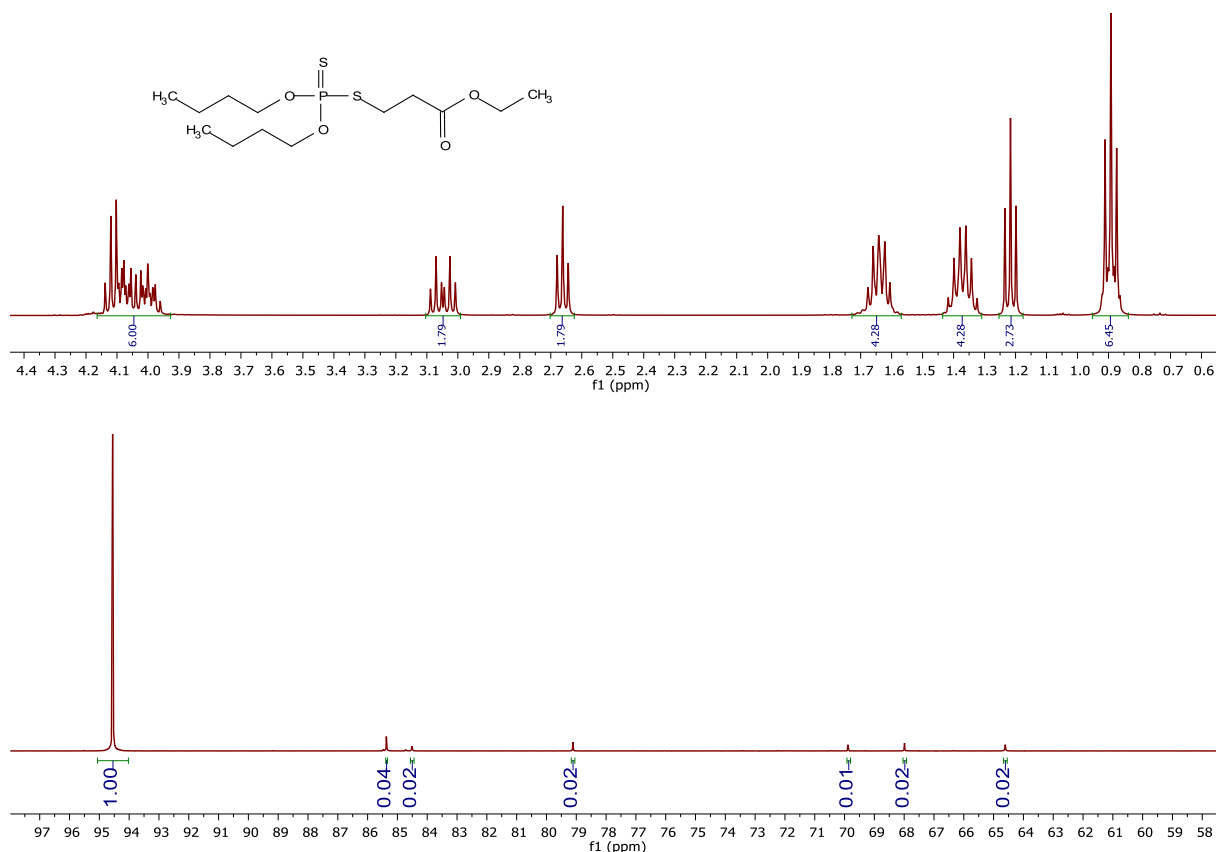


Figure 19. ^1H - and ^{31}P NMR of the dibutyl dithiophosphoric acid ethyl acrylate adduct. Solvent: CDCl_3 .

The ^1H -NMR spectra of the product confirmed the basically quantitative conversion of dibutyl dithiophosphoric acid to the acrylate adduct (Figure 19). Furthermore, no remaining acrylate peaks (approx. 5.8 to 6 ppm)¹⁴⁷ were observed in the product. The peak at 4.05 ppm corresponds to the two PO-CH_2 groups as well as the P-S-CH_2 group, leading to an overlapped signal with the integral of 6. The signal at 3.05 ppm corresponds to the CH_2 -group adjacent to the dithiophosphate ester group. The signal at 2.65 ppm is assigned to the OCH_2 group of the ethyl ester. The signals at 1.4 ppm and 1.65 ppm belong to the two CH_2 groups in the butyl rest. The signal at 1.2 ppm corresponds to the CH_3 group of the ethyl rest, and the signal at 0.9 ppm corresponds to the two CH_3 groups of the butyl rest.

The ^{31}P -NMR spectra are also consistent to the substantial conversion of the dibutyl dithiophosphoric acid to the Michael product (Figure 20). The corresponding signal is at 95 ppm.¹⁴⁴ Only a minor rest of the free acid (peak at 85.5 ppm¹⁴⁴) remained in the model reaction product (approx. 3.5 %). A possible explanation for its presence could be the inversion of the addition reaction. Alternatively, some of the free acid may have

been oxidized to disulfide, which has a comparable shift. The ^{31}P -NMR spectra revealed a purity of approx. 88.5 %.

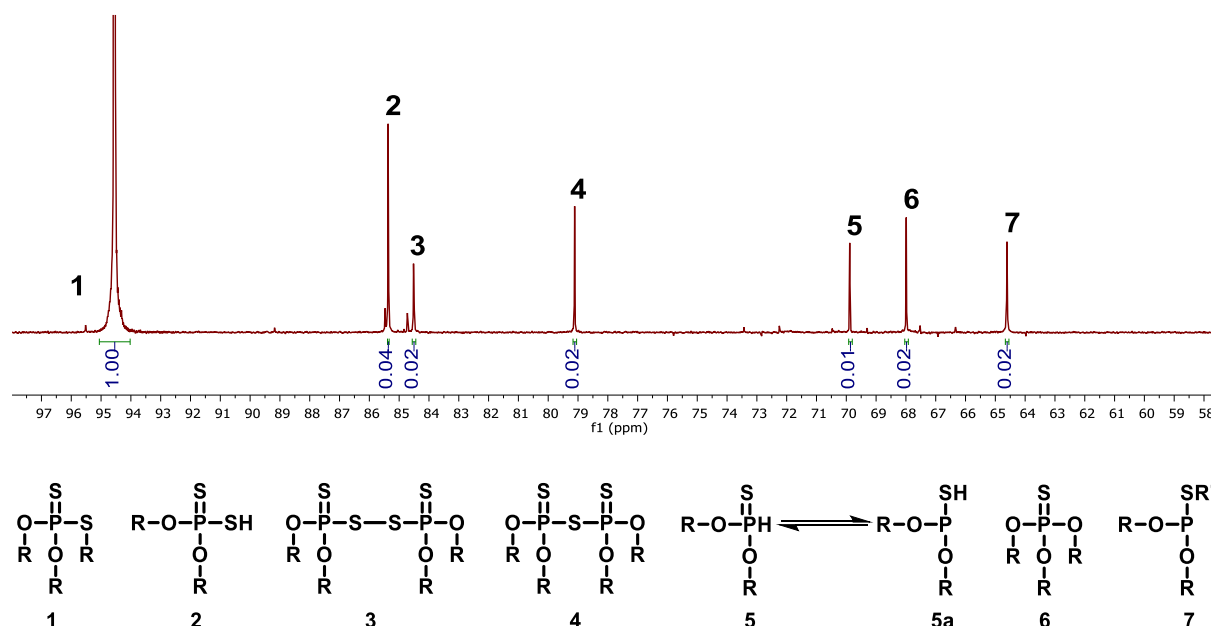


Figure 20. Zoomed in ^{31}P -NMR spectra of the final reaction product of dibutyl dithiophosphoric acid and ethyl acrylate. NMR solvent: CDCl_3 . R = butyl, R' = ethyl acrylate

The ^{31}P -NMR spectra of the final product revealed changes compared to the ^{31}P -NMR spectra of the dibutyl dithiophosphoric acid. A peak no. **7** at 65 ppm is observed in addition to peak no. **2** at 85.5 ppm of the starting material and peak no. **1** at 95 ppm of the product. The signal **7** could possibly be assigned to the product of a reaction of the SH-functionality of **5a** (62 ppm) with ethyl acrylate, forming a further a Michael-adduct. The integrals of species **5** and **5a** in the ^{31}P -spectra of the dibutyl dithiophosphoric acid were 0.05 and 0.04 of the total intensity. In the ^{31}P -spectra of the final product, the integrals of **5** and **7** were 0.01, 0.02, which needs some explanation. The overall amount of **5** and **7** is lower than could be assumed from the spectra of the starting material. A likely explanation for this finding may be that species **5** is distilled off under these conditions, resulting in change of equilibrium leading to conversion of **5a** to **5**. As a consequence, only a minor fraction of **5a** is reacting to **7**. Species **6** can be used as internal standard with integrals of 0.02 in both spectra, thus being inert towards the addition of ethyl acrylate as well as no distillation under the given reaction conditions.

The results indicate two disadvantages of the conducted reaction: firstly, the addition of excess acrylate bears difficulties with regard to the possible formation of polyacrylates, secondly the use of the relatively heavy dibutyl dithiophosphoric acid (molecular weight 242.33 g/mol) bears difficulties with regard to the purification of the

crude product by distillation. The impurities resulting from preparation of dialkyl dithiophosphoric acid, in contrast may be distilled off in case of the isopropyl esters at temperatures around 65 °C in vacuum. To resolve these disadvantages, the aforementioned products derived from alternative acrylates (Figure 16) were synthesized with an excess of diisopropyl dithiophosphoric acid, which can be formed in higher qualities than the dibutyl dithiophosphoric acid due to the volatility of the undesired impurities and the inverted reaction conditions regarding the Michael addition.

The synthesis of the diisopropyl dithiophosphoric acid was performed according to the described method in 6.4 Synthesis of Dialkyl Dithiophosphates. The product appeared as a clear violet to green liquid with an unpleasant smell.

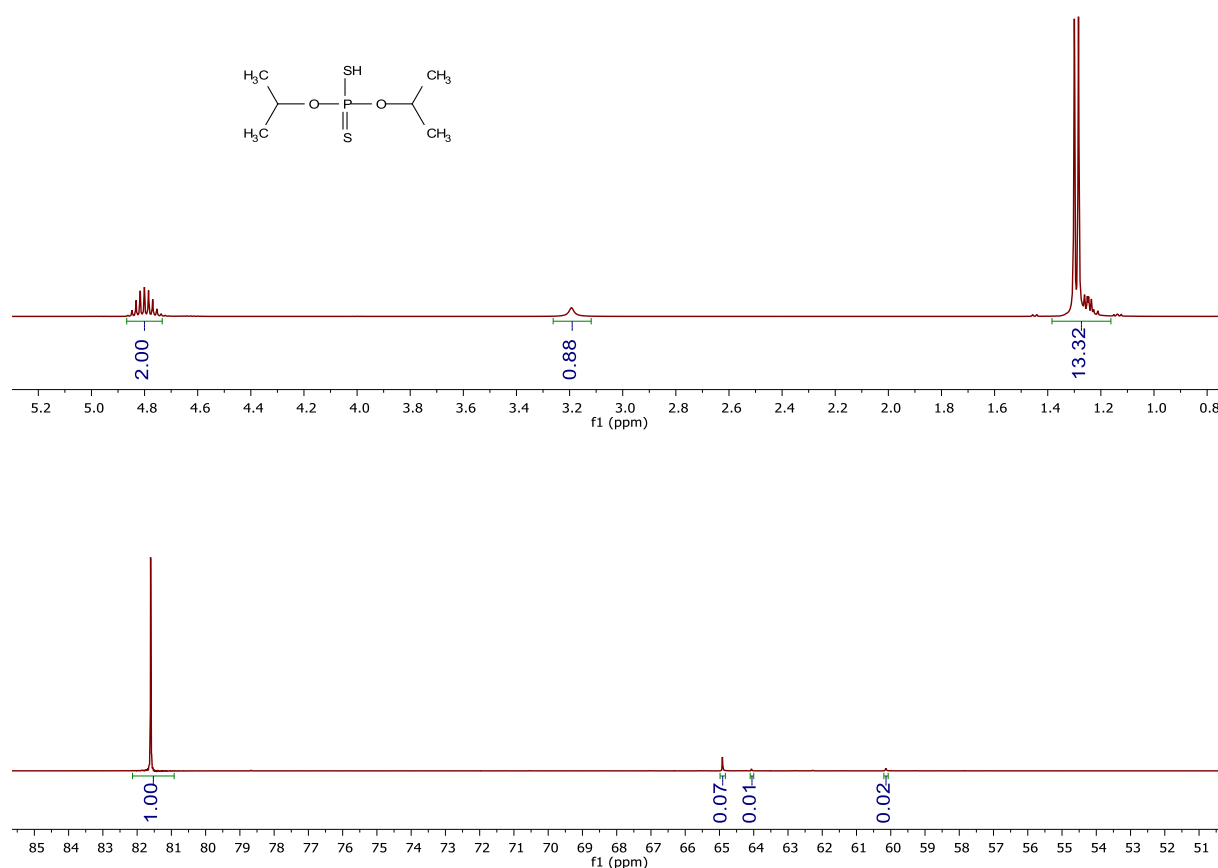


Figure 21. Top: ^1H -NMR spectra of diisopropyl dithiophosphoric acid in CDCl_3 . Bottom: ^{31}P -NMR of diisopropyl dithiophosphoric acid in CDCl_3 .

The ^1H NMR spectra show the expected shifts, integrals and patterns (Figure 21). A signal at 4.8 ppm with an integral of 2 is found, which is assigned to the two CH -groups of the isopropyl residues adjacent to the phosphor atom. The signal at 3.2 ppm would derive from the SH group. The signal at 1.3 ppm corresponds to the four CH_3 -groups

of the two isopropyl rests. The ^{31}P -NMR spectrum exhibits the product peak at 81.5 ppm. Minor peaks are at 65 ppm, 64 ppm and 60 ppm. The signal at 65 ppm corresponds to triisopropyl thiophosphate $\text{S}=\text{P}(\text{OR})_3$, the signals at 64 and 60 ppm are presumably thiophosphonates, respectively the tautomeric form (see Figure 18, structures 5 and 5a). The purity of the diisopropyl dithiophosphoric acid is about 90 %, as based on the ^{31}P -NMR.

Additions of diisopropyl dithiophosphoric acid (15 mol% excess) to acrylates was also performed at 90 °C. Therefore, 0.85 equivalents of 2-ethylhexyl acrylate (EHA) and phenoxyethyl acrylate (POEA), respectively 0.42 equivalents of hexanediol diacrylate (HDDA) were added over a period of 30 min. The color of the reaction solution changed in the process from green violet to colorless to slightly yellow. After complete dosage of acrylate, the reaction was allowed to stir for 2 h. Again a dynamic vacuum (10^{-1} mbar) was applied to remove excess diisopropyl dithiophosphoric acid. The product appeared as a slightly yellow to colorless liquid with an unimpressive scent.

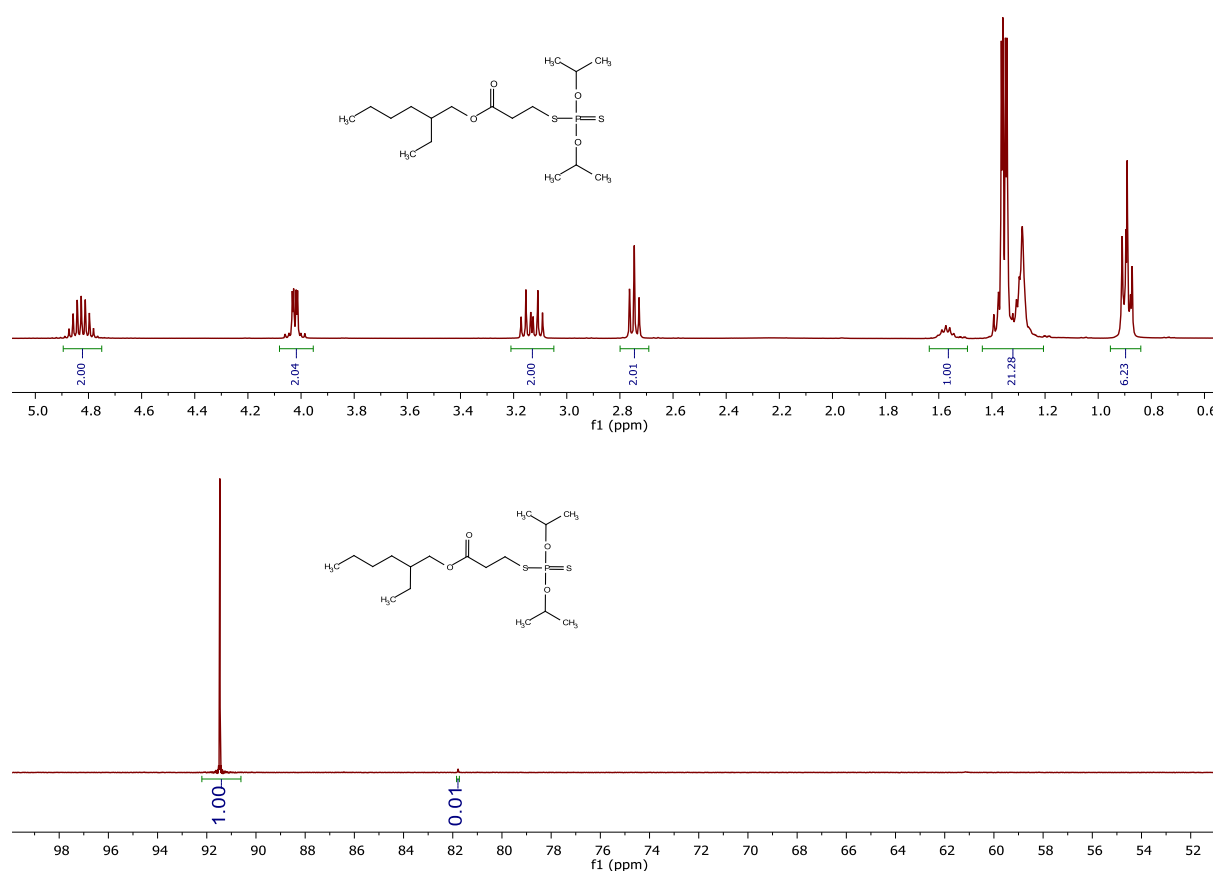


Figure 22. ^1H -NMR spectra of ethylhexyl acrylate dithiophosphate adduct (top). ^{31}P -NMR of ethylhexyl acrylate dithiophosphate adduct (bottom). NMR solvent: CDCl_3 .

NMR spectroscopical evidence is in agreement with the formation of the Michael-adduct (Figure 22). The signal at 4.82 ppm are assigned to the two *CH*-groups adjacent to the phosphor atom. The signal at 4.02 ppm would correspond to the *CH*₂-group adjacent to the ester of the ethyl hexyl alcohol. The signal at 3.13 ppm corresponds to the *SCH*₂-group coupling with the phosphor atom, leading to a doublet of triplets (dt). The signal at 2.75 ppm corresponds to the *CH*₂-group next to the ester. The ³¹P-NMR reveals the desired product with a signal at 91.45 ppm. A minor impurity can be found at 81.77 ppm with an integer of 0.01. This impurity may be the oxidation product of the diisopropyl dithiophosphoric acid. The purity was determined by ³¹P-NMR spectra to be 99 % (Figure 23).

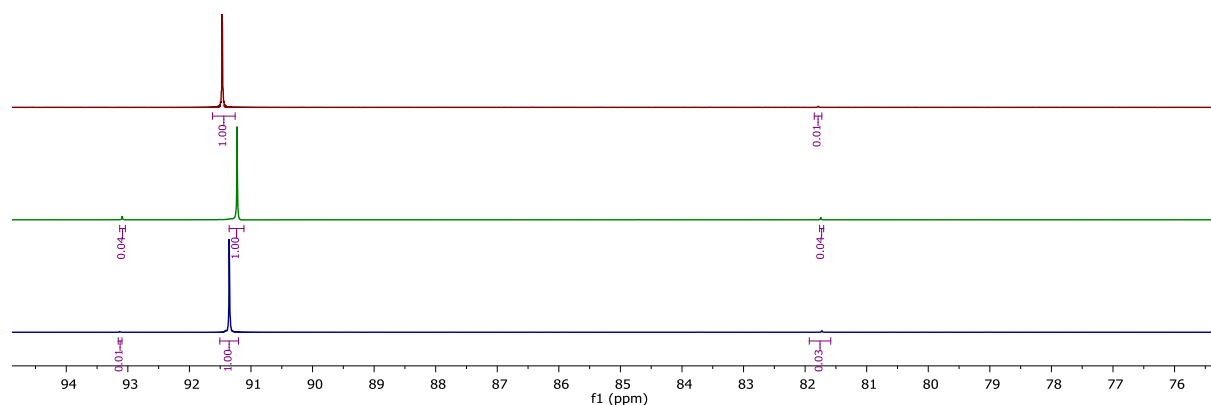


Figure 23. ³¹P-NMR spectra of the ethylhexyl acrylate dithiophosphate adduct (top), phenoxyethyl acrylate dithiophosphate adduct (middle) and the hexanediol diacrylate dithiophosphate adduct (bottom). NMR solvent: CDCl₃.

The products obtained are clear colorless to slightly yellow liquids with an agreeable smell, i.e. much less pungent than Irgalube 63 ®. The purity for all novel dithiophosphates was determined by ³¹P spectra to be >92%. Thus, the first objective of developing novel dithiophosphate-acrylate-adduct based anti-wear additives with mild odor was accomplished.

Menthol was chosen as an alcohol obtainable from renewables for the synthesis of further dithiophosphoric acids. Ethanol can also be obtained from renewable sources, however the solubility of resulting dithiophosphoric acid in mineral oils is expected to be poor on account of the polarity differences. In addition, diethyl dithiophosphoric acid may exhibit an unpleasant smell as it is quite volatile. Menthol is readily available, thus synthesis of dithiophosphoric acids derived from menthol is an attractive route to novel dithiophosphate based lubricant additives. Menthol may exhibit pleasant esthetics next to good AW properties after reaction with P₂S₅.

The preparation of dithiophosphoric acids derived from menthol revealed difficulties, which result from the low reactivity of menthol towards phosphor pentasulfide. Since the sterically hindered secondary OH group required higher reaction temperatures of around 80 °C, the selectivity became much lower. The reaction mixture contained a larger amounts of phosphor species, showing signals between 70 to 110 ppm in the ^{31}P -NMR. Thus, the experiments with menthol were abandoned as no easy purification was in sight.

5.1.2 Novel Thiophosphates

Thiophosphates are ubiquitous components of oil and grease formulations¹⁴² and are generally formed by reaction of appropriate alcohols with phosphor trichloride in toluene in the presence of a base (e.g. triethylamine), followed by sulfur oxidation.^{14,15} The oxidation of trivanilline phosphite to the corresponding thiophosphate with sulfur was carried out in boiling toluene.

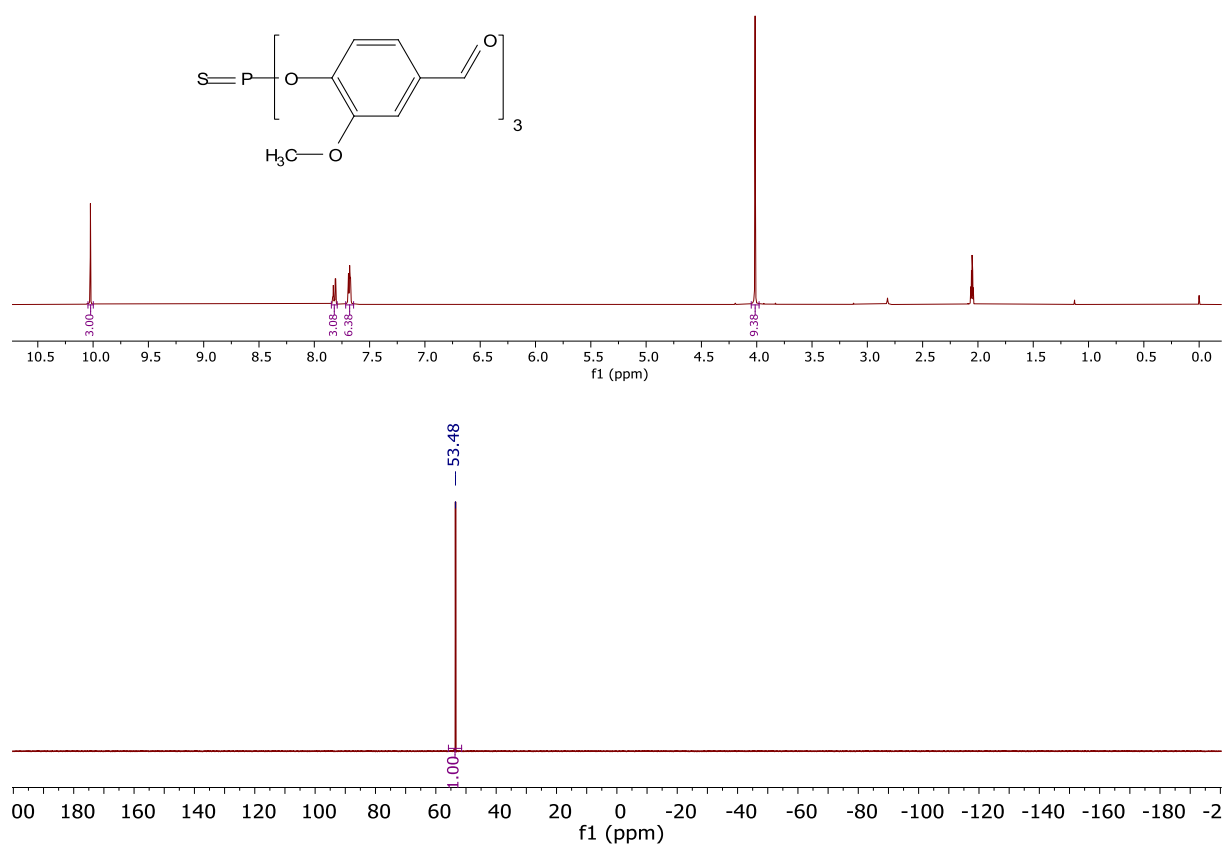


Figure 24. Top: ^1H -NMR spectra of vanillin thiophosphate in acetone-d_6 . Bottom: ^{31}P -NMR of vanillin thiophosphate in acetone-d_6 .

The ^{31}P -NMR spectra of the product reveal the successful transformation of the phosphite (typical shift for triphenyl phosphite 120 to 130 ppm¹⁴⁸) to the corresponding thiophosphate (typical shift 50 to 75 ppm¹⁴⁹) (Figure 24). The product appeared as a powder with the scent of vanilla, but it showed a very poor solubility in toluene, CDCl_3 and was only slightly soluble in acetone- d_6 . A dissolution of the obtained product in Tudalen 12 ® failed. Based on the poor solubility of vanillin thiophosphate in mineral base stock, ethyl vanillin- and eugenol thiophosphate were assumed to behave comparably, thus experiments towards thiophosphates based on such lignin derived alcohols were abandoned. As an alternative alcohol from renewables, oleic alcohol was considered. Therefore, technical trioleyl phosphite was reacted with sulfur to yield the thiophosphate.

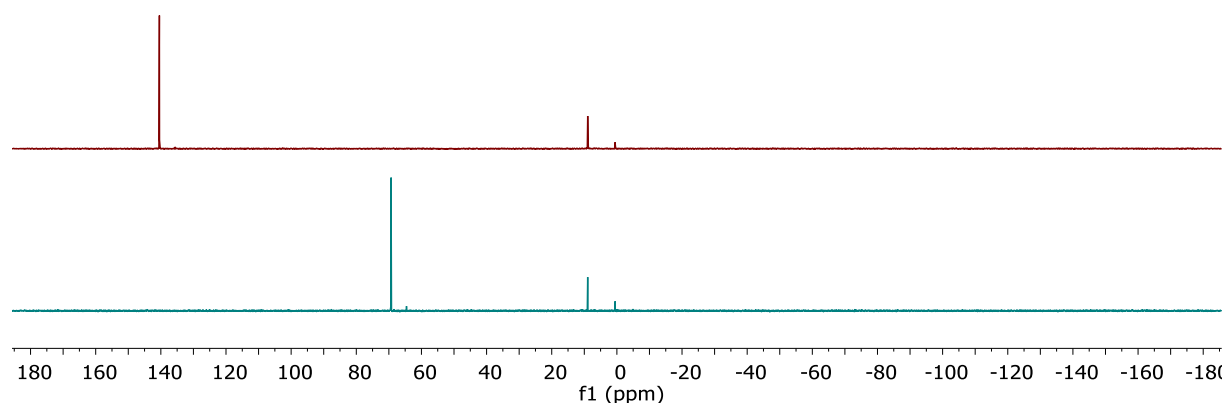


Figure 25: ^{31}P -NMR spectra of trioleyl phosphite (top) and trioleyl thiophosphate (bottom) in CDCl_3 .

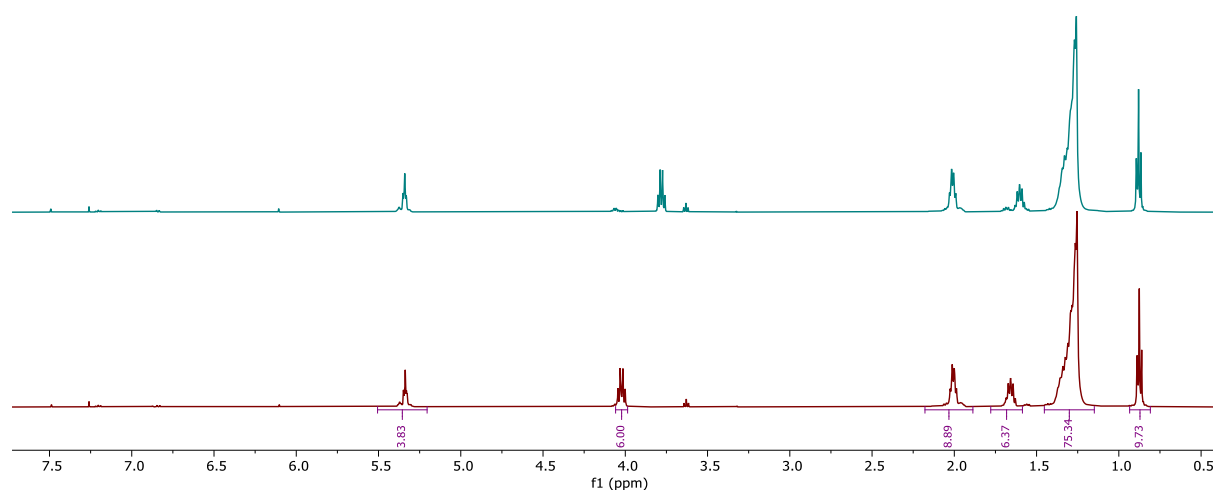


Figure 26. ^1H -NMR spectra of trioleyl phosphite (top) and trioleyl thiophosphate (bottom) in CDCl_3 .

The ^{31}P NMR spectrum of technical trioleyl phosphite exhibits characteristic signals at 140 ppm and impurities in the range of 0 to 10 ppm (Figure 25). The signals at 9 ppm

may be assigned to diolel phosphonate.¹⁵⁰ Oxidation to thiophosphate was successful as indicated by the peak at 65 ppm in the ^{31}P -NMR. The shift of the impurities remained unchanged. This is consistent to the assumption of the impurities to be diolel phosphonate. Another hint is the signal in the ^1H -NMR at 6.10 and 7.49 ppm, which fits to a $\text{PO}(\text{H})$ tautomerism (Figure 26).¹⁵¹

5.1.3 Renewable Phosphonates

A synthesis of oleyl stearyl phosphonates from dimethyl phosphonate by transesterification seemed an interesting route of preparation.^{71,72} Therefore, a mixture of 70 mol% oleyl alcohol and 30 mol % stearyl alcohol was reacted with excess dimethyl phosphonate at elevated temperatures. The reaction was driven by the removal of methanol by distilling it off. The resulting product was obtained as waxy liquid, which further solidified at room temperature.

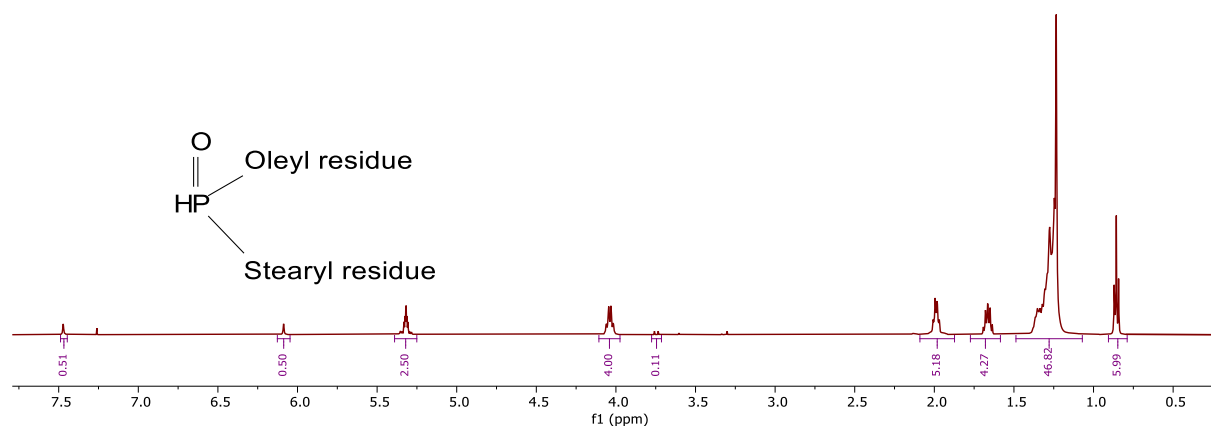


Figure 27. ^1H -NMR spectra of oleyl-stearyl phosphonate in CDCl_3 .

The ^1H -NMR spectrum of the solid shows that conversion has taken place (Figure 27). The signals at 7.47 ppm and 6.08 ppm are assigned to the $\text{PO}(\text{H})$ POH tautomerism; they have an accumulated integral of 1 proton relative to the $\text{P}(\text{OCH}_2)_2$ -moiety. The signal at 5.31 ppm can be assigned to the unsaturated olefinic protons of the oleyl residue. The signal at 4.04 ppm corresponds to the $\text{P}(\text{OCH}_2)_2$ esters of oleyl and stearyl alcohol with an integral of 4 and a splitting of the signal due to coupling with phosphorus leading to a doublet of quartets. The signal at 3.75 ppm can be assigned to a POCH_3 entity with either mono oleyl or mono stearyl residues resulting from excess dimethyl phosphonate and thus incomplete transesterification. The amount of mono methyl mono oleyl-stearyl phosphonate calculated by ^1H -NMR was to be approx.

3.5 mol%. The signals between 0.8 and 2.05 ppm can be assigned to the oleyl-stearyl residues. The NMR analysis confirmed no residual dimethyl phosphonate in the product.

5.1.4 Innovative Polysulfides

Polysulfides are routinely used extreme pressure additives.¹¹³ Common derivatives are di-tert. butyl polysulfides like RC 2540® or TBPS454®, di tert. nonyl polysulfides like TNPS537®. These products can be formed by reaction of olefins with sulfur/H₂S at elevated temperatures and pressure. The suitability of synthetic dipentene (a 50:50 mixture of D- and L-limonene) and turpentine (a crude mixture of terpenes) for the synthesis of lubricant additives is also known.^{108–115,152,153} The most common used olefins are isobutylene and isononylene, obtained from cracking crude oil.¹⁵⁴ Due to environmental and sustainability issues of crude oil based products¹⁵⁵, renewable alternatives would be appreciated.

In lieu of latter argumentation, the synthesis of dialkyl polysulfides derived from renewables such as oleic acid, eugenol, eugenyl acetate and citrus D-limonene respectively balsam oil (α & β pinene) was performed to determine their relevance as alternative extreme pressure additives. The used terpenes can be harvested from pine turpentine, while D-limonene is a side product of the production of lemon, orange and lime juice. D-limonene can also be extracted from the peels by steam distillation.¹²⁸ Since adding value to industrial byproducts is of general interest, sulfidic derivatives were prepared with the objective to screen them for extreme pressure properties in the context of lubrication.

Reactions of oleic acid, as well as eugenyl derivatives with sulfur led to solid products, containing precipitated sulfur and showing poor solubility in mineral base oil. Further efforts with these starting materials were not undertaken, and experiments were directed to the natural terpenes. The company Weissmeer Baltische Export GmbH located in Hamburg donated samples of D-limonene as well as brazilian balsam turpentine oil, which contains alpha and beta pinene (Figure 28).^{156,157}

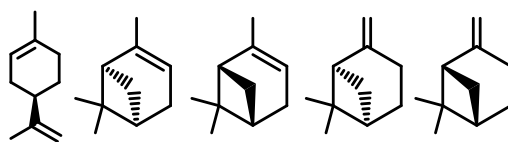


Figure 28. From left to right: structures of D-limonene, (+)-α-pinene, (-)-α-pinene, (+)-β-pinene and (-)-β-pinene.

The double bonds in these terpenes should be converted to polysulfides in the presence of sulfur to yield novel EP additives. The reaction between double bonds and sulfur can occur via two reaction pathways : I) a free radical process involving the homolytic cleavage of an S-S bond yielding S-S_x-S and II) an electrophilic attack of S-S_x-S⁺ following the heterolytic cleavage of an S-S bond.¹⁵⁸ Independent of the reaction mechanism, complex mixtures of polysulfides can be expected due to the multitude of double bonds of the applied terpenes. An indication of putative products is given in Figure 29, i.e. without considering the stereochemistry. The reaction products yielded from the “vulcanization” of limonene are statistically distributed oligomers, respectively rings. The majority products from vulcanization of balsam turpentine oil were expected to be statistically distributed dimers of alpha and beta pinene.¹⁵⁹ According to literature reports, Markovnikov products are most propable.¹⁶⁰

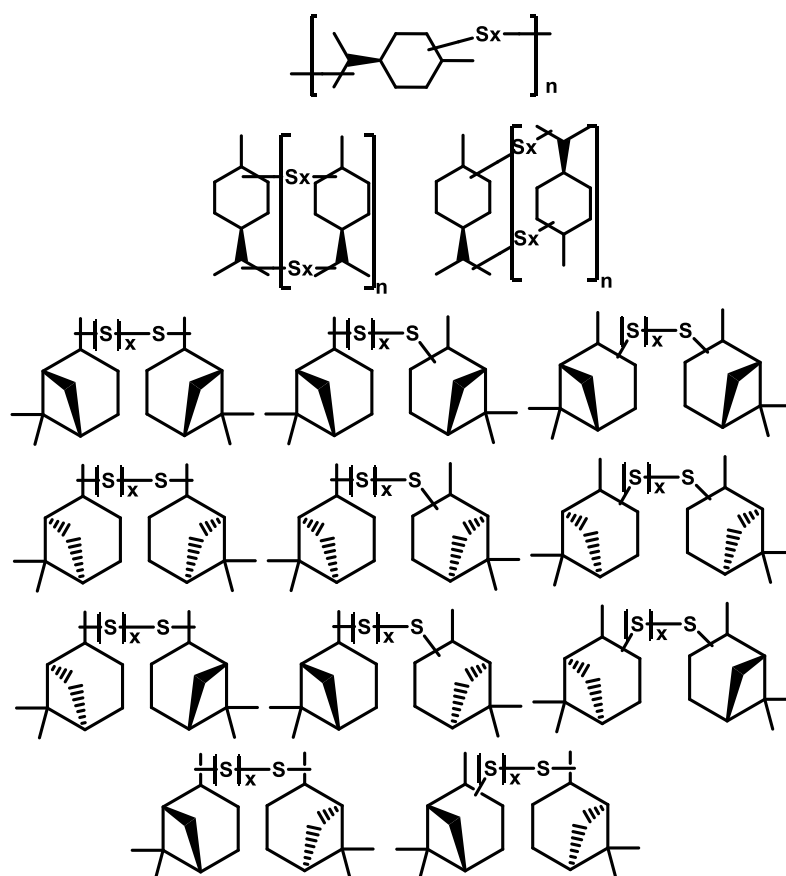


Figure 29. Possible structures of the resulting polymeric polysulfides from limonene (top and second row) and polysulfides resulting from pinene.

Three stoichiometries were used to gain some insight into the reaction mixture formed from D-limonene (33 wt% S, 41 wt% S and 50 wt% S). The reagents were placed in a round bottom flask equipped with a condenser and a stirring rod and heated. The chosen reaction temperature for the vulcanization of D-limonene was approx. 175 °C. At a temperature of around 120 °C sulfur melted to give a separate yellow liquid. Under vigorous stirring the two liquids homogenized and formed a blood colored reaction liquid. After stirring for 6 h at 175 °C, the reaction mixture was allowed to cool to ambient temperature. A detailed procedure is given in 6.10 Synthesis of Renewable Terpene Polysulfides.

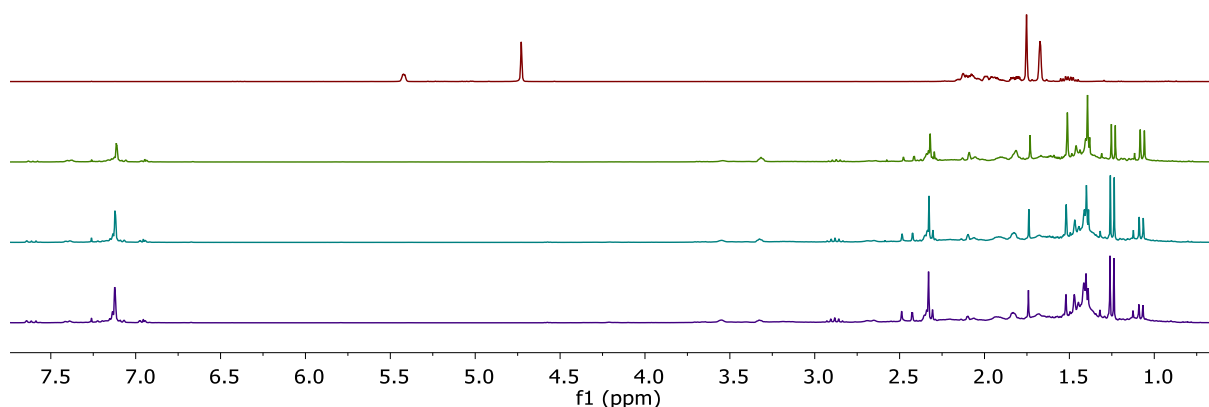


Figure 30. ^1H -NMR of D-limonene, 33 wt% S, 41 wt% S and 50 wt% S (from top to bottom) in CDCl_3 .

The NMR spectra of the reaction mixtures gave evidence for the complete conversion of the double bonds as well as formation of aromatic compounds and unknown compounds in the aliphatic range. (Figure 30). Most likely is formed p-cymene with signals at 1.25 ppm, 2.36 ppm 2.85 ppm and 7.12 ppm.¹³¹ These fit to a simulated ^1H -NMR spectra of p-cymene (Figure 33). To check the stability of the resulting products, the probes were put aside for 14 days and evaluated for the precipitation of sulfur (Figure 31).

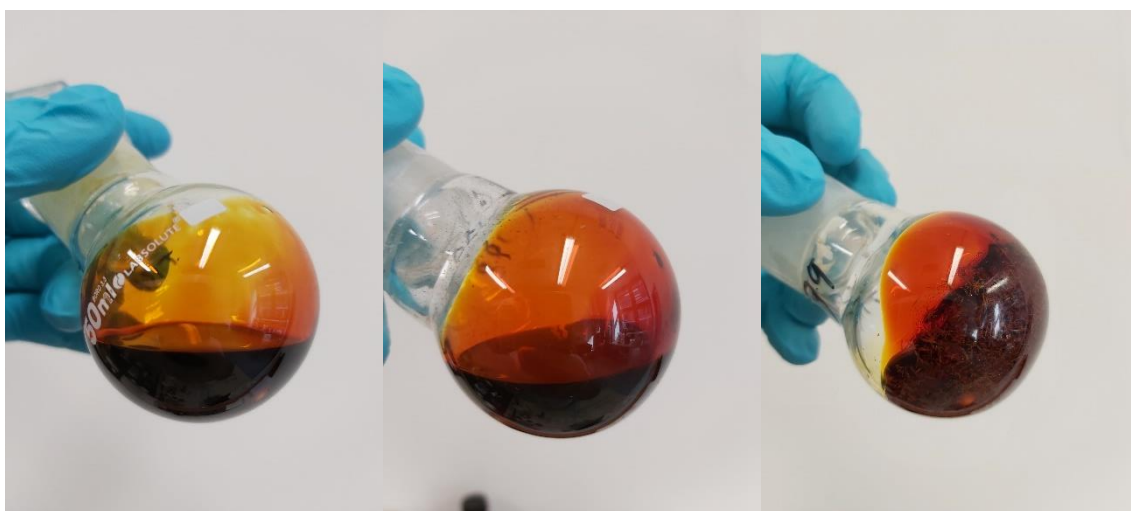


Figure 31. Reaction products with 33 wt% S (left), 41 wt% S (middle) and 50 wt% S (right) after 14 d.

The reaction product with 50 wt% S showed some precipitation of sulfur resulting in a disqualification as extreme pressure additive. The incomplete solubility of the 41 wt% product in the base stock for EP tests led also to its disqualification as potential EP additive. The reaction product of limonene and 33 wt% S was found suitable with respect to giving a single phase in the standard lube oil base. The obtained product was set aside for potential precipitation of sulfur. After three weeks, no precipitation

was observed and samples for determination of the EP properties were prepared. The elemental analysis of the crude reaction mixture showed 33.78 wt% sulfur. Based on the results from the elemental analysis, sulfur-equivalent molecular masses (g/mol S), samples with 1 mmol, 1.5 mmol and 2 mmol S/50g base stock were prepared. These were screened to determine the EP properties.

Prior to the EP investigation, the matter of compulsivity to REACH was considered. Unknown monomeric compounds result in an obligatory registration for novel chemical compounds. Therefore, further syntheses routes and properties examination of the limonene-33wt% S sample were performed. In detail, another work-up strategy was carried out, including a vacuum distillation of the crude product at 175 °C. This led to the removal of approx. 25 wt% of volatile compounds (3.6 g of distillate relative to 14.94 g of total reagent mass). ¹H-NMR of the distillate indicated p-cymene next to some not identified compounds (Figure 32).

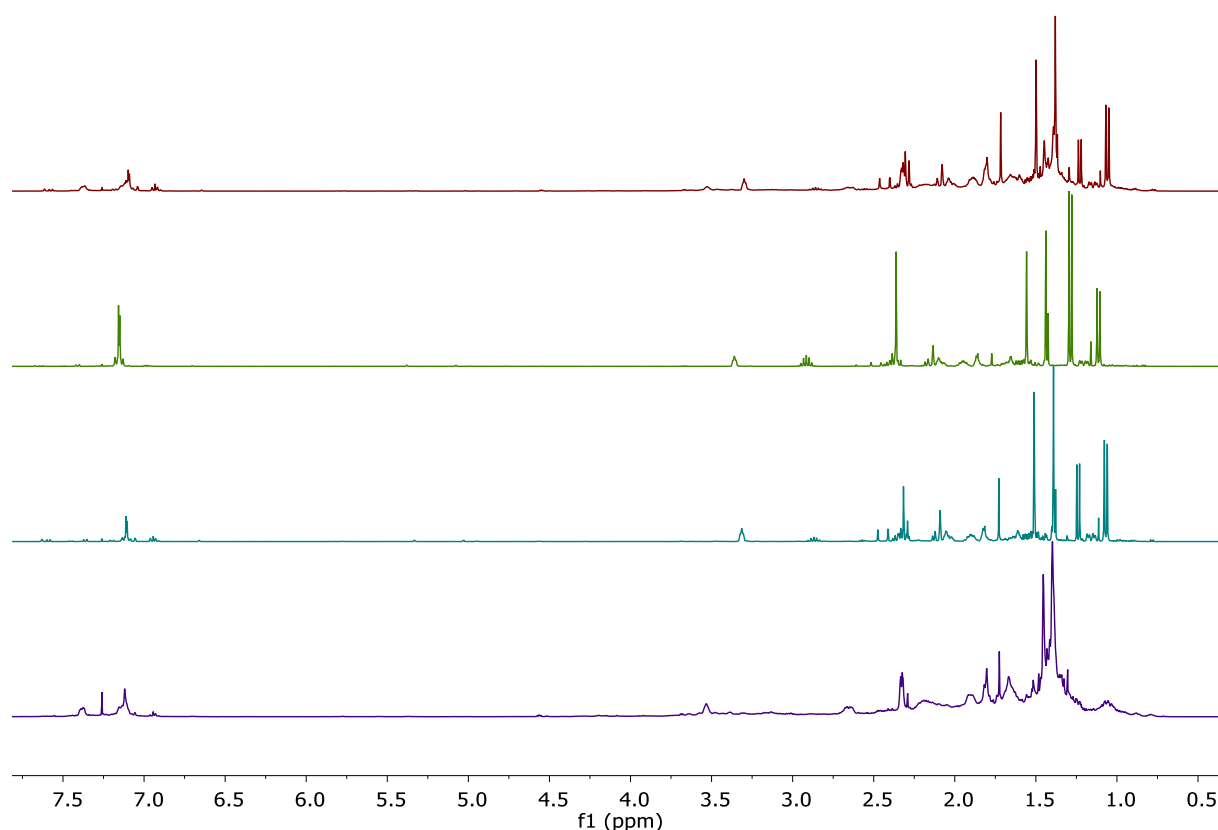


Figure 32. ¹H-NMR spectra of 33 wt% S crude product, first distillate fraction, last distillate fraction, final product in CDCl₃ (from top to bottom).

The NMR spectra show differences between the collected fractions. Most significant are the changes in the intensity of the signals at approx. 1.10 ppm, 1.20 ppm, 2.36 ppm, 2.85 ppm and in the aromatic region around 7.10 ppm. The first distillate

fraction reveals increased intensity of the signals at 1.20 ppm, 2.36 ppm, 2.85 ppm and 7.10 to 7.20 ppm, consistent with p-cymene (Figure 33).

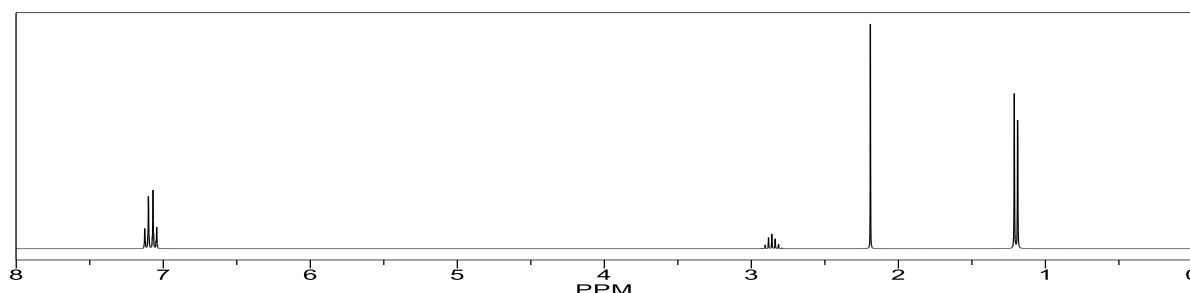


Figure 33. Simulated ^1H -NMR spectra of p-cymene using ChemDraw Professional 16.0.

Integration of the signals were in good agreement with the theoretical integrals of 6:3:1:4 for p-cymene. The last distillate fraction provides evidence for p-cymene, but in significant lower amounts. Intensified signals at 1.10 ppm and 1.50 ppm may fit to volatile sulfur containing compounds. The collected volatile samples during the distillation exhibit a strong unpleasant smell indicating volatile sulfur compounds. The obtained distillates show broad signals in the spectra, which are not original ones from after the synthesis. This finding strengthens the assumption of oligomer formation of the main product and quantitative removal of volatile compounds by distillation. The viscosity and color of the collected fractions of the distillation are in agreement with the conclusion of the removal (and/or formation) of byproducts (Figure 34). The obtained product after vacuum distillation was a dark red tacky resin with mild esthetics.



Figure 34. Crude product with 33 wt% S, first collected drops of distillate, last collected drops of distillate, obtained product after vacuum distillation (from left to right).

The raw product is a liquid, the obtained product after vacuum distillation a clear sticky resin with mild odor. The change in viscosity further strengthens the assumed formation of oligomeric polysulfides. In addition, formation of polymeric species was reported and discussed in the literature.¹³¹

The obtained resin-like product obtained after vacuum distillation was further analyzed by MALDI-MS and elemental analysis. The elemental analysis revealed 50.24 wt% carbon, 42.92 wt% sulfur and 6.64 wt% hydrogen. Based on the elemental analysis a median empirical formula of $C_{10}H_{16}S_{3.2}$ can be calculated. This finding again strengthens the assumed formation of polysulfides with an average of 3.2 sulfur atoms per limonene (C_{10} unit; Figure 35).

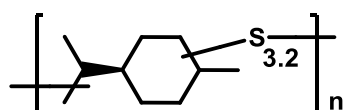


Figure 35. Repeating unit of D-limonene polysulfide.

The degree of polymerization and the molecular weight distribution was obtained from a MALDI-MS analysis using silver trifluoroacetate and 9-nitro-anthracene as matrices. The ions could not be assigned to limonene polysulfides but $(Ag_2S)_nAg^+$ salts, which is in good accordance to the literature.¹⁶¹ The detection of silver sulfide salts and the absence of limonene polysulfide related ions strongly indicate the reaction of the product accompanied by the formation of silver sulfides. The ability of polysulfides to extract metals is known.^{129,162}

The crude product as well as the resin-like product obtained after vacuum distillation were used for EP tests, and the results of their EP properties are given in chapter 5.3.10 Extreme Pressure Performance of Dialkyl Polysulfides.

Analogous to experiments with D-limonene, balsam turpentine oil was screened for the options of getting to novel EP additives. The isomeric character of the used terpenes (both $C_{10}H_{16}$; $M = 136.24$ g/mol), molecular weights and thus the weights of the reactants were the same as for experiments with limonene. The reactants were put in a round bottom flask equipped with a condenser and stirring rod, and heated to approx. 155 °C to reflux for balsam turpentine oil. Sulfur melted again at around 120 °C, resulting in a homogenous reaction liquid which turned blood red in time with increasing temperature. The reaction mixture was stirred for 6 h, after which it was cooled to ambient temperature. A blood red liquid was received as product. A detailed procedure is given in 6.10 Synthesis of Renewable Terpene Polysulfides.

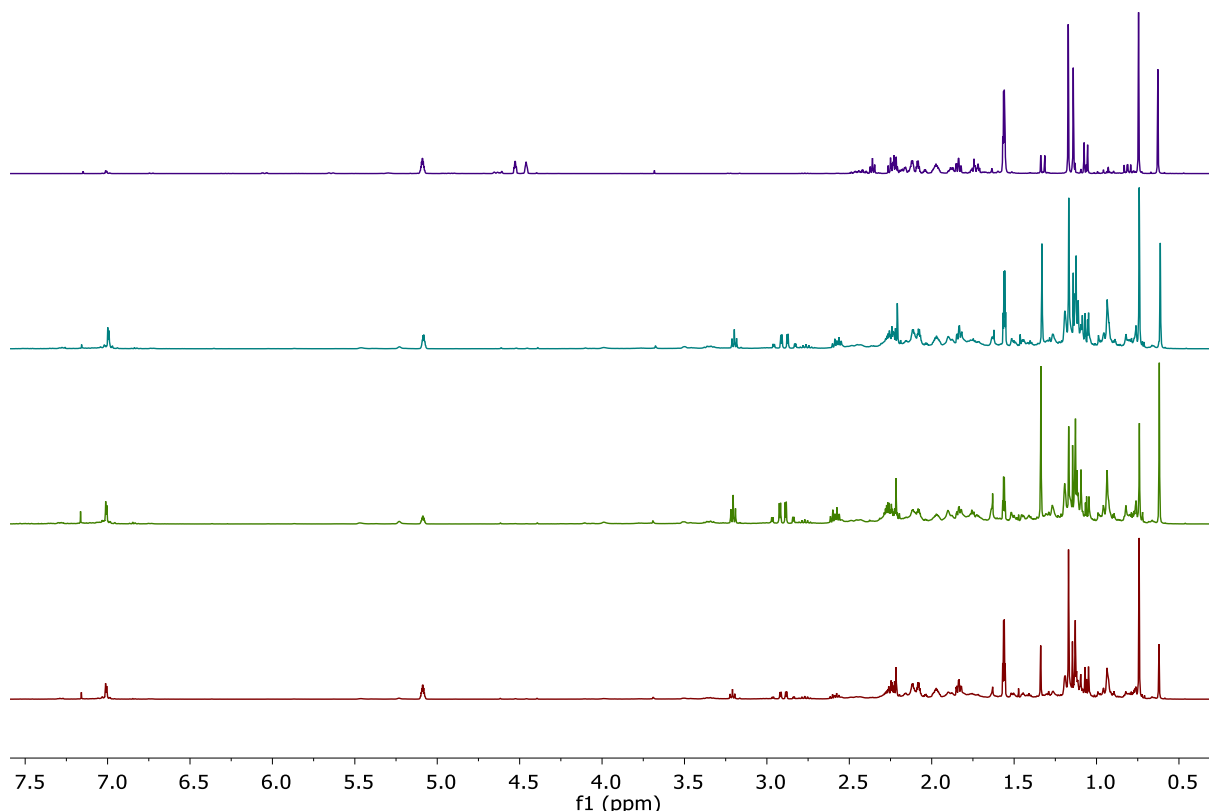


Figure 36. ^1H -NMR spectra of pure turpentine oil, 33 wt% S, 41 wt% S, 50 wt% S (from top to bottom) in CDCl_3 .

^1H NMR signals of olefinic protons in the products are found at 4.50 ppm¹⁶³ for the exocyclic proton (β -pinene) respectively 5.10 ppm¹⁶⁴ for the cyclic proton (α -pinene; Figure 36). The spectra of the crude product reveal different reactivities of the different pinene derivatives. The spectra indicate that the cyclic double bond of the alpha pinene does not react with sulfur under the reaction conditions. This unexpected finding is interesting, a complete conversion of the cyclic double bond of the limonene was found. This suggests, that the pinene reacts with sulfur along different pathways under the examined reaction conditions. The double bond is much less accessible and in contrast contains readily accessible allylic H-moieties. As a result, an electrophilic attack of sulfur at the double bond is not observed. It was found, that these products are not soluble in lube base oil. Thus, balsam turpentine oil disqualified as a renewable source for synthesis of EP additives.

5.2 Anti Wear Performance

A comprehensive set of experiments were carried out to gain insight into structure-response relationships between functional groups and lubrication performance (AW performance). The functional groups considered are shown in Figure 37. Species with varying ratios of phosphor to sulfur (e.g. dithiophosphoric acids and dithiophosphates 2 mol S/1 mol P) were tested with regard to the phosphor equivalent mass and with regard to the sulfur equivalent mass in separate formulations. This enables a direct comparison within a family of functional groups.

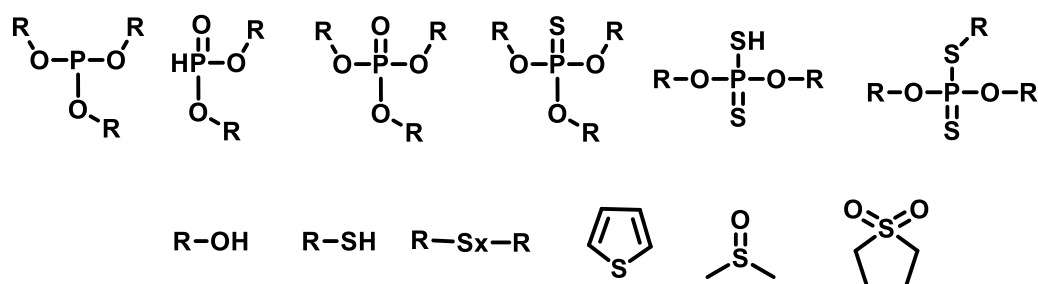


Figure 37. Examined functional groups with regard to the AW performance. From left to right, top row: phosphites, phosphonates, phosphates, thiophosphates, dithiophosphoric acid, neutralized dithiophosphates. bottom row: alcohols, mercaptans, polysulfides, thiophenes, sulfoxides, sulfolan.

5.2.1 Anti Wear Benchmark

Benchmark tests for AW performance were carried at concentrations of 0.01, 0.1, 1, 1.5 and 2 mmol substance per 50 g of base stock (Figure 38). The equivalent molar mass was calculated by $M_{eq} = \text{molar mass} / \sum \frac{\text{sulfur/phosphorous}}{\text{molecule}}$. The R group (Figure 37) in tests was a butyl moiety which is favorable for the solubility in the base stock, and allows a straight forward interpretation of the results. The wear scar diameter (WSD) again was used as a measure. The base stock Tudalen 12® with no additives as lubricant leads to a WSD of 619 μm . The use of butyl alcohol as AW additive yields no significant benefits over the base stock, indicating that indeed the butyl moiety is of little relevance to the WSD.

The remaining functional groups show increasing anti-wear performance with increasing concentration. Phosphonates, phosphites, phosphates and dithiophosphoric acids show moderate wear-reducing properties, already at concentrations of 0.01 mmol P. The WSDs range from 460 μm to 500 μm . The

thiophosphate and dithiophosphates seem to have no wear-reducing effect at this concentration. Especially the mediocre performance of neutral dithiophosphates relative to the free dithiophosphoric acid is interesting. A possible explanation could be the tentatively higher reactivity (acid-base coupled redox reaction) toward the metal surface of dithiophosphoric acid. Its action seems to have more aspects as it increases and then decreases with concentration.

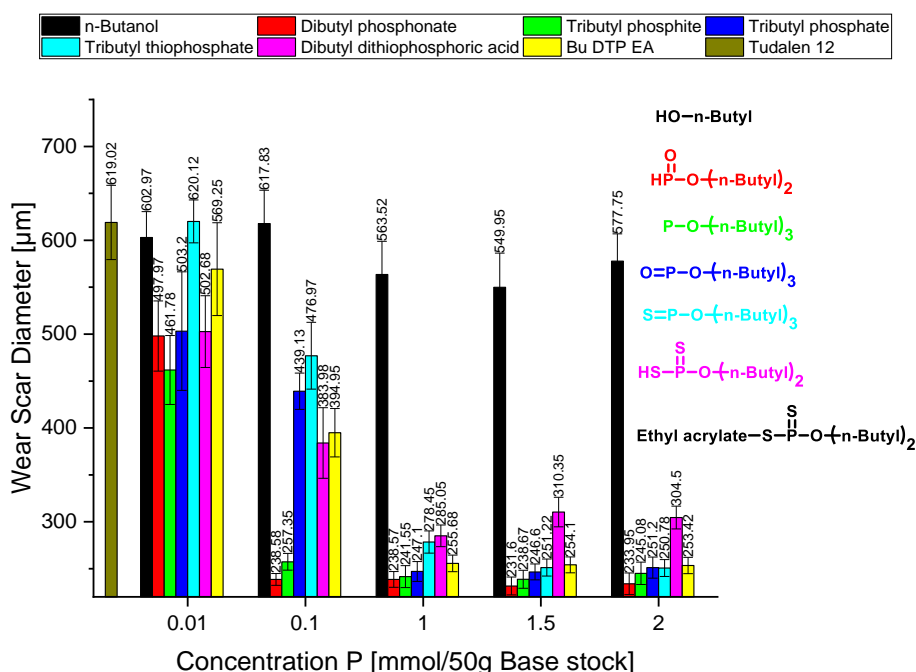


Figure 38. Wear scar diameter of the benchmark experiments. Test conditions: 150 N, 60 min 1450 rpm.

More significant differences between the examined compounds are observable at a concentration of 0.1 mmol P entities. Particularly, the phosphonate and the phosphite exhibit superior wear-reducing properties with low WSDs of approx. 240 μm and 260 μm . Higher concentrations of these phosphor containing compounds give no significant increase in wear reduction. A concentration of 0.1 mmol P seems to be sufficient in the time frame of the testing for these compounds. The dithiophosphoric acid and the dithiophosphate exhibit effective AW properties with somewhat higher WSDs between 384 μm to 394 μm at such a concentration. The phosphates respectively thiophosphates show no significant anti-wear performance for concentrations of 0.1 mmol P. The WSDs are found between 440 μm and 474 μm closer to those of the base stock of 619 μm at 0.1 mmol P.

Thiophosphates and dithiophosphoric acids are the compounds with the smallest action in the context of anti-wear. This becomes in particular obvious at higher concentrations of 1 mmol P with WSDs of 280 μm to 285 μm . The dithiophosphoric acids exhibit their best AW performance at 1 mmol P with a WSD of 285 μm and this decreases at concentrations of 1.5 and 2 mmol P yielding WSDs of 305 μm to 310 μm . Thiophosphates show their critical concentration at 1.5 mmol P with WSDs around 250 μm .

5.2.2 Anti Wear Performance of Alcohols

The benchmark substance chosen in this study for alcohols was butanol. Geraniol and oleyl alcohol as renewable alcohols were tested for anti-wear properties (Figure 39). Oleyl alcohol is unsaturated and a C_{18} fatty alcohol, geraniol has two double bonds and a branched C_{10} alkyl chain.^{165,166}

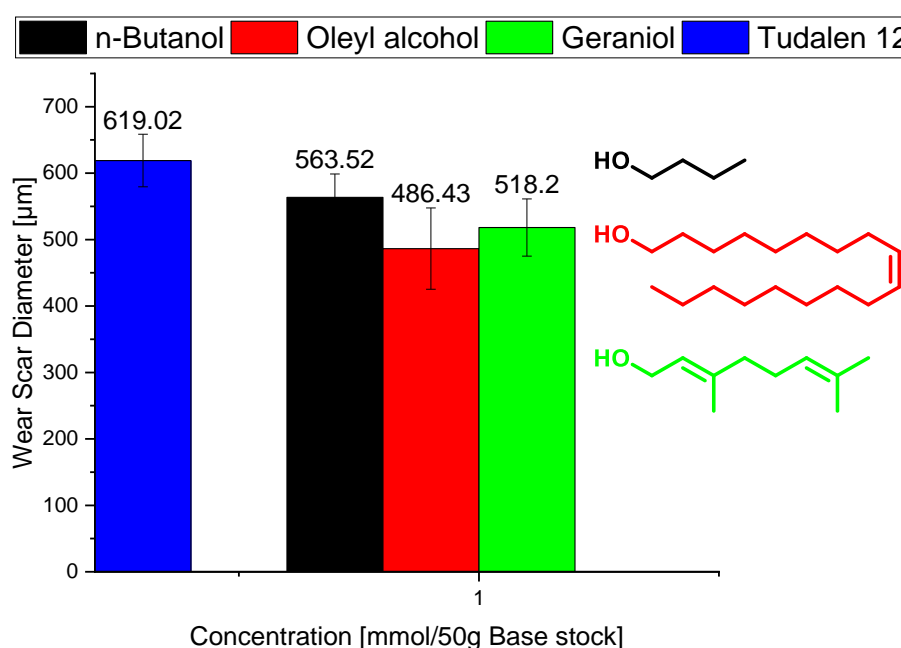


Figure 39. Wear scar diameter using different alcohols as additive. Test conditions: 150 N, 60 min 1450 rpm.

The benchmark alcohol butanol gives a WSD of 564 μm when used as a lubricant. The alcohols geraniol and oleyl alcohol show comparable WSDs with 486 μm respectively 518 μm (619 μm for the base stock). These values are within the accuracy of the method. The developed tribolayers were analyzed using EDX mapping. Oleyl alcohol was chosen as representative (Figure 40).

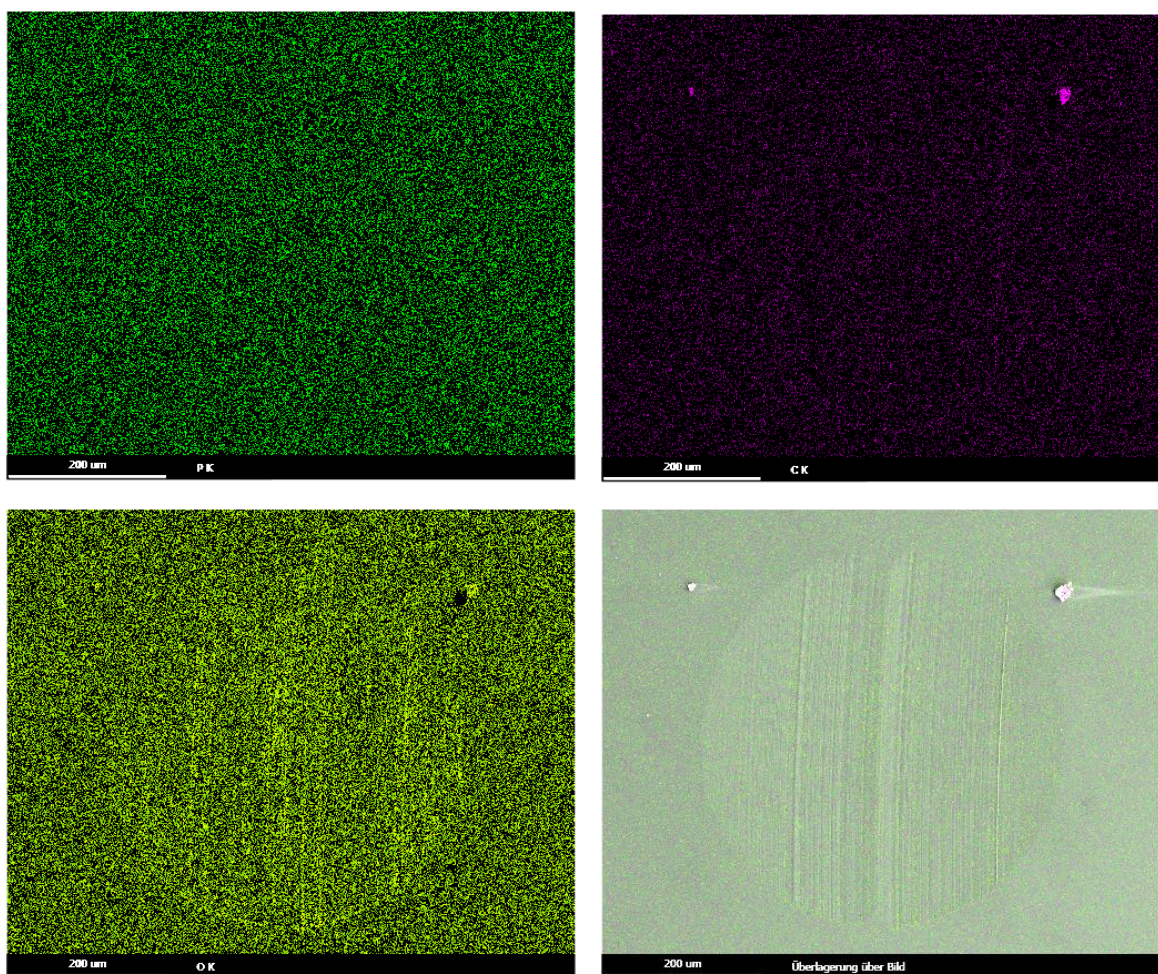


Figure 40. Top row: EDX mapping of phosphor (left) and carbon (right). Bottom row: EDX mapping of oxygen (left) and overlay of all mapped elements and the electron microscope image of the wear scar using oleyl alcohol at 1 mmol in base stock.

The EDX analysis revealed no phosphor as expected for a phosphorous free lubricant. Additionally, putative phosphorous contained in the steel alloy is beneath detection limit of the method. The carbon mapping revealed that also no substantial amount of carbon is in the surface layer, indicating that the alcohol did not react to carbides or similar entities, which are known to be very resistant to wear and friction (e.g. used as coatings for tools).¹⁶⁷ The oxygen mapping exhibits minor oxygen distributions, especially in the long scratches as can be seen in the electron microscope image with the mapped elements overlay. The EDX determined oxygen content in the depicted area adds up to 2.4 wt%, respectively 6.63 atom% with an error of about 10 % with regard to the measured value. It is assumed that the oxygen in the tribolayer is coming from the oil and not from the alcohol. Alcohols thus show no significant wear reducing properties at the examined concentration and further experiments were not carried out. The EDX analysis revealed some formation on tribolayers.

5.2.3 Anti Wear Performance of Mercaptanes

The screening of the alcohols as additives in base stock in lubrication test showed no wear reducing properties. Next sulfur containing compounds in form of mercaptanes (octyl mercaptane, dodecyl mercaptane and dipentene dithiol), sulfoxides (DMSO), sulfones (sulfolane) and a cyclic thioether (dibenzothiophene) were considered as additives (Figure 41).

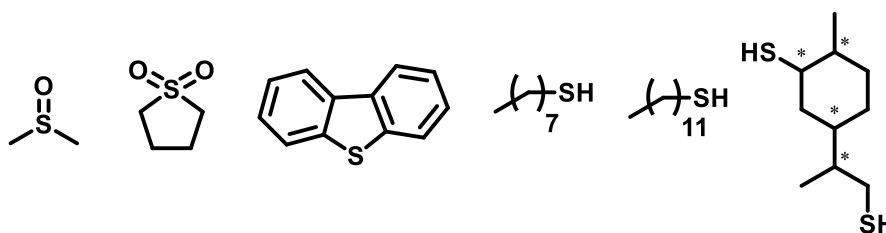


Figure 41. Examined mercaptans and related compounds. From left to right: DMSO, sulfolane, dibenzothiophene, octyl mercaptane, dodecyl mercaptane and dipentene dithiol.

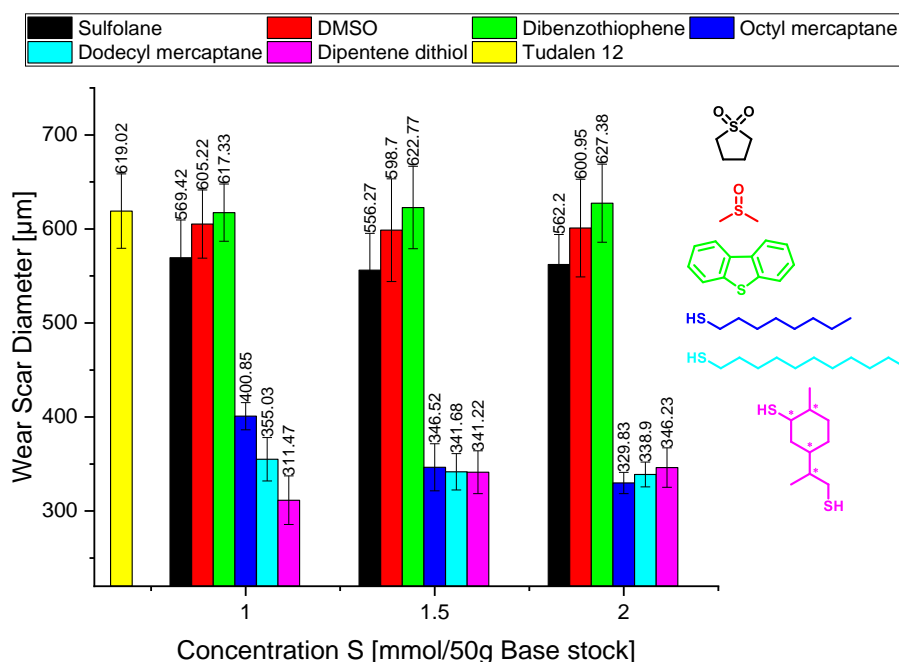


Figure 42. Wear scar diameter of different mercaptanes and related compounds. Test conditions: 150 N, 60 min 1450 rpm.

The AW performance of the various sulfur containing derivatives in concentrations of 1, 1.5 and 2 mmol S per 50 g base stock is observable (Figure 42) as far as these are having an S-H moiety. These results show, that sulfur compounds without an S-H bond as in sulfoxides (DMSO), sulfones (sulfolane) or thioethers exhibit a low wear protection. The WSDs range from 550 μm to 627 μm , not substantially different from

that of the base stock. A possible explanation for this observation is in the chemical property of those sulfur atoms. These are much less reactive and in part will not even be able to coordinate directly to the metal-surface. The tribofragmentation might require more severe conditions.

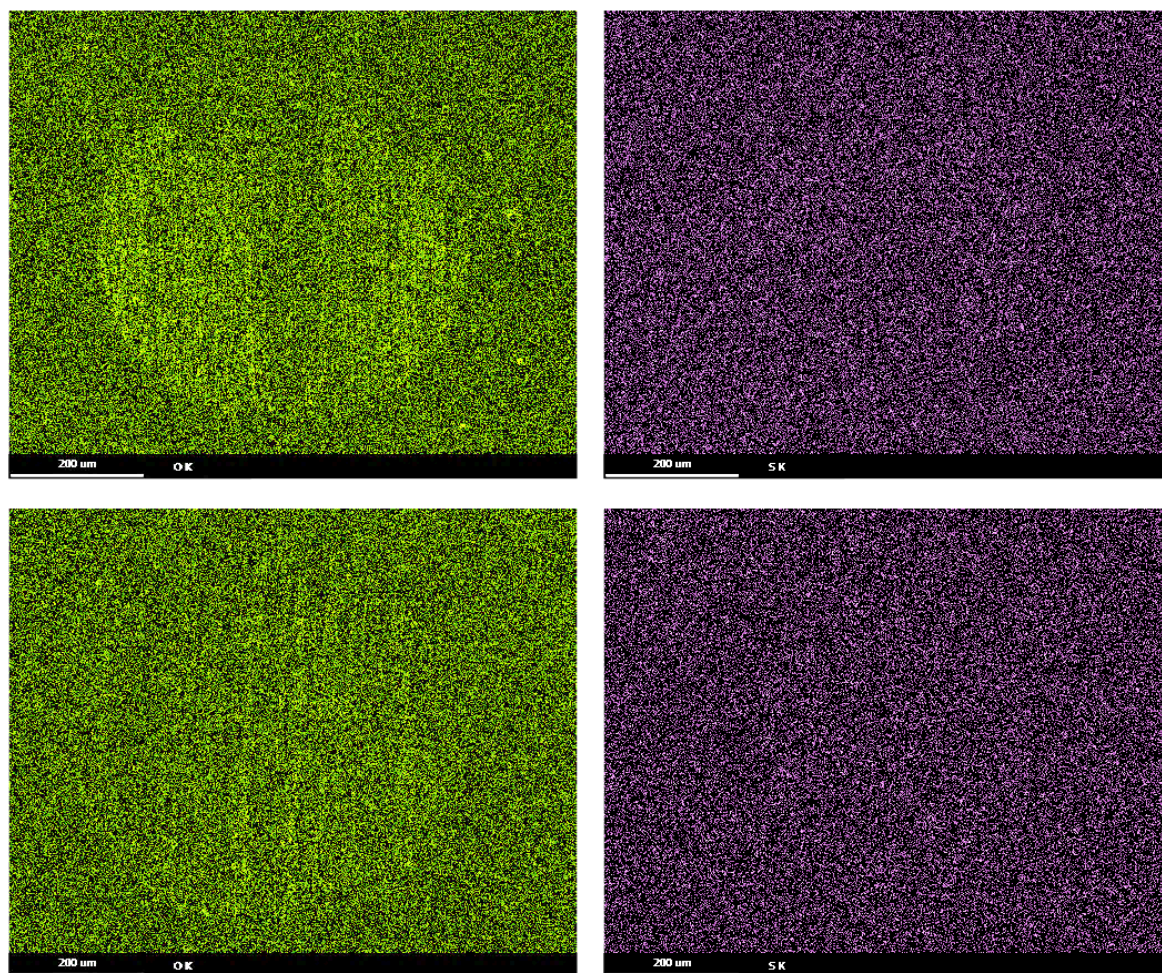


Figure 43. EDX mapping of oxygen (left column) and sulfur (right column) from the wear scars yielded from the 2 mmol experiments of DMSO (top row) and dibenzothiophene (bottom row).

EDX mapping of the wear scar surfaces from sulfoxide species (DMSO, also representative for sulfolane) and thioethers (dibenzothiophene) gave no evidence for the formation of sulfur species on the surface (Figure 43). The oxygen mapping (green) shows a slight increase within the tribolayer of the wear scar (vertical lines). This was also observed for the neat base stock. It can be assumed, that these low amounts of oxygen derive from dissolved oxygen in the oil.

The AW properties of the examined mercaptanes show a moderate wear reduction. This is consistent throughout the examined concentration range. The experiments with 1 mmol S per 50 g base stock yield WSDs of 400 μm for the C₈-mercaptane, 355 μm

for the C₁₂-mercaptane and 311 μm for the dipentene dithiol. It is remarkable that within the 1 mmol experiments longer alkyl chains decrease wear better (C₈ vs C₁₂). This possibly related to the vapor pressure. Dipentene dithiol gives best AW properties. A possible explanation could be the ability of coordination to the metal surface. Increasing the concentrations to 1.5 and 2 mmol sulfur give no further decrease in the WSDs; values ranging from 330 μm to 346 μm and the difference between the additives disappears.

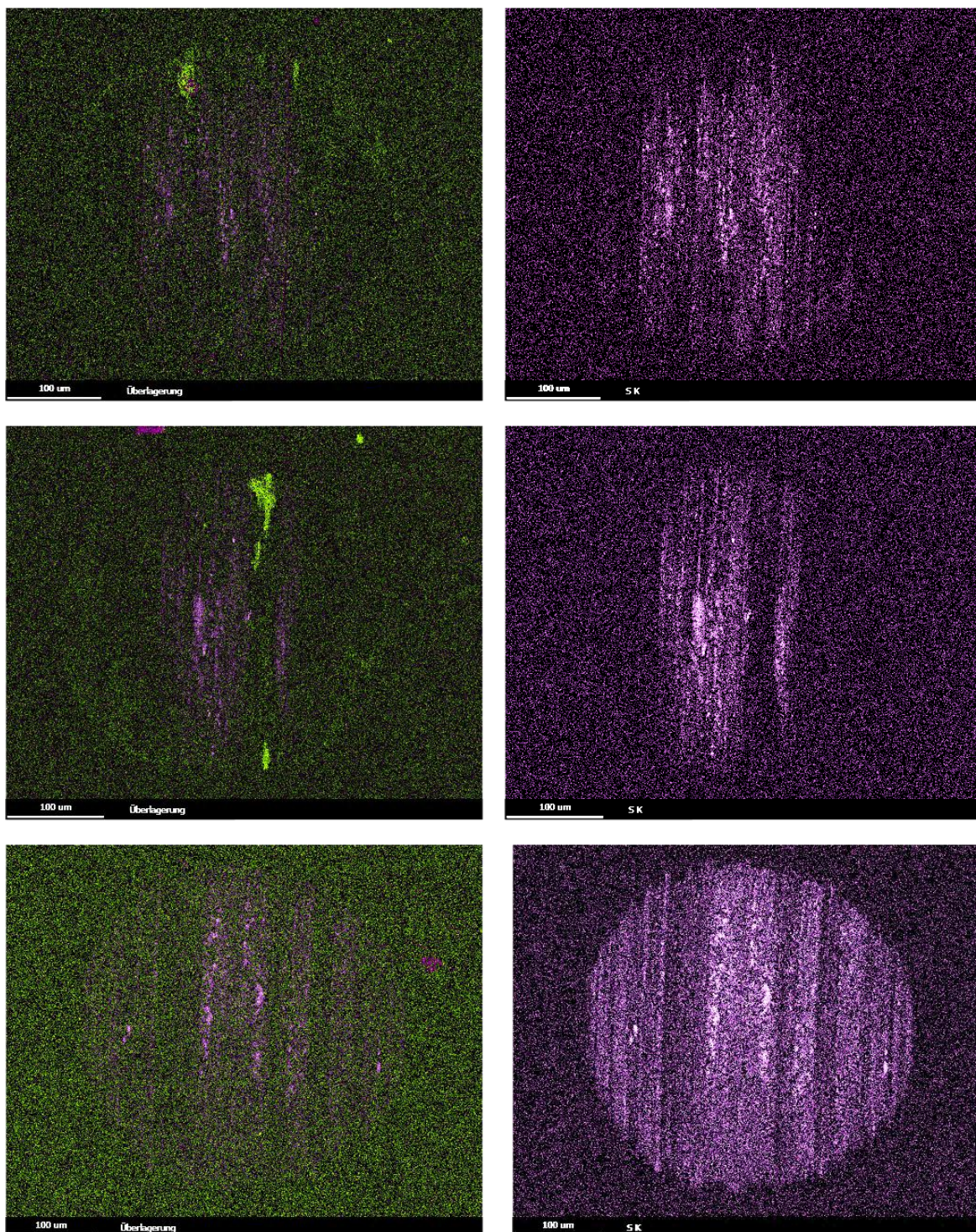


Figure 44. EDX mapping of 2 mmol experiments of octyl mercaptane, dodecyl mercaptane and dipentene dithiol (from top to bottom). From left to right: top row: octyl mercaptane oxygen and sulfur, exclusive sulfur. middle row: dodecyl mercaptane oxygen and sulfur, exclusive sulfur bottom row: dipentene dithiol oxygen and sulfur, exclusive sulfur.

The EDX mapping of the wear scars from using mercaptanes as additives reveal sulfur in the tribolayers (Figure 44). The sulfur traces are in linear formation in the center of the scar in case of the C₈- and C₁₂-mercaptanes. The geometry of the four-ball system

gives this region of highest pressure. The mercaptanes could decompose under such circumstances and the favorable formation of a tribolayer results.

The situation for dipentene dithiol is comparable, except that the sulfur mapping shows equal distribution of sulfur within the wear scar. A possible explanation for this observation could be that the decomposition of dipentene dithiol requires lesser pressure. The formation of sulfur-containing tribolayers occurs then throughout the wear scar. Furthermore, the coordination to the surface might be stronger due to the presence of two sulfur atoms per molecule.

Another possible explanation for the different reactivity of sulfoxides, sulfolane, thioethers and mercaptanes could be the bonding enthalpy. Sulfur-oxygen double bonds, as can be found in DMSO and sulfolane, exhibit bonding enthalpies of 420 kJ/mol. Sulfur-carbon single bonds, as in dibenzothiophene have bonding enthalpies of 296 kJ/mol, the expulsion of S requiring twice that energy. The aromatic structure of dibenzothiophene increases the bonding enthalpy, so that the real value is higher. Mercaptanes have S-C bonding enthalpies of 361 kJ/mol, making a reaction at the surface more likely.¹⁶⁸ The relative bonding enthalpies as well as the coordinative bonding energies from the spectrochemical series support the thesis that mercaptanes can interact with the metal surface.^{168,169}

Mercaptanes build up tribolayers and thus reduce wear. The limonene dithiol exhibits the highest sulfur content in the wear scar, the linear derivatives lead to less sulfur on the surface (Figure 45). These findings are in agreement with the observed wear reduction. Sulfoxides, sulfolanes and thioethers respectively dibenzothiophenes are not capable of significant wear reduction under the examined conditions. The experiments carried out with regard to EP properties of these compounds are in chapter 5.3 Extreme Pressure Performance.

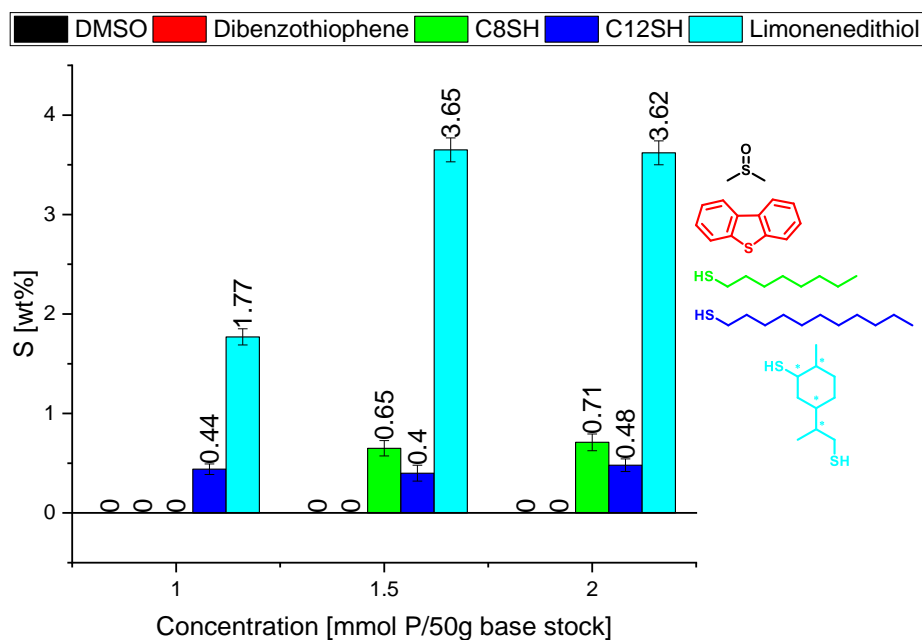


Figure 45. Weight fractions of sulfur detected in the wear scar.

5.2.4 Anti-Wear Performance of Phosphites

Various phosphor species were tested with the aim to reach a comprehensive overview of AW performance, and also with the objective to build an understanding of the underlying processes. The WSDs of the examined oxo-phosphites indicate wear reduction over the base stock, which is in agreement to literature reports (Figure 46).⁶⁹ The WSDs of the oxo-phosphites exhibit values of 233 μm to 246 μm within the concentration range of 1 to 2 mmol. These values are close to the theoretical minimum of 220 μm for the conditions. These values depict the resolution limit of the four-ball apparatus. Trends between structure and lubrication action are not observable.

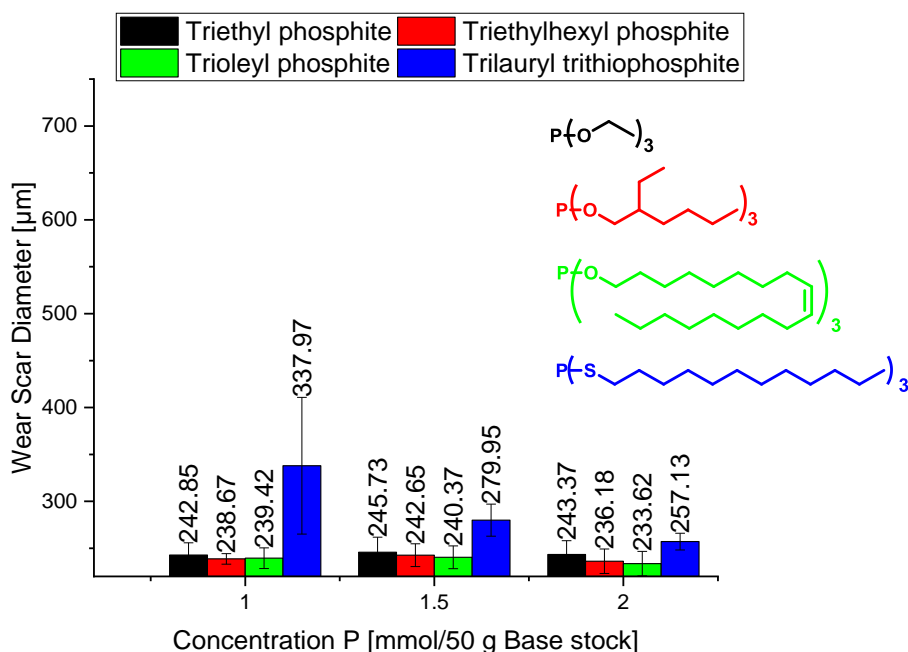


Figure 46. Wear scar diameter of different phosphites. Test conditions: 150 N, 60 min 1450 rpm.

Trithiophosphites exhibit significant wear reduction only at higher concentrations. Experiments with the trilauryl trithiophosphate revealed WSD of 338 μm at 1 mmol down to 257 μm at 2 mmol. Wear in the presence of trioleyl phosphite leads to a tribolayer with oxygen and phosphor atoms (Figure 47). The amounts of oxygen and phosphor in the tribolayer are lower than observed with additivation with oxo-phosphites (Figure 48).

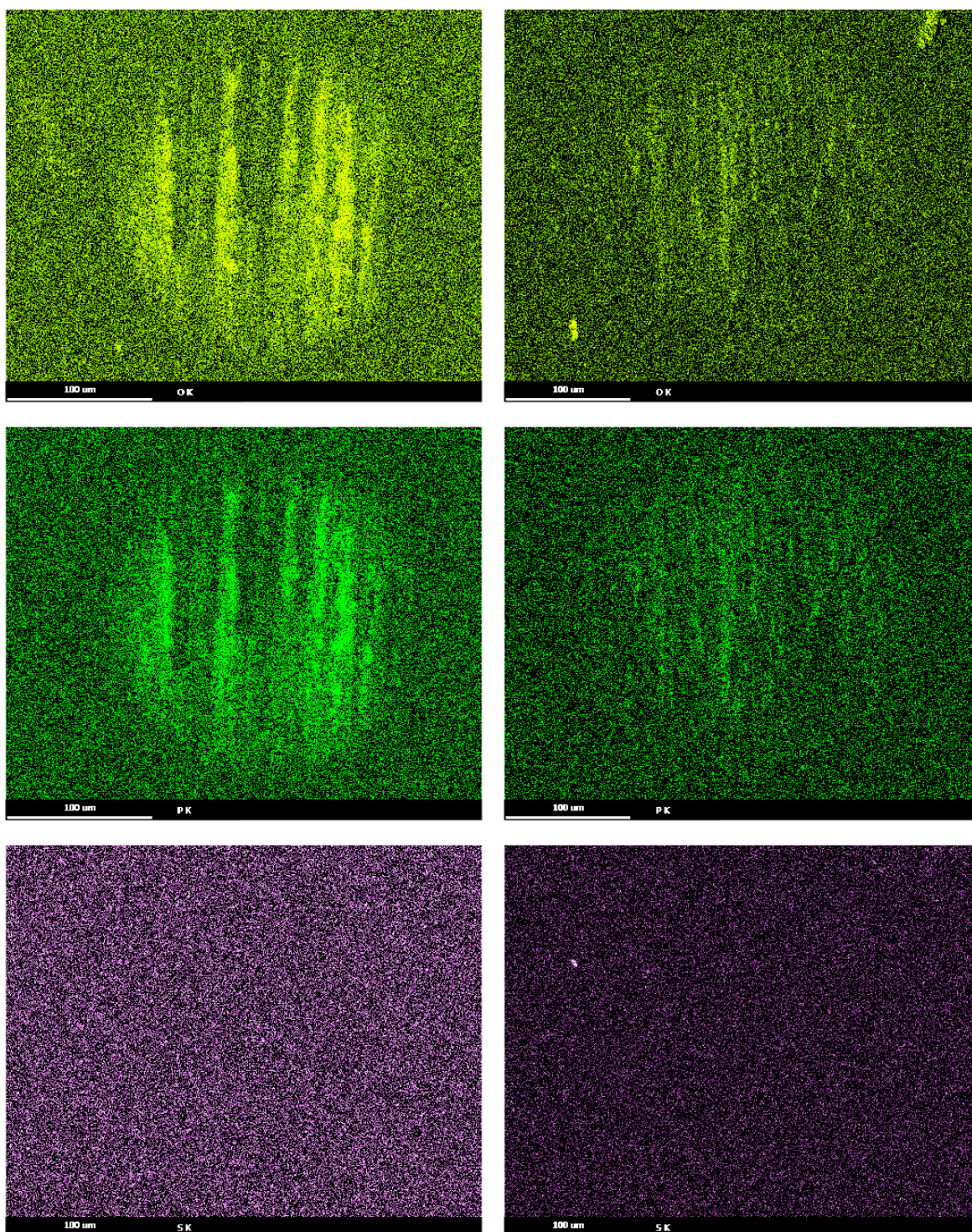


Figure 47. EDX mapping of oxygen (top row), phosphor (middle row) and sulfur (bottom row) for 2 mmol P trioctyl phosphite (left column) and 2 mmol trilauryl trithiophosphite (right column).

Sulfur could not be detected in the tribolayer when using trithiophosphites, just as is found for the oxo-phosphite additive, despite the three sulfur atoms per molecule and detectable phosphor atoms in the tribolayer. The question arise why no sulfur is found. A possible explanation could be, that the activation energy for the formation of sulfur containing tribolayer is not sufficient at the examined conditions. Alternatively, sulfur

could serve as a carrier for the phosphor, which is then integrated into the tribolayer. Sulfur would react to soluble compounds like disulfides or mercaptanes that remain in the base stock oil. Longer times of observation would be necessary to gain further insights.

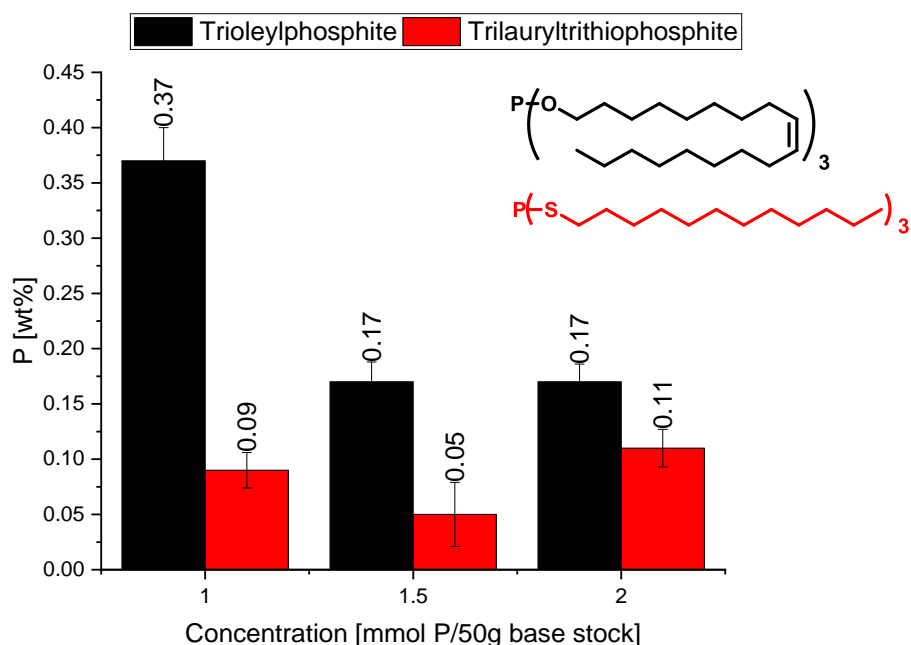


Figure 48. Phosphor content in the wear scars.

The phosphor content of the tribolayer overall ranges from 0.37 wt% at 1 mmol to 0.17 wt% at higher concentrations. The phosphor content when using the trithio-phosphite additivation is much lower with values ranging from 0.09 wt% to 0.11 wt%. In contrast, the trioleyl phosphite yields higher amounts of phosphor in the wear scar which is in good agreement with the concentration dependent wear reduction. This is remarkable, because the superior performance of the oxo-phosphites can be weakened by the exchange of the oxygen (POR_3) by sulfur (PSR_3). These experiments give reason that sulfur may be substituted in AW additives, which is interesting with regard to esthetic appearance. Experiments to illuminate the EP properties are shown in 5.3 Extreme Pressure Performance.

5.2.5 Anti Wear Performance of Phosphates

Phosphates are the corresponding P(V) equivalents of the phosphites. The good AW properties of phosphites led to the idea of evaluating their lubrication properties too.

Figure 49 shows the WSDs after using triethyl phosphate, triethylhexyl phosphate, tributyl phosphate and triphenyl phosphate as additivation for the base stock. Their WSDs range from 239 μm to 269 μm shows that phosphates are excellent AW additives. No concentration related trend with regard to the WSD is observed. This implies that 1 mmol added substance already leads to an effective tribolayer. The compounds have about the same AW properties (differences are within the experimental error).

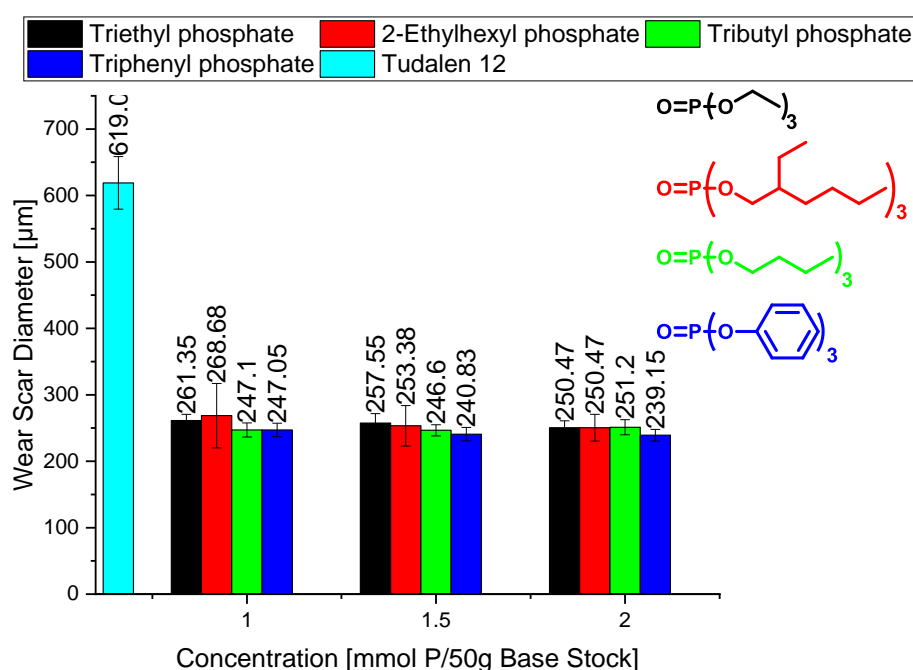


Figure 49. Wear scar diameter of different phosphates. Test conditions: 150 N, 60 min, 1450 rpm.

The phosphates are less effective than the corresponding phosphites at equal concentrations. This observation may underlie the fact that the $(\text{RO})_3\text{P}=\text{O}$ have weaker coordination abilities. Furthermore, the reducing properties of phosphites can enhance the formation of tribolayers by reacting with the oxidized passive layer of the metal. The examination of triphenyl phosphate as an aromatic example revealed, that aromatic esters do not exhibit any advantage over alkyl esters with regard to the WSD. This is interesting concerning ecofriendly and toxicologically acceptable additives.

EDX analysis of the wear scar revealed oxygen and phosphor as major components in the wear scars (Figure 50). This result parallels those from experiments with phosphites. The weight fractions of phosphor in the wear scar determined by EDX were around 0.10 wt%. This is significantly lower than that with phosphites (0.17 wt% for

2mmol) additivation. It is congruent to the lower wear reduction of phosphate additivations. These findings support a mechanism of tribolayer formation by reduction of the passive layer followed by incorporation of phosphor atom from decomposition of the additives.¹⁰²

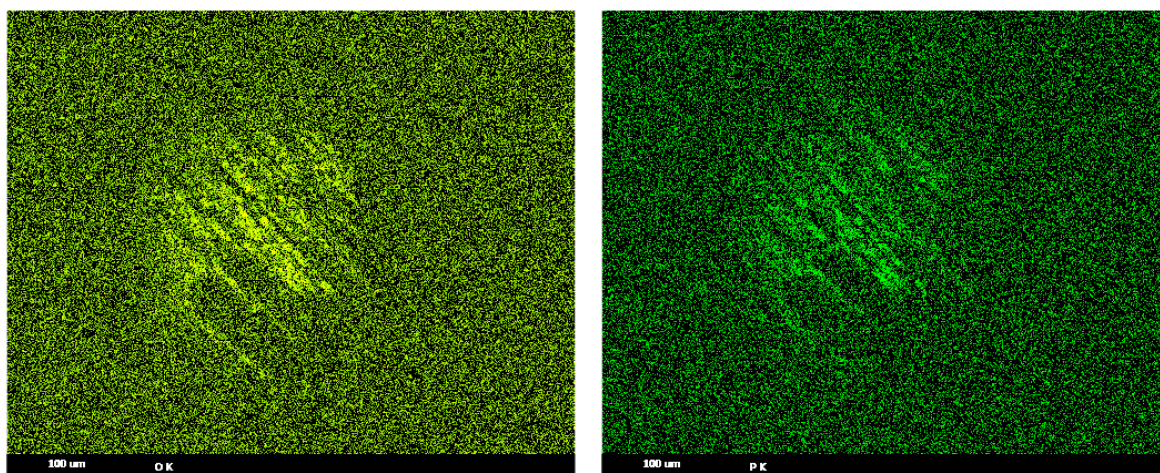


Figure 50. EDX analysis of wear scars derived from the 2 mmol triethyl phosphate experiment of oxygen (left) and phosphor (right).

5.2.6 Anti Wear Performance of Thiophosphates

Replacing the oxygen in phosphates by sulfur leads to thiophosphates, a ubiquitous class of additives in industrial and commercial lubricant formulations.^{90,141,142} Prominent derivatives are triphenyl phosphorothionate (TPPT) and tertiary butylated phenol thiophosphates (TPPT+).^{170–172} The indicated severe health issues of these compounds are given in 2.2 Types of Additives. Lubricant additives that are ecologically and toxicologically acceptable may be thiophosphates from renewable natural vanillin and oleyl alcohol. The poor solubility of vanillin thiophosphate was a KO criterium, thus only results of oleyl- and butyl thiophosphate are given (Figure 51).

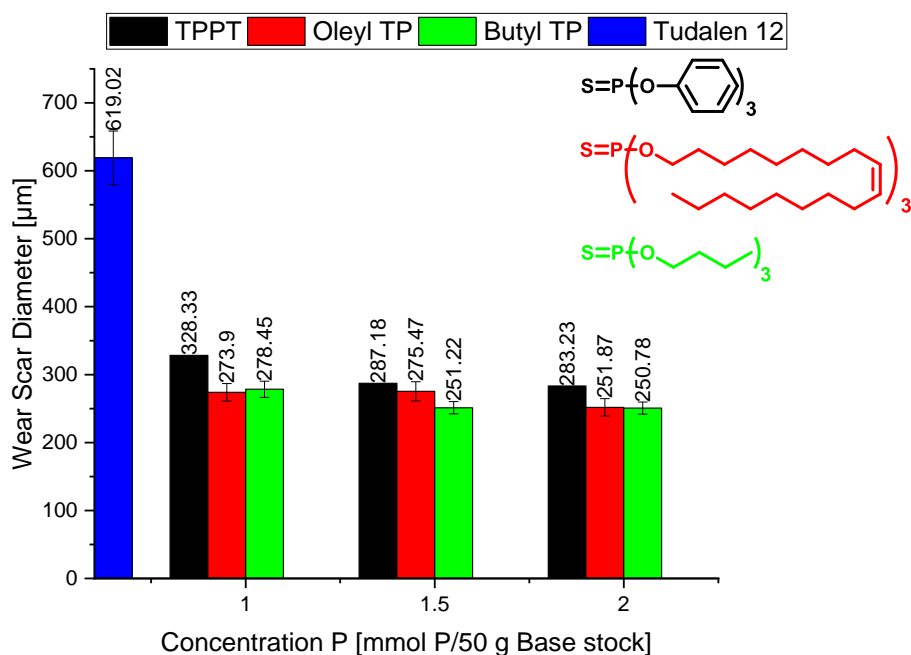


Figure 51. Wear scar diameter of thiophosphates. Test condition: 150 N, 60 min, 1450 rpm.

All thiophosphates exhibit significant wear reduction with regard to the base stock. TPPT shows WSDs ranging from 328 μm at 1 mmol over 287 μm at 1.5 mmol to 283 μm at 2 mmol. The required minimum concentration can be determined around 1.5 mmol to yield best AW performance. The thiophosphates derived from oleyl and butyl alcohol yield equal AW properties (within the error of the method). The WSDs range from 273 μm to 278 μm at 1 mmol, over 251 μm to 275 μm at 1.5 mmol to 251 μm to 268 μm at 2 mmol. The slight decrease of the WSD from 1 mmol to 1.5 mmol gives the required minimum concentration between 1 and 1.5 mmol for best AW performance. Oleyl thiophosphate seems to be an attractive substitute to TPPT with regard to the AW performance, the ecological sourcing of the alcohol¹⁶⁵ as well as its estimated toxicologically acceptable profile. Thus, the synthesis and characterization of bio related thiophosphates as alternatives for TPPT and TPPT+ was successful.

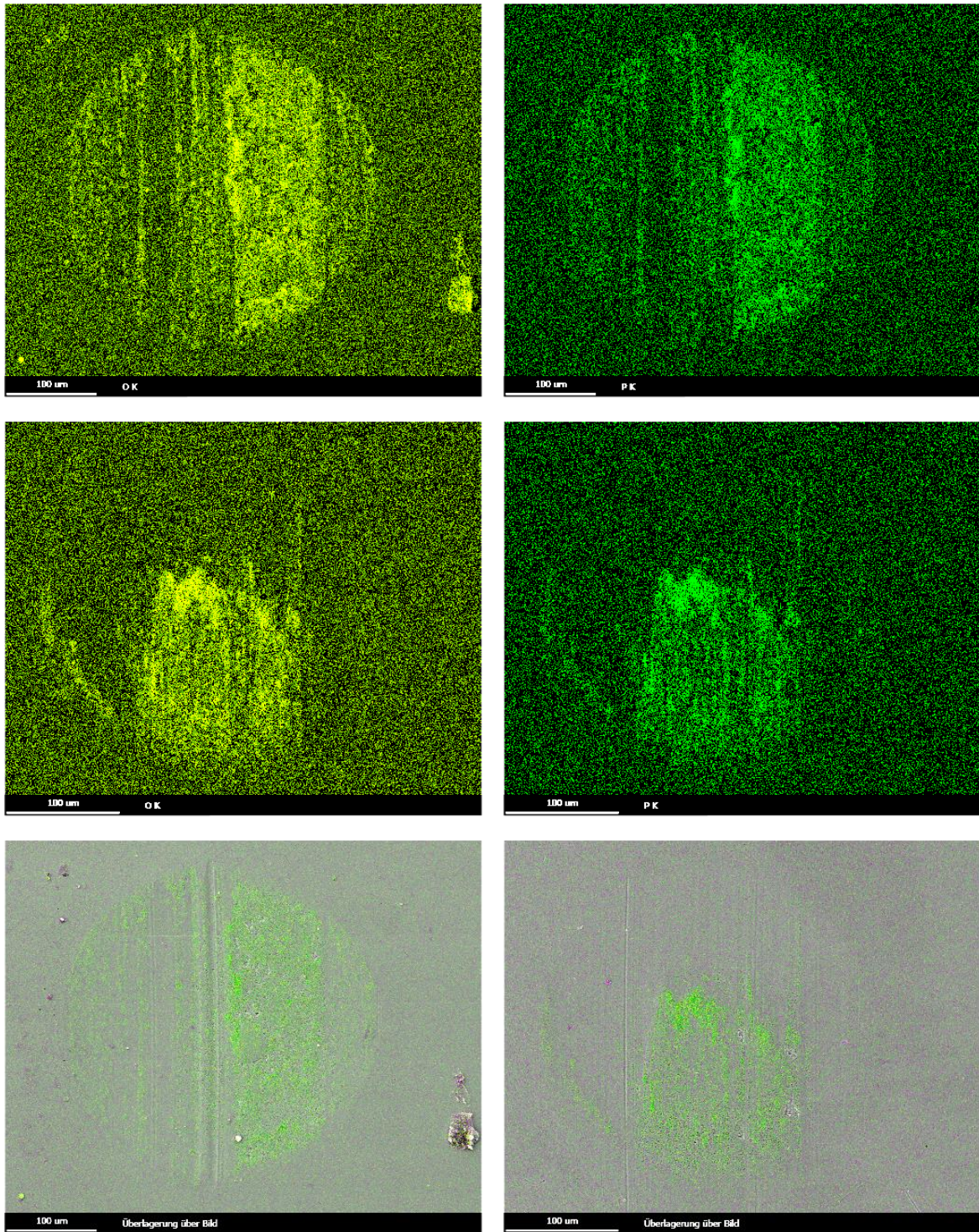


Figure 52. EDX analysis of oxygen (left column) and phosphorus (right column) of the wear scars yielded from the 1 mmol experiments of TPPT (top row) and oleyl thiophosphate (middle row). Bottom row depicts the overlay of oxygen, phosphorus, sulfur and the electron microscope image of the wear scars of TPPT (left) and oleyl thiophosphate (right).

The EDX analysis of the balls revealed the presence of phosphor and oxygen in the tribolayer obtained using TPPT and oleyl thiophosphate as additives (Figure 52). No significant differences in the EDX image of the wear scars can be observed.

The buildup of a tribolayer and thus the effective inhibition of wear may possibly be related to the activation energy for reaction between the AW additive and the metal surface. TPPT contains stable aromatic residues, which may not react as fast as alkyl derived units such as in oleyl thiophosphate thus leading to a slightly larger WSD. On top, coordination of additives to metal surfaces is faster and potentially stronger for flexible alkyl chains. Long alkyl chains may also act as a local thickener of the base stock. A higher viscosity involves longer contact times and the fluid layer more effectively separates the metal balls.

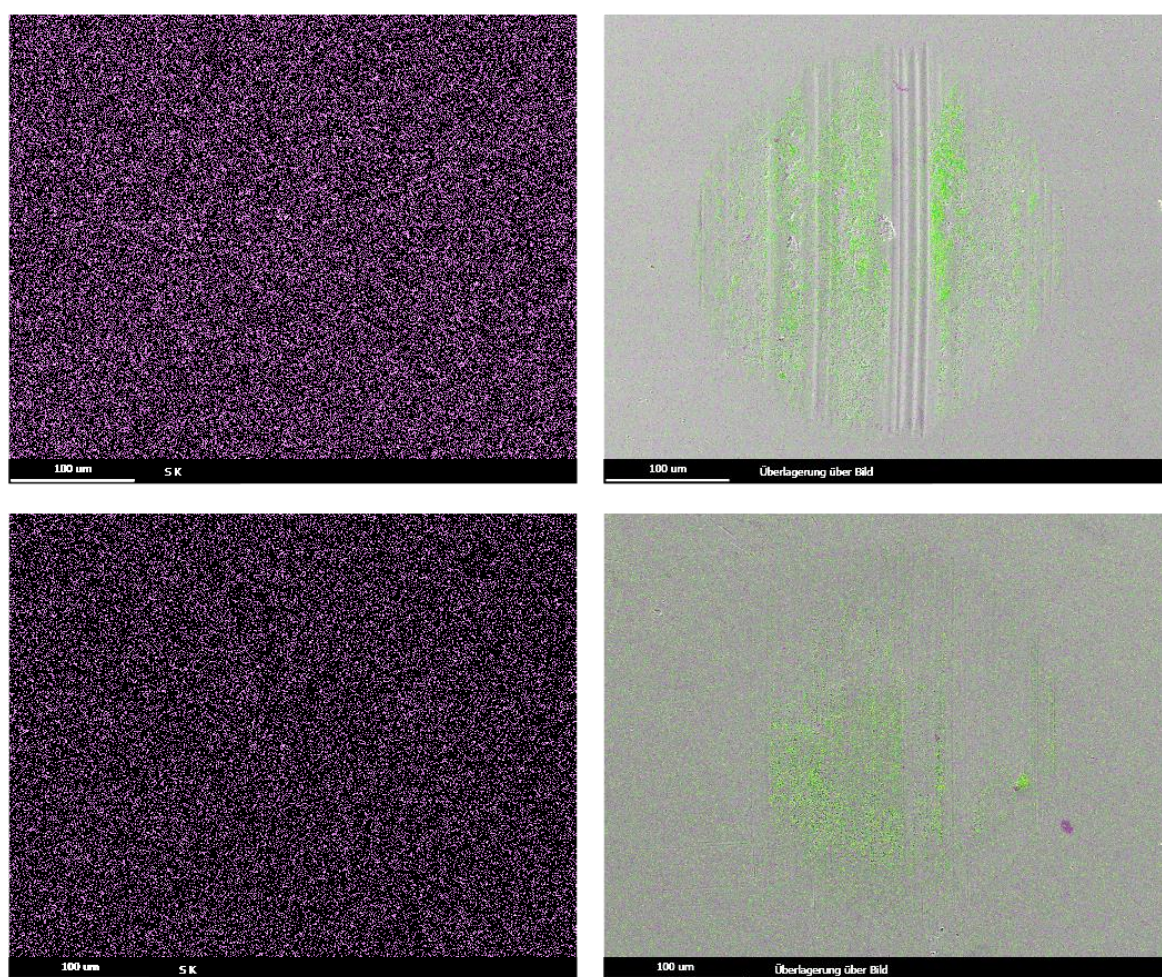


Figure 53. EDX mapping of sulfur (left column) and overlay of oxygen (yellow) and phosphor (green) on the electron microscope picture of the wear scar (right column) for wear scars yielded at 1.5 mmol for TPPT (top row) and oleyl thiophosphate (bottom row).

The EDX mapping for sulfur of tribolayers from experiments at 1.5 mmol addition gives no evidence for sulfur, like in the experiment with 1 mmol, oxygen and phosphorus are the dominant elements of the tribolayer (Figure 53). A presumption that the oleyl derivative provides sulfur for the tribolayer and therefore exhibited a significantly lower WSD than TPPT would be wrong. The similar WSDs of 287 μm for TPPT and 276 μm (i.e. within the sensitivity of the four-ball apparatus) at the 1.5 mmol loading, supports the assumption of different rates of surface functionalization.

5.2.7 Anti Wear Performance of Dithiophosphates

Dithiophosphates are also ubiquitous in AW additives.^{90,141,142} Substitutes for ashless derivatives like the commercially available Irgalube 63®¹⁷³ are focused in this thesis (cf. 2.2 Types of Additives & 2.5 Mechanism of Action).

Irgalube 63 ® is prepared by reaction of diisopropyl dithiophosphoric acid with ethyl acrylate.^{74,75} This product yields moderate AW action but has a rather unpleasant smell. Residual ethyl acrylate can cause severe irritations of the respiratory system.¹⁷⁴ Therefore, novel dithiophosphate based additives are synthesized and characterized with regard to their odor and their AW properties. Three acrylates, phenoxyethyl acrylate (POEA), ethylhexyl acrylate (EHA) and hexanediol diacrylate (HDDA) were reacted with dithiophosphoric acid in order to prepare the analogous dithiophosphoric acids.

The 2:1 ratio of sulfur to phosphorus in dithiophosphate derivatives gives the same ratio of sulfur and phosphorus contents in formulations with the base stock. Therefore, AW experiments with a sulfur content (concentration S given in mmol/50g base stock) and a phosphorus content (concentration P given in mmol/50g base stock) were performed (Figure 54).

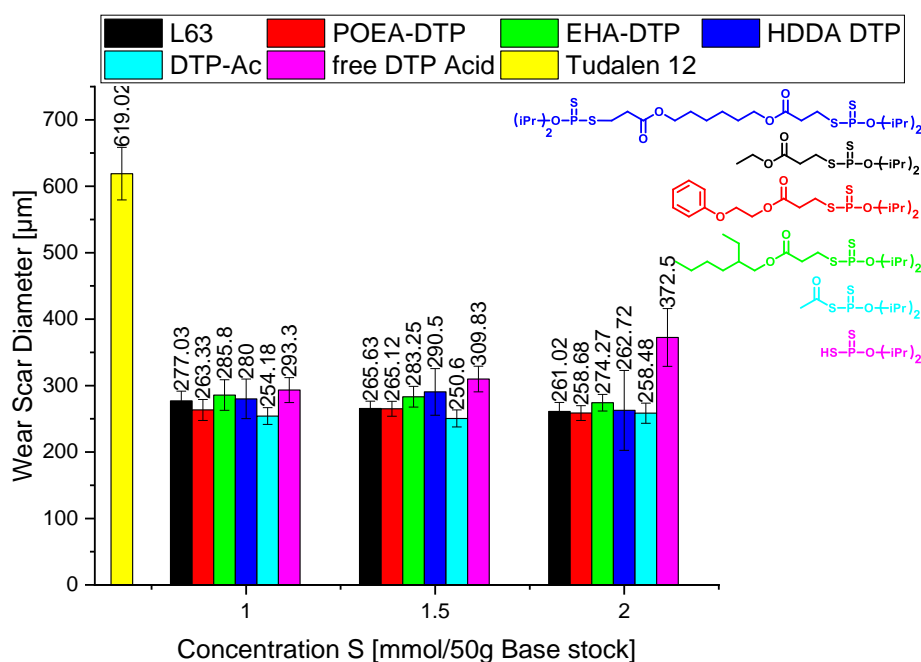


Figure 54. Wear scar diameter of DTP derivatives. Test conditions: 150 N, 60 min, 1450 rpm.

The wear reduction of base stock with free dithiophosphoric acid is significant. Unexpectedly, the WSDs is larger at higher starting concentrations. The WSDs exhibit 293 μm at 1 mmol to 310 μm at 1.5 mmol, climaxing to 373 μm at 2 mmol. The VKA experiments with free dithiophosphoric acid additive led to a deep green color of the used oil. The color is stronger at higher concentration of the additive. A complexation reaction of iron and chromium atoms or ions to dithiophosphoric acid can be assumed to be the cause.^{175–177} The color intensity correlates positively with the wear. This ongoing reaction of iron and chromium may underly in the higher wear.

The higher wear at higher additive concentration of the free DTP and the assumed ability to develop slightly shearable tribolayers possibly makes the free dithiophosphoric acid a promising extreme pressure additive. While AW additives need to build up robust and friction reducing tribolayers, EP additives need to separate the contact surfaces to inhibit friction welding of metal. Thus, a continuous solvation and reformation of tribolayers by free acid could describe the effective mechanism.

Alkyl derivatives are more effective AW additives than the free acid, especially at higher concentrations. The AW properties of neutral dithiophosphates possess no concentration dependence within the examined concentration range. The tested dithiophosphates exhibit WSDs of 263 μm to 285 μm at 1 mmol, 265 μm to 290 μm at 1.5 mmol and 261 μm to 263 μm at 2 mmol. The acetylated dithiophosphoric acid

shows WSDs of 254 μm , 251 μm and 259 μm at 1, 1.5 respectively 2 mmol. The acetylated dithiophosphoric acid have a slightly better AW performance at lower concentrations than acrylate derived dithiophosphates. The AW performance of dithiophosphates converges to a similar range around 260 μm . These experiments show that acrylate entities can be varied without loss of AW performance, which is in agreement with earlier studies on dithiophosphates.⁷⁶ The objective of finding alternatives to Irgalube 63 ® with comparable performance with regard to the toxicological profile was successful. It could be shown, that the Michael reaction of the dithiophosphoric acid with various acrylates (thereunder a diacrylate) leads to products with acceptable AW properties.

EDX analyses of wear scars for a better understanding of the AW action as function of the different functional groups were performed for oxygen, phosphor and sulfur (Figure 55 & Figure 56).

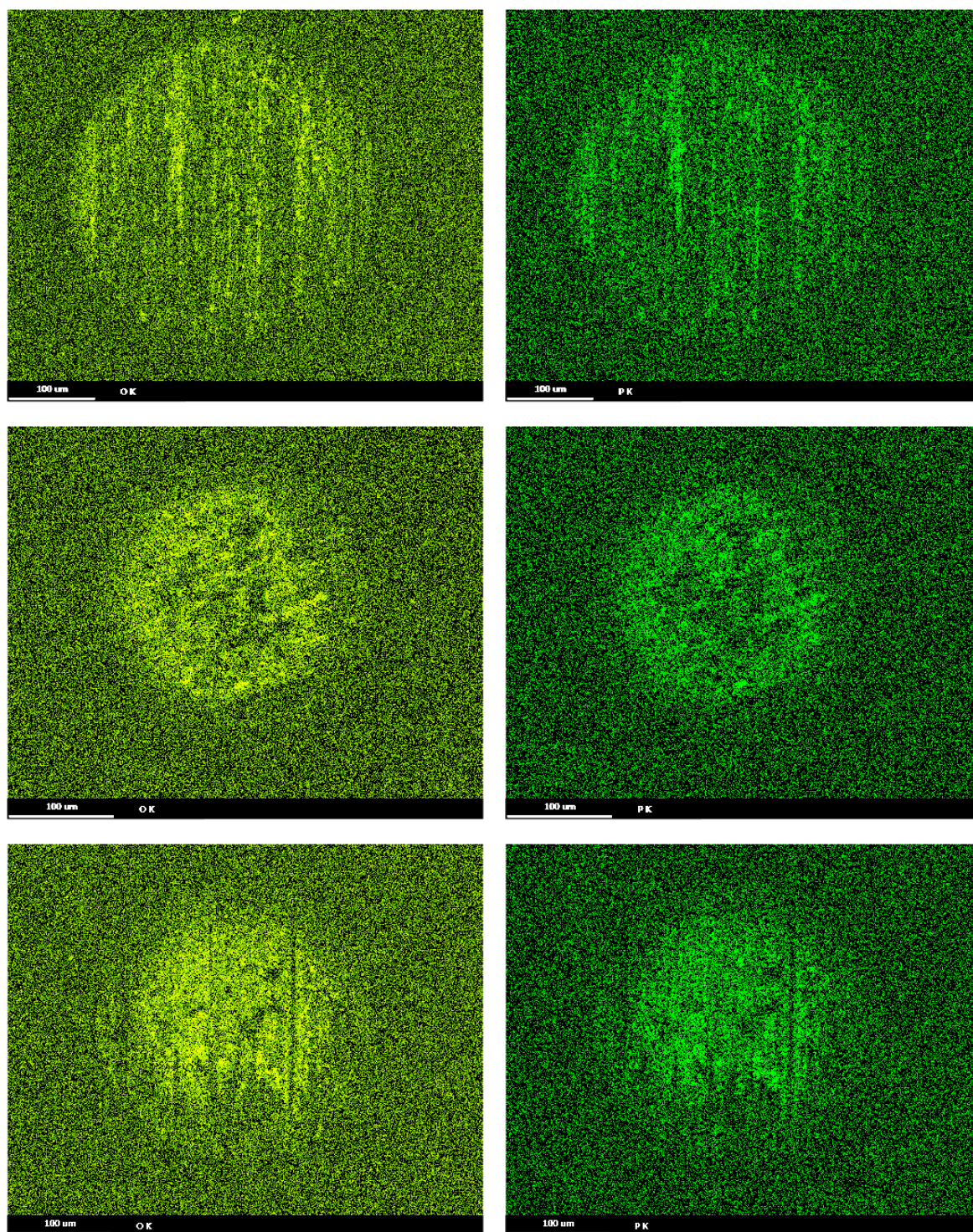


Figure 55. EDX analysis of the wear scars using 2 mmol in base stock of diisopropyl dithiophosphoric acid (top row), Irgalube 63 [®] (middle row) and ethylhexyl acrylate dithiophosphate (bottom row) for oxygen (left column) and phosphor (right column).

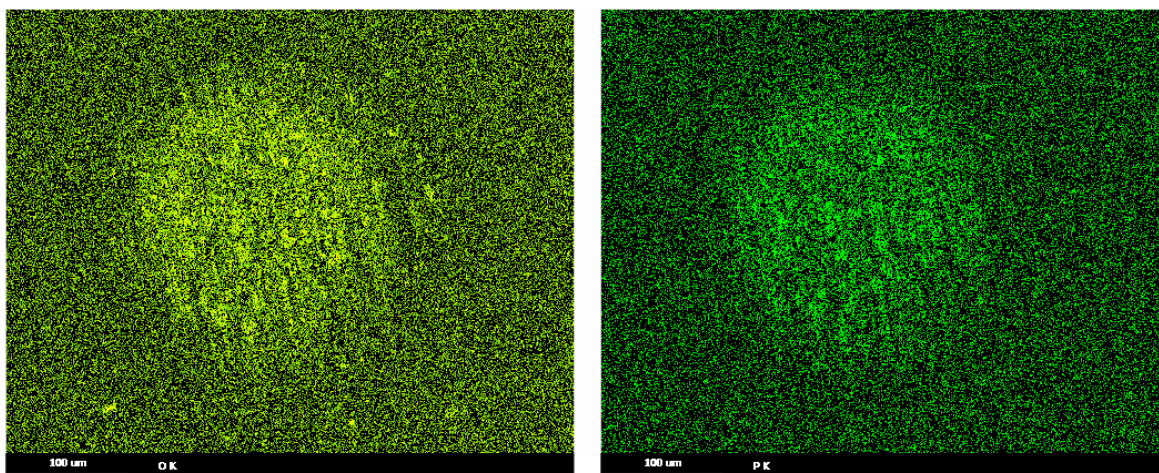


Figure 56. EDX analysis of the wear scars using 2 mmol of acetylated dithiophosphoric acid in base stock for oxygen (left column) and phosphor (right column).

The EDX analysis revealed oxygen and phosphor as major components of the tribolayers. These findings are comparable to the EDX analyses of the phosphite and phosphate studies. Surprisingly it was found, that the dithiophosphate derivatives as AW additives yielded no sulfur in the tribolayer. Especially for the free dithiophosphoric acid these results are against expectation of favorable coordination ability of the acid to (ions in) the metal surface.

Dithiophosphates inflict a wear resistance involving the phosphate part, the sulfur reacting to organic compounds remaining in the oil. Experiments with mercaptanes as AW additives gave sulfur in the tribolayer. Apparently, sulfur containing species from dithiophosphates do not react with the surface at the examined conditions or the formed intermediates are not stable against the phosphate (derived) entities. The formed sulfur compounds may consist of disulfides or sulfur oxo-derivatives.

The dithiophosphoric acid behaves different from the neutral derivatives in AW experiments. Deeper scratches from debris can also be seen. The EDX analysis of the scars from performance test with dithiophosphoric acid as AW additive reveals that the amounts of oxygen and phosphorus in the scar are lower and their distribution more evenly. This finding leads to the hypothesis of continuous solution and reformation of tribolayers, resulting in significant wear, and therefore less oxygen and phosphorus is found in the wear scar.

Furthermore, the color of the oil after the experiments suggests the formation of iron and chromium dithiophosphate complexes. These complexes can be derived from reaction of dithiophosphoric acid with iron or chromium salts (e.g. chlorides, hydroxides

or iron powder).^{175–177} In terms of the four-ball system iron and chromium oxides of the passive layer on the surface of steel ball¹³⁷ can serve as reactants for these complexes.

In summary, the AW and EDX results revealed, acrylate-based dithiophosphates as well as novel acetylated dithiophosphoric acid to be proper alternatives to Irgalube 63® with acceptable toxicological properties and pleasant esthetics. The EP properties of the examined dithiophosphoric acid derivatives can be found in chapter 5.3.7 Extreme Pressure Performance of Dithiophosphoric Acids.

5.2.8 Anti Wear Performance of Phosphonates

Phosphonic acid is the P(III) analogue to phosphoric acid (Figure 57).

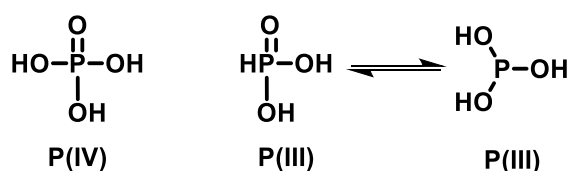


Figure 57. Phosphoric acid (left) and phosphonic acid (right).

Phosphonate esters have two ester groups and a P-H moiety, whereas trialkyl phosphites do not (Figure 58).

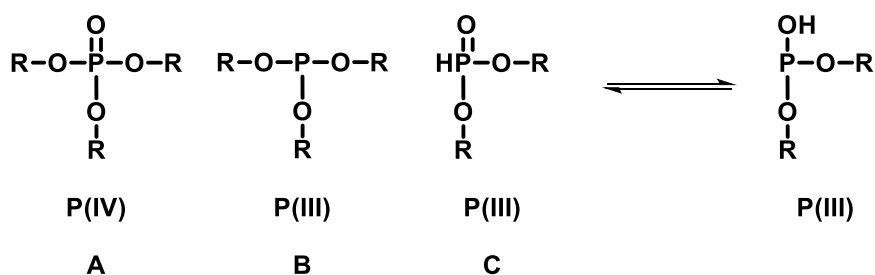


Figure 58. Phosphate esters (A), phosphite esters (B) and H-phosphonate esters (C) respectively the tautomeric structure of H-phosphonate esters.

Phosphite esters and phosphate esters are accessible by an acid base reaction of phosphor trichloride with alcohols respectively followed by oxidation.¹⁴ Phosphonates can be accessed by reaction of phosphor trichloride with alcohols yielding an equivalent of chloro alkane.^{14,70} This leads to problems of separation by distillation for higher alcohols (higher molecular weight thus higher boiling point). A more convenient method especially for the preparation of phosphonates is transesterification of dimethyl phosphonate with an alcohol.^{71,72} The formed methanol can easily be removed, e.g. by application of vacuum. Following this route, derivatives of renewable oleyl and stearyl

alcohol were prepared. Phosphonate esters in which the hydrogen is substituted by an alkyl chain were examined too. These derivatives are accessible by a Michaelis-Arbuzov reaction of triethyl phosphite with bromo alkanes or by palladium catalyzed addition of hypophosphorous acid to alkenes followed by oxidation.^{85,178,179}

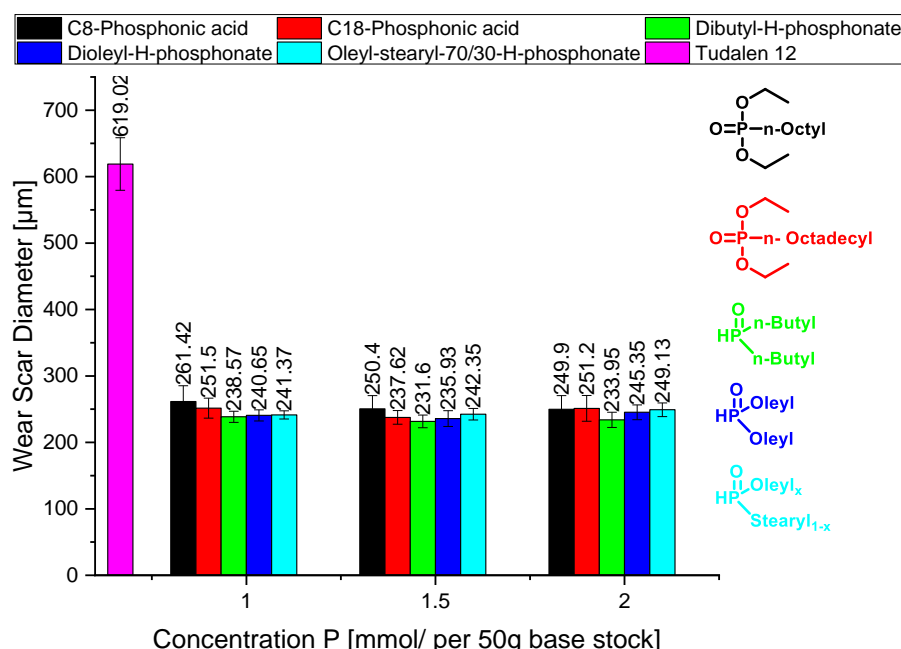


Figure 59. Wear scar diameter of phosphonate derivatives. Test conditions: 150 N, 60 min, 1450 rpm.

AW experiments with these derivatives in base stock gave the best wear protection of all compounds in this thesis. The phosphonate esters (C₈-diethyl phosphonate & C₁₈-diethyl phosphonate) show slightly worse AW values than the H-phosphonate esters, having WSDs from 261 µm to 250 µm. The AW performance is in good accordance to literature reports.⁸⁰

The H-phosphonates exhibit WSDs of 250 µm to 232 µm. Values around 230 µm resemble the lowest values the four-ball apparatus is able to measure. The theoretical minimum diameter of the wear scar at the tested conditions according to Hertzian contact mechanics is 220 µm (see 4.1 AW & EP determination with the Four-Ball Apparatus (VKA)). The experiments reveal no dependence of the WSDs with regard to the type of organic residue. This is in good accordance with the aforementioned experiments which also suggest that the organic residues contribute to their solubility in the base oil, but have no impact on the AW performance (Figure 60). Furthermore,

their esthetics as well as their estimated toxicological and ecological profiles are acceptable.

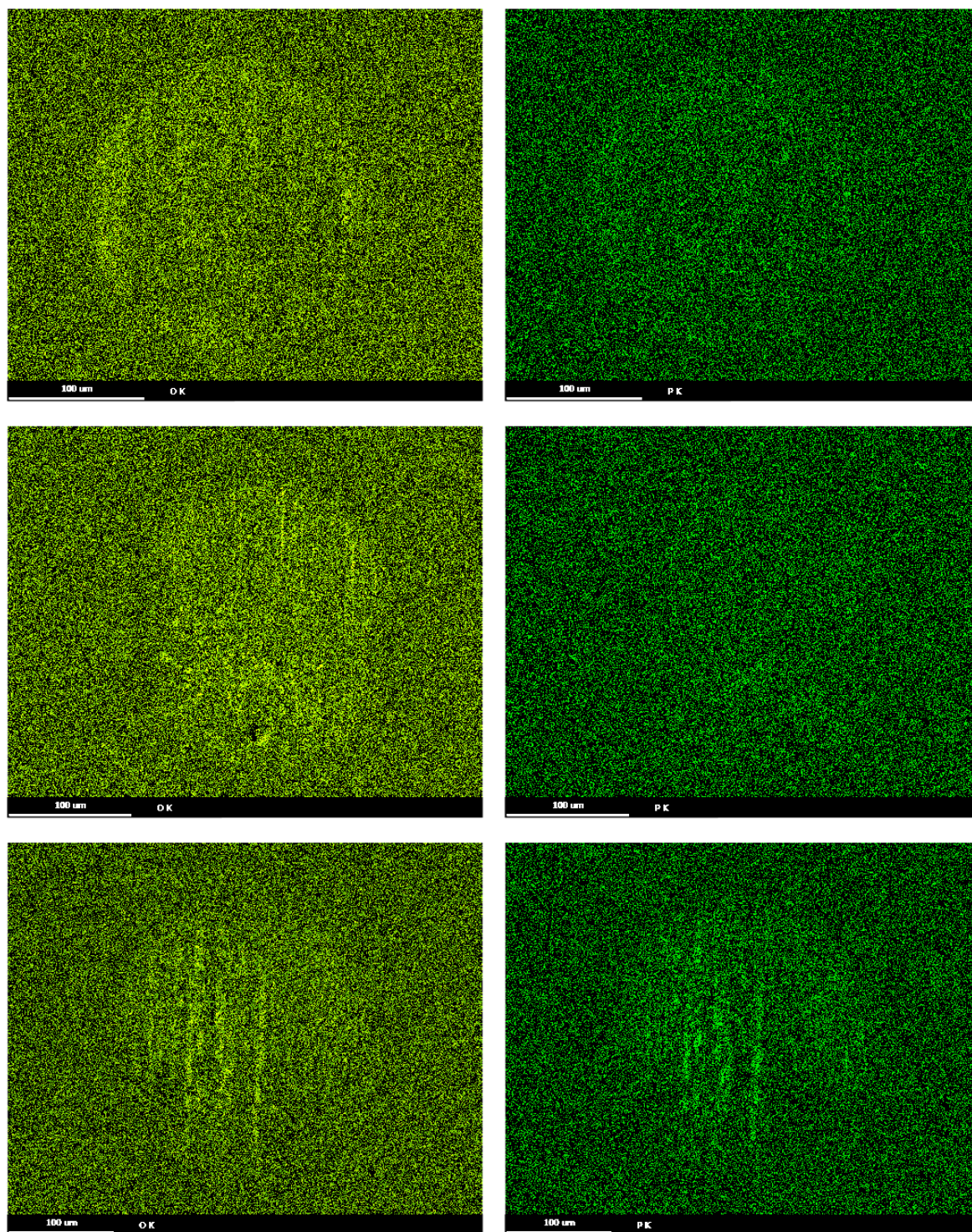


Figure 60. EDX mapping for oxygen (left column) and phosphor (right column) of wear scars in AW experiments with base oil containing 2 mmol of C_8 -phosphonate (top row), C_{18} -phosphonate (middle row) and dibutyl-H-phosphonate.

5.2.9 Anti Wear Performance of Benchmark on 1.0616 and 1.4034 Steel

The AW test along DIN 51350-3 dictates the use of steel balls with the EN 10027-2 identification number¹⁸⁰ 1.3505 (100Cr6) with a G20 surface grade or better.²⁵ This steel has a medium content of chromium, leading to a medium oxidation and corrosion stability.¹³⁷ EDX analysis of wear scars revealed phosphor and oxygen as essential elements for AW protection, sulfur was only detectable in studies with mercaptanes. It was surprising to find a lack of sulfur in the wear scar in AW experiments with phosphor and sulfur containing additives, like thiophosphates and dithiophosphates. This led to the question, whether sulfur would bind to the surface of steel as a function of load or as a function of its constitution.

Two additional steel alloys were tested to gain a further understanding of the different anti-wear mechanisms in the context of surface chemistry. A pure iron steel with EN 10027-2 identification number 1.0616¹⁸⁰ having lower oxidation and corrosion stability¹³⁸ than that of 100Cr6 (1.3505) was chosen. In addition, a high chromium steel having higher oxidation and corrosion stability with EN 10027-2 identification number 1.4034 was chosen.^{140,180} The 100Cr6 steel balls were G10 grade, the 1.0616 G200 grade and the 1.4034 were G100 grade. The absolute AW values will have to be considered with some restraints, but trends and insights into surface chemistry may be interpreted. It was expected, that additives react readily with pure iron balls, whereas for high chromium alloy steel a reaction of additives might be significant slower or absent. Large wear scar diameters would indicate the absence of a reaction resulting in the formation of a tribolayer. The different steel qualities were tested in AW experiments with the butyl derivatives of phosphonates, phosphites, phosphates, thiophosphates, dibutyl dithiophosphoric acid as well as dibutyl dithiophosphate acrylate Michael-adducts (dibutyl dithiophosphoric acid reacted with ethyl acrylate) as additives (Figure 61).

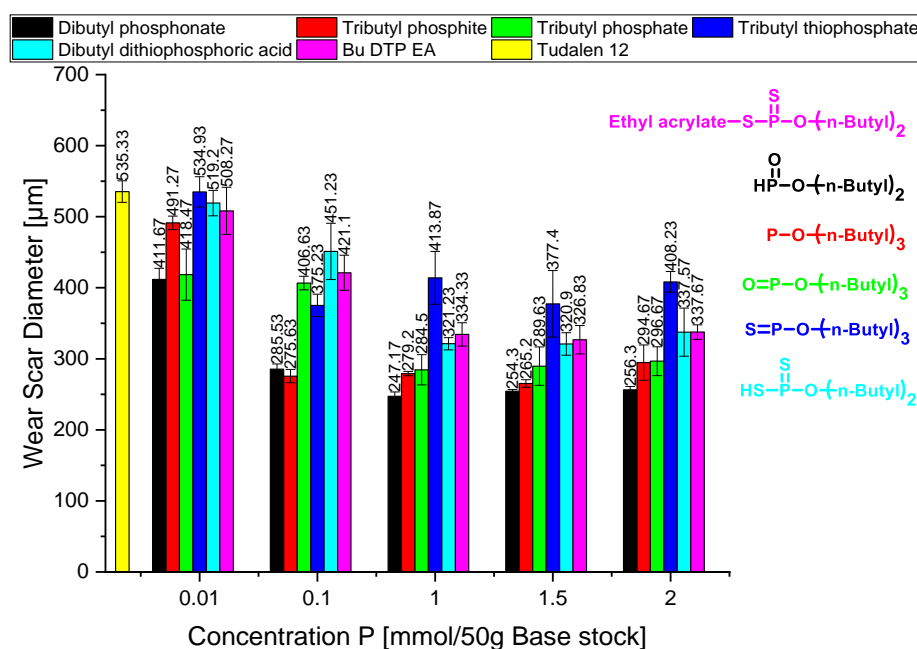


Figure 61. AW performance on 1.0616 steel. Test conditions: 15 kg, 60 min, 1450 rpm, 25 °C.

The tests with 1.0616 steel reveal minor differences between phosphor(III) and phosphor(V) systems. The AW performance lay at a similar level, especially at higher concentrations. As seen in the experiments with 100Cr6 steel, phosphonates exhibit best AW performance. The AW experiments on 1.0616 steel reveal significant wear reduction for the additives over the base stock for phosphonates and phosphates at concentrations equal or larger than 0.01 mmol P/50g base stock. The dibutyl dithiophosphoric acid and the dithiophosphate acrylate adduct exhibit no wear reducing properties at the lowest concentration of 0.01 mmol P/50g base stock. Phosphonates and phosphites show their maximum performance at concentrations equal or larger than 0.1 mmol P/50g base stock. The WSDs of 286 μm respectively 276 μm of phosphonates and phosphites indicate a significantly better AW performance than phosphor(V) systems with WSDs of 375 μm and 451 μm. Phosphonates have the best AW properties with WSDs between 247 μm and 256 μm. Phosphites and phosphates exhibit comparable WSDs with 265 μm to 297 μm for concentrations larger than 1 mmol/50g base stock. The thiophosphate reveals poor AW performance with WSDs between 377 μm and 414 μm at concentrations equal or larger than 1 mmol P/50g base stock. This may indicate slower reaction between thiophosphate and the iron steel surface.

The AW experiments show no difference between dithiophosphoric acid and acrylate adduct (WSDs between 321 μm and 337 μm), which was unexpected with regard to the potential hydrogen corrosion of the acid. Tests on 100Cr6 had revealed a higher WSDs at higher increasing concentrations of the free acid. The results of experiments with 1.0616 steel could indicate a reaction between steel and wear reducing additives, leading to a more protective tribolayer.

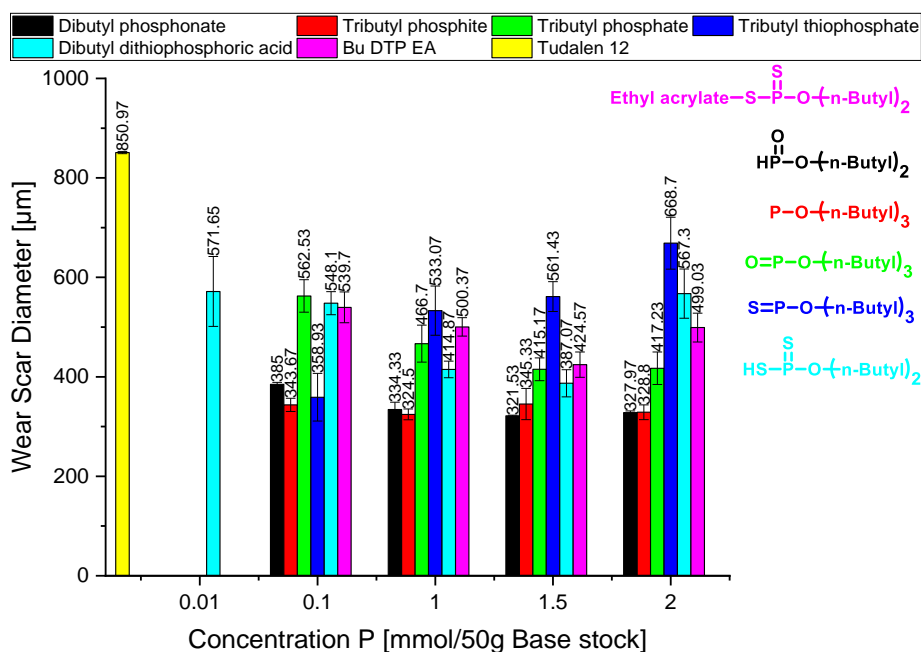


Figure 62. AW performance on 1.4034 steel. Test conditions: 15 kg, 60 min, 1450 rpm, 25 °C.

Experiments with 1.4034 steel reveal major differences between the AW additives (Figure 62). AW tests with additive concentrations of 0.01 mmol P/50g base stock show only effects for dithiophosphoric acid. Experiments of the other additives could not be completed due to repeated heavy vibrations, contrary to the run with base stock which could be completed. Experiments with 0.1 mmol P/50g base stock show no trend of wear scar diameter with regard to the use of phosphor(III) or phosphor(V) compounds. The results for H-phosphonate, phosphite and thiophosphate all lay within the same range of 344 μm to 385 μm . Similar results were found for phosphate, dithiophosphoric acid and its acrylate adduct, showing larger WSDs between 540 μm and 563 μm .

Experiments with concentrations of ≥ 1 mmol P/50g base stock reveal the distinct differences, phosphonates and phosphites yield WSDs between 322 μm and 345 μm , substantiating the superior AW performance of phosphor(III) systems over a broad range of concentration. Phosphates and thiophosphates exhibit significant higher

WSDs with values between 416 μm and 669 μm , whereas phosphates reveal a trend of lower WSDs of 467 μm to 417 μm with increasing concentrations. Thiophosphates show opposed behavior, resulting in higher WSDs values of 533 μm to 669 μm with higher concentrations.

Both dithiophosphoric acid and the corresponding acrylate adduct behave similar at concentrations of 0.1 mmol P/50g base stock (Figure 63). Relevant differences are visible at higher concentrations of 1 mmol P/50 g base stock with WSDs of 415 μm for dithiophosphoric acid respectively 500 μm for the corresponding acrylate adduct. This may indicate a higher reactivity of the free acid towards the surface, leading to a tribolayer. A better AW performance of the acrylate adduct is unexpectedly found with WSDs of 425 μm to 387 μm at AW additive concentrations over 1.5 mmol P/50 g base. This observation may still be explained in terms of the hydrogen corrosion of the free acid, leading to formation of protective tribolayers at low to medium concentrations, but high wear by ongoing metal dissolution at higher concentrations (i.e. when the tribolayer is broken).

Experiments with different steel qualities showed different reactivities of the additives. Point of interest were the oxidation state of the phosphorous species and the Brønsted acidity. The best performance for all examined steel qualities, especially the tests with 1.4034 steel showed superior performance of the phosphor(III) additives. These species may be more reactive towards the metal (oxide) surface. The assumption concerning the reducing character of the phosphor(III) systems with regard to removal of the passive layer followed by formation of a protective tribolayer was strengthened.

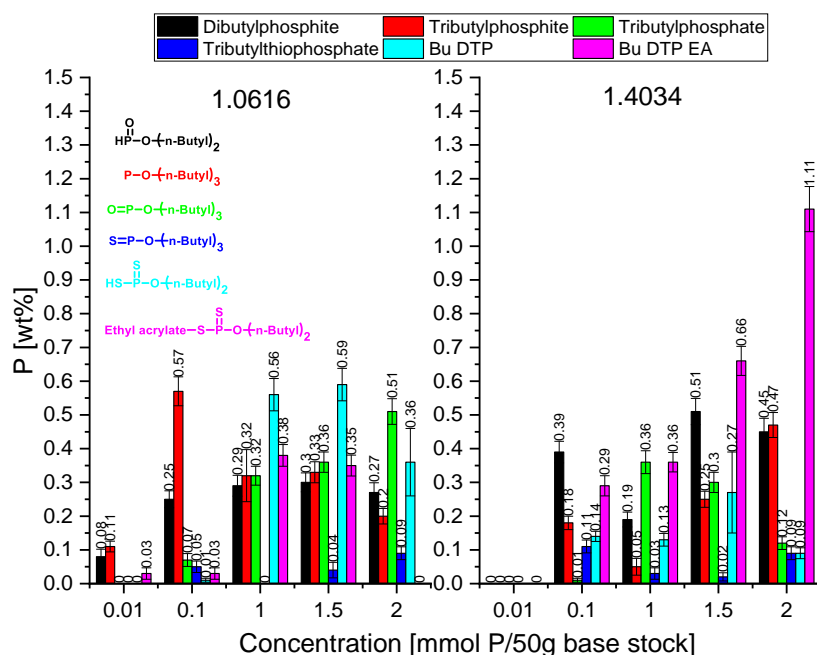


Figure 63. EDX analysis of P for 1.0616 (left) and 1.4034 (right).

The phosphor EDX analysis gave no compelling evidence for a dependence of the resulting tribolayer, respectively the reactivity of the additive towards the various steels. The EDX analysis of the surface of the 1.0616 and 1.4043 steel balls after the wear experiments gave very low P contents within the scars when using additive concentrations of 0.01 and 0.1 mmol P/50 g of base stock (Figure 63). Results using 1 mmol P/50 g of base stock or higher, show detectable phosphor contents in the range of 0.1 to 1.1 wt%. The action of tributyl phosphate and tributyl thiophosphate is the same for all types of steel. One significant difference is observed for dibutyl dithiophosphoric acid, which yields phosphor contents from 0.4 to 0.6 wt% for 1.0616 steel and significantly lower contents ranging from 0.1 to 0.3 wt% for experiments with the 1.4034 steel. This observation might be an effect of the chromium in 1.4034 alloy, resulting in higher chemical resistance¹⁴⁰, thus lower incorporation of phosphor in the tribolayer.

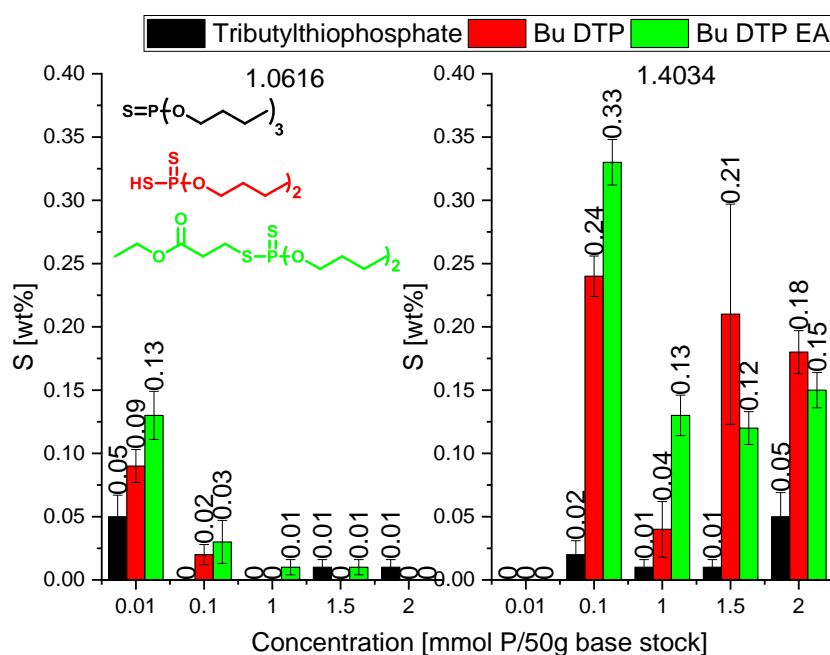


Figure 64. EDX analysis of S for 1.0616 (left) and 1.4034 (right).

The sulfur EDX analysis gave more differentiated results. Experiments with 1.0616 steel yielded questionable sulfur contents in the wear scar at or below the lowest concentration of detection. On the contrary, experiments with 1.4034 steel gave sulfur contents ranging from 0.05 to 0.33 wt% in the wear scar. The more corrosion stable steel thus picks up more readily sulfur atoms from the additive to remain in the scar. A possible explanation for these findings could be the steel alloy. The 1.4034 alloy contains additional chromium¹⁴⁰, which might support adhesion (growth) of the resulting tribolayers.¹⁸¹ Considering the different chemical composition (the different chemical properties), the 1.0616 steel forms sulfur containing tribolayers, but the adhesion on the substrate is weak, thus the build-up of detectable amounts of sulfur is not possible. The differences in adhesion of phosphor containing tribolayers (e.g. iron phosphates) and sulfur containing tribolayers (e.g. iron sulfide) are too severe. As a consequence the sulfur containing tribolayers dissipate, while the phosphor containing tribolayers adhere to the substrate. Thus, formation of inhomogeneous tribolayers on 1.0616 steel alloy consisting of phosphor and minor shares of sulfur are observed.

These results indicate, that the chemical composition of the material has impact on the reactivity with the additive, respectively the growth and adhesion of tribolayers. Experiments with ashless AW additives on different steel alloys yield comparable conclusions for the dependence of the formation of tribolayers on different steel alloys, in contrast the considered alloy (440C) did not yield tribolayers.¹⁸¹

5.2.10 Anti Wear Performance in Ester Oils

The prior experiments led to the insight that phosphonates may be superior AW additives. Comparable AW experiments were conducted in a more polar ester oil, also to verify whether the performance of the oleyl-stearyl phosphonate is also superior. Therefore, 1 mmol P/50g base stock of TPPT and OSHP7030 were tested in AW experiments on the performance on 100Cr6 steel balls (Figure 65). The amounts of TPPT and phosphonate in these experiments are 0.68 wt% for TPPT and 1.16 wt% for phosphonate.

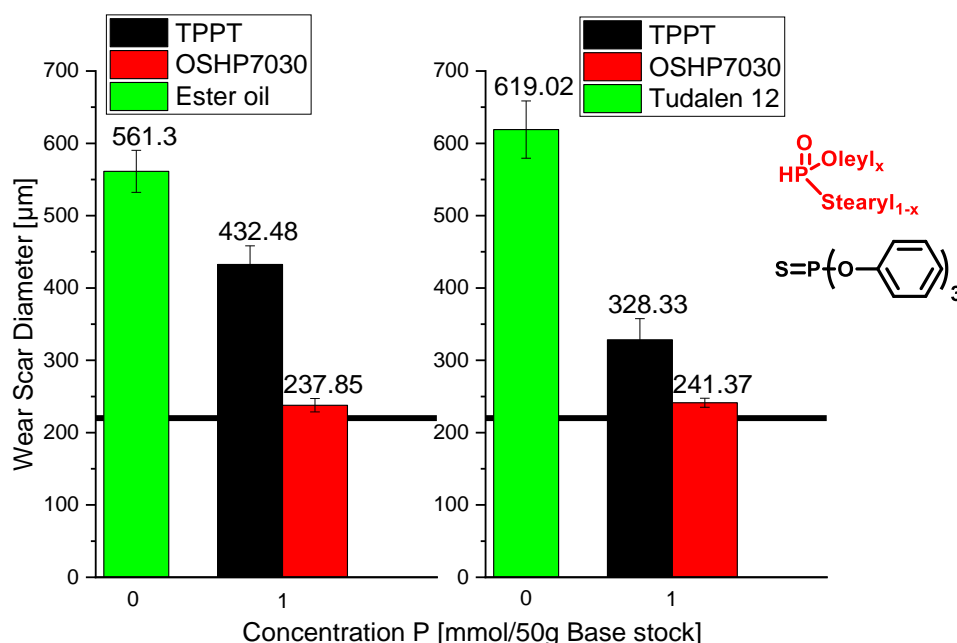


Figure 65. Comparison of AW performance of 1 mmol TPPT and OSHP7030 in an organic ester oil (left) and Tudalen 12® (right). Test conditions: 15 kg, 60 min, 1450 rpm, 25 °C.

Employing the polar ester oil results in slightly smaller WSDs of 561 μm over the 619 μm of the Tudalen® 12 mineral oil. This is as expected as the ester oil with their ester groups would adsorb better to metal (oxide) surfaces. The importance of AW additives is also lesser with regard to wear; the performance of TPPT in an ester oil is significantly inferior to the performance in a mineral oil. The WSDs were 432 μm in the ester oil against 328 μm in mineral oil at a TPPT concentration of 1 mmol/50 g of stock. The metal surface is covered by ester oil and adsorption of TPPT is less.

The AW performance of OSHP7030 is independent of the base oil. The WSD values obtained in ester oil and in mineral oil are with WSDs of 238 μm respectively 241 μm the same within the significance of method. This shows the superior performance of

phosphonates as AW additive and also its independence of the base oil. Experiments in mineral oil revealed phosphonate to exhibit the maximum AW performance for concentrations as low as 0.1 mmol P/50g base stock. This fact leads to a weight fraction of 0.12 wt% resulting in maximum AW performance. This aspect should be pointed out for commercial aspects.

The AW experiments yielded phosphor (III) substances as superior AW additives, and especially oleyl stearyl phosphonate (OSHP7030) was found to exhibit extraordinary AW properties. The presence of sulfur in the additives was found of minor impact on AW performance. The EDX analysis did not show sulfur incorporation within the wear scars when using phosphor-sulfur containing additives. It is assumed, that at the applied load conditions, reaction of sulfur entities do not take place after absorption of phosphorous from the compounds. Phosphor containing tribolayers are of superior stability. Studies with 1.0616 and 1.4034 steel indicated no dependence of AW additive performance (same trend compared to 100Cr6) on the material composition, tribolayer composition did show differences in dependence of the alloy. Experiments with an ester oil indicated a consistent AW performance of OSHP7030. The performance of TPPT is stronger dependent on the base stock.

5.3 Extreme Pressure Performance

5.3.1 Concept of a Novel Extreme Pressure Screening Method

The EP (extreme pressure) performance of lubricant additives is, next to the AW performance, also of interest. EP additives are capable of preventing damage in mechanical systems under severe loads and insufficient part surface separation by the base lubricating fluid.¹⁰⁷

Determination of EP properties was realized by an adapted dynamic load screening method.²⁷ A load increase in the four-ball system was imposed by sliding a weight on the lever, thus increasing the pressure between the four balls. The load lever has eighteen steps. Available lever weights are 1 kg, 2 kg, 2.5 kg, 5 kg, 10 kg, 20 kg, 30 kg, 40 kg and 50 kg. Loads ranging from 70 kg to 240 kg on the four-ball system can thus for example be applied with the 10 kg lever weight. This scales linearly, using 20 kg as

sliding weight allows a load from 140 kg to 480 kg. The maximum lever weight is 50 kg which delivers peak loads of 1200 kg.

The DIN 51350-2 procedure demands to charge the VKA with cleaned balls and lubricant system.²⁶ Subsequently, a load lower than the weld load is applied on the lever and the test is run for 60 s. After 60 s the system is relieved, the system cleaned, charged with new balls and the next load is applied. The load is increased stepwise, until the weld load is reached. According to DIN 51350-2, the weld load needs to be the same in two of three runs for a significant value.²⁶ Thus ninety individual runs are necessary for a complete screening of an EP additive, i.e. 18 steps with five lever weights.^{28,135} This procedure is exceedingly time and material intense. The used balls burden cost of about 1.30 €/ball at four balls/test. Furthermore, large amounts of substances are needed for comprehensive EP characterization and providing large amounts of substances is not only a challenging task in academic surroundings but also expensive. Therefore, a more effective way to determine EP values of novel substances would be of use.

Here, a new method based on a known concept²⁷ is disclosed, which is validated by comparing collected data with industrial EP product data. The principle of the method is to linearly increase the load over 60 s by adjusting the lever within one lever weight. This leads to decent load-torque curves within one test setup with four balls per lever weight and a single charge of lubricant. The general layout is shown in Figure 66.

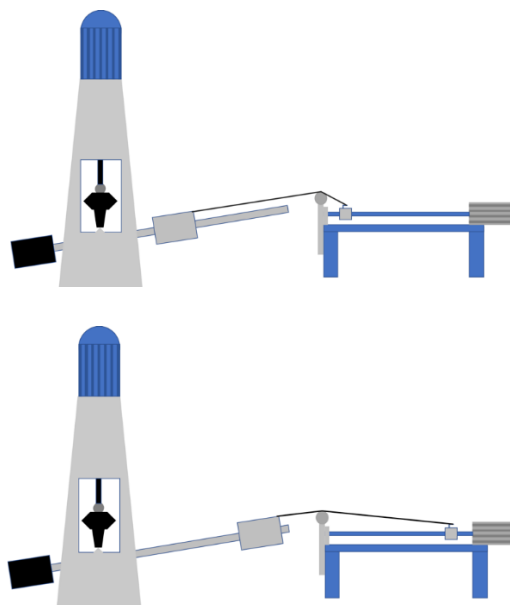


Figure 66. Advanced EP screening method. Top image displays the situation before the experiment, bottom image displays the situation at the end of the experiment, sliding the weight up the lever.

The set-up comprises of the four-ball apparatus (VKA) from Hansa Press- und Maschinenbau GmbH and a linear drive system capable of moving the lever weight on the lever (Figure 66). The eighteen steps on the lever to increase the load on the four-ball system are now equally distributed over a length of 42.5 cm (length of weight lever). The linear drive is controlled by Grbl-Software version 1.1 installed on an Arduino Uno®. The step motor pulls the weight over 42.5 cm during 60 s test time. This set-up condenses eighteen single experiments to only one experiment yielding load-torque curves. In combination with the 2 kg, 5 kg, 10 kg, 20 kg, 30 kg, 40 kg as well as 50 kg lever weight, seven experiments yield data regarding the EP properties over a broad load range. The added linear drive is a modern so to speak upgrade for the standard four-ball apparatus with regard to the characterization of additives.

5.3.2 Validation of the novel Extreme Pressure Screening Method

Torque-load curves for each lever weight are the outcome of the novel procedure, which are combined in a single graph (the detailed procedures for the linear drive method and the DIN method are summarized in chapter 6.11 Linear Drive Screening Procedure & 6.12 DIN 51350-2 Procedure). The combination of the data sets yield a comprehensive torque-load curves over a broad load range (Figure 67).

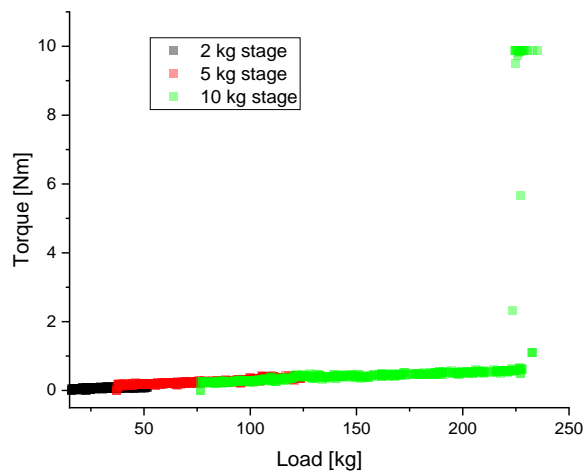


Figure 67. Torque-load curves from the new method: 2 kg stage in black, 5 kg stage in red, 10 kg stage in green.

The merged data yield a continuous torque-load curve, climaxing in the weld point of the additive. Vibration during the starting period or transitions in wear are possible, resulting in torque peaks and false associated load values (Figure 68). The curve shows two vibration effects resulting from different sources. The vibration effect in the measurement during the 10 kg stage occurred simultaneously with an increase in torque of approx. 1.5 Nm. This may be associated to a transition in the tribolayer or hint of beginning failure. Literature reports associate this transition as the scuffing point.²⁷ The second vibration effect is visible at the beginning of the 20 kg stage, suggesting that the starting period of the test is critical. The final increase in torque at approx. 420 kg indicates failure (seizure) of the lubricant respectively the welding of the four-ball system. The resulting curves are comparable to literature reports, concluding a viable experimental setup.²⁷

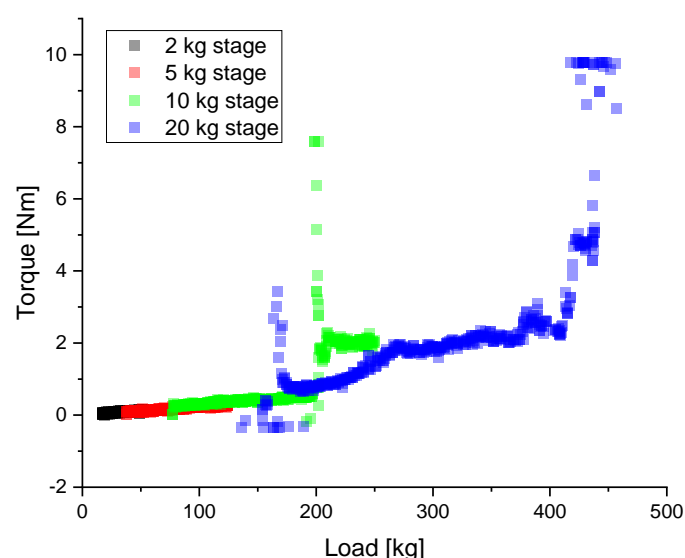


Figure 68. Combined load stage graphs and torque peaks during a test, resulting from transition effects or starting effects.

Irgalube 63® (diisopropyl dithiophosphoric acid ethyl acrylate adduct) was chosen as test substance for validating the method and comparison to DIN 51350-2. The tests were performed with 1 mmol P/50g base stock using the same steel balls (Figure 69). The left part depicts a proper set of EP screening experiments with the linear drive method yielding the weld load at approx. 225 kg indicated by a significant increase in torque. The right part is derived from the DIN 51350-2 method, giving a weld load of 200 kg. The novel linear drive method covers the load range from 15 kg to 225 kg in six experiments. The linear drive method generates multiple values through the load range, giving a more robust assessment.

The DIN method covers the range of 140 kg to 200 kg with eight experiments necessary. It only gives multiple values for the weld load. A complete reproduction (blue curves) of the DIN method would have taken fourteen tests, compared to six tests for the novel method. This shows the considerably larger content of information obtained from the novel method.

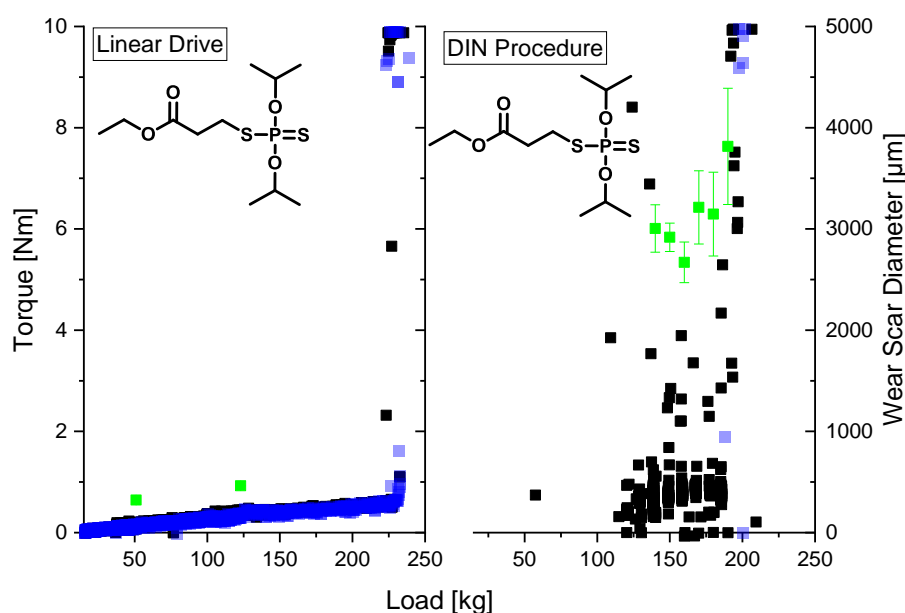


Figure 69. Torque-load curves and the WSDs (green) resulting from novel EP screening method (left) and the DIN method (right). Test conditions: 1 mmol P/50g base stock, test time 60 s (for each load), 1450 rpm, 25 °C.

The collected torque data of the linear drive method gives a torque-load continuum climaxing in the weld point, while the torque data resulting from the DIN method are quite diffuse. This finding can be explained by fluctuation of the torque during the starting period of the four-ball apparatus, lasting about 6 s. The torque values obtained from the DIN method level off between 0.5 and 1 Nm after the starting period, climaxing at 200 kg, when the weld point for failure of lubricant action is reached.

The welding point determined by the novel linear drive approach was determined approx. 10 % higher with a weld load of 225 kg. A possible explanation for this observation could be the constant increase in load of the linear drive method, during which the additive can react with the metal surface to form tribolayers. In case of the DIN method, the welding occurred within a few seconds at the 200 kg load mark, indicating the time until welding occurred to be too short to build up a proper tribolayer.

In conclusion, the linear drive method yields more reliable information with regard to the torque-load behavior as well as the resulting WSD with significant less effort. The DIN method yields the weld-load and WSDs with limited interpretability regarding torque values and WSD.

The torque-load curve of 1 mmol P/50g base stock for tributyl phosphite shows no discrete welding point (Figure 70). The curve shows a break in the smooth linear increase of the torque at approx. 115 kg. Severe vibration effects occurred at this point, resulting in swinging of the weight lever leading to loading and unloading of the four-ball system, thus torque data are “outlier” load data. The vibration stops at a distinctive point, resulting in the standard weight lever position and correct load data. This point is reached at around 180 kg accompanied by a interpretable torque-load increase. Considering the resulting WSD of the load stages, the steel balls suffered significant wear at about 115 kg load, indicating failure of the lubricating system. The load at which severe wear occurs is defined as initial seizure load.⁸⁵ One possible explanation, why a decent torque-load curve is measurable after reaching 180 kg might be a sufficient contact area between the running ball, capable of sustaining the load. Nevertheless, the WSD of nearly 5 mm diameter indicates severe wear and thus failure of the lubricating system is assumed.

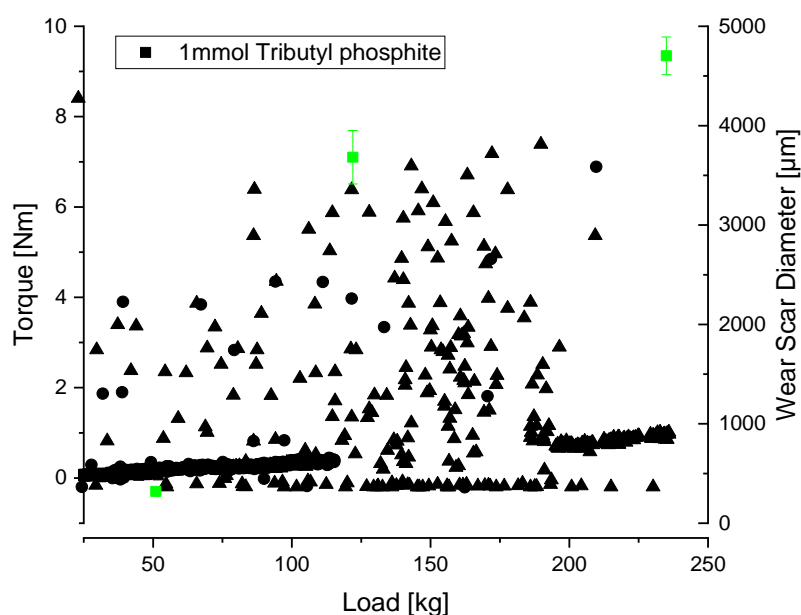


Figure 70. Torque-load curves and the WSDs (green) of an additive without weld point (new method). Test conditions: 1 mmol P/50g base stock, test time 60 s (for each load step), 1450 rpm, 25°C.

In conclusion, the new approach was useful obtaining valuable data on EP behavior. It yields much more information, and in a fraction of time and effort of the DIN 51350-2 method. The data, including scientific reproduction for a lubricant action by much fewer experiments, compares well to generated numbers by the DIN method. In addition, additives with longer periods of little action can be characterized properly.

The DIN method is limited to additives with fast tribofragmentation, however, it should be mentioned, that EP additives need to cover a broad load range. Therefore, additives which deplete very fast at high loads may not show any useful EP properties at low or medium loads. In addition, severe conditions typically occur during a run in time, thus instantaneous depletion may be a disadvantage with regard to service life of the lubricant. Thus, the novel developed method yields information of the complete range load in combination with torque data.

5.3.3 Extreme Pressure Performance of Tudalen 12 ®

The EP screening of the base stock (Tudalen 12 ®) revealed a failure at 70 kg (Figure 71). This is accompanied by an increase of the WSD from 337 to 4233 µm within the second load stage. This low EP performance is expected on account of the low sulfur content of the mineral oil (vide infra).

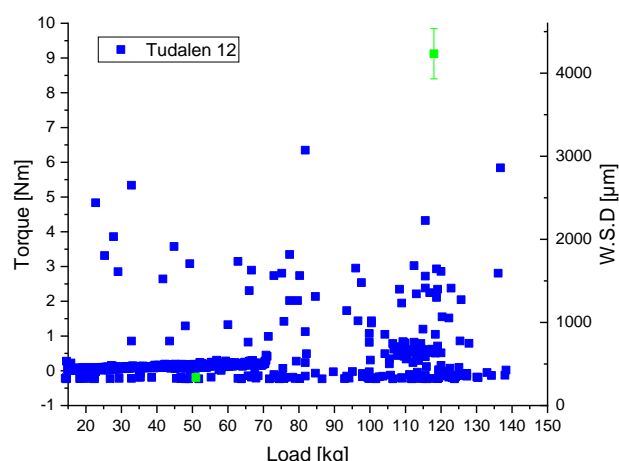


Figure 71. Torque-load curves and the WSDs (green) of Tudalen 12® (new method).

5.3.4 Extreme Pressure Performance of Phosphites

Trialkyl phosphites have poor EP properties with failure loads in the range of approx. 120 kg accompanied by failure WSDs in the range of 3700 µm and larger. The experiments are characterized by severe vibration effects accompanied with significant wear indicated by the tremendous WSD. The failure load is independent from the concentration. The EP properties of phosphites were measured at concentration of 1 and 2 mmol (Figure 72). The 2 kg load stage with peak loads of 51 kg yields WSDs of

320 μm , 322 μm and 323 μm . The 5 kg load stage with resulting peak loads of 120 kg yielded WSDs from 3700 μm to 3900 μm , indicating failure. The testing of the 10 kg stage climaxing at 250 kg confirmed the observations with the high WSD in the range of 4000 to 5600 μm .

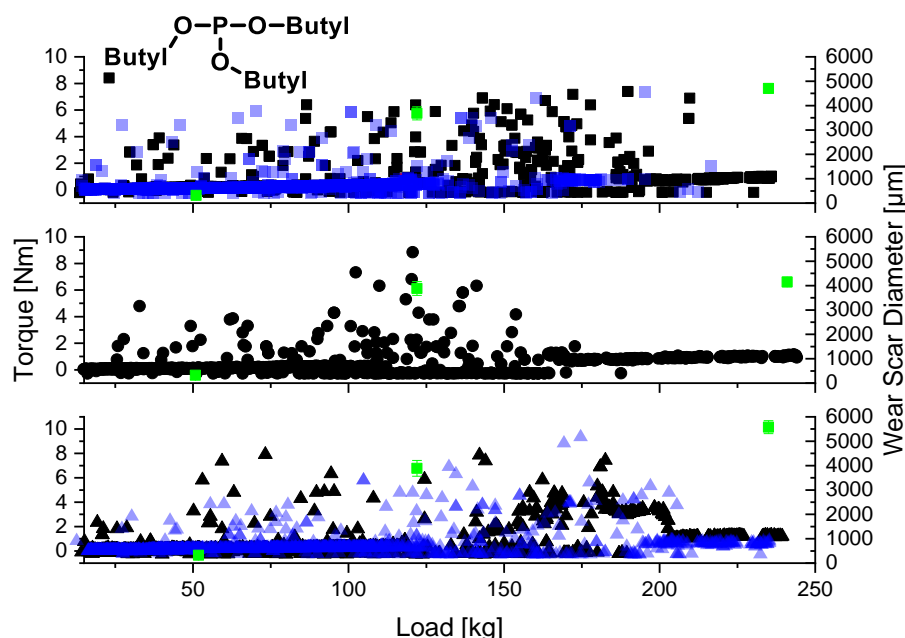


Figure 72. Torque-load curves and the WSDs (green) of tributyl phosphite. Concentrations: 1 mmol P/50g base stock (squares), 1.5 mmol P/50g base stock (spheres) 2 mmol P/50g base stock (triangle). Duplicates in blue.

5.3.5 Extreme Pressure Performance of Phosphonates

The EP characteristics of phosphonates were tested with dibutyl phosphonate as representative dialkyl phosphonate (Figure 73), showing a failure load (initial seizure load) beneath 200 kg which is in good agreement for di-O-alkyl-alkyl-phosphonates.⁸⁵ The WSDs after the lowest load stage with peak loads of 50 kg are in the range of 320 to 360 μm . The next higher load stage climaxing at 120 kg yields WSDs of 600 to 865 μm indicating acceptable EP performance at moderate loads. The next load stage climaxing at 250 kg, led to vibration effects accompanied with diverse WSDs ranging from 1041 to 3693 μm , indicating failure. The torque data strengthens vibration effects and indicates failure at loads of approx. 170 kg, accompanied with tremendous wear. Higher load stages climaxing at 500 kg confirm the failure load beneath 200 kg.

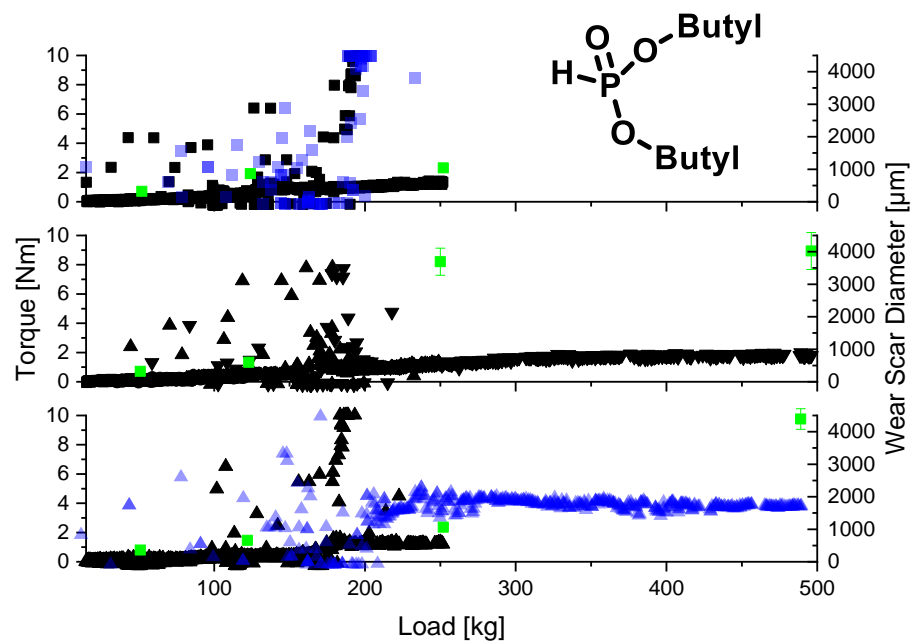


Figure 73. Torque-load curves and the WSDs (green) of dibutyl phosphonate. Concentrations: 1 mmol P/50g base stock (squares), 1.5 mmol P/50g base stock (spheres) 2 mmol P/50g base stock (triangle). Duplicates in blue.

5.3.6 Extreme Pressure Performance of Thiophosphates

The EP testing experiments were performed with tributyl thiophosphate (Figure 74) and triphenyl thiophosphate (TPPT: Figure 75).

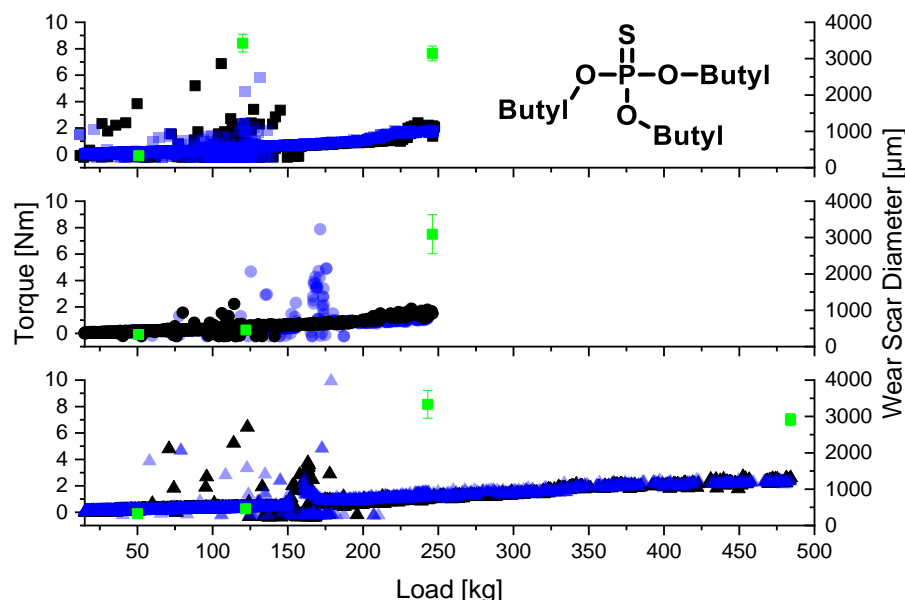


Figure 74. Torque-load curves and the WSDs (green) of tributyl thiophosphate. Concentrations: 1 mmol P/50g base stock (squares), 1.5 mmol P/50g base stock (spheres) 2 mmol P/50g base stock (triangle). Duplicates in blue.

The WSDs using tributyl thiophosphate as additive after the lowest load stage are 328, 330 and 325 μm . The next higher load stage with peak loads of 120 kg, however, already leads to failure at an amount of 1 mmol in 50 g base stock. The inferior performance is indicated by a high WSD of 3426 μm (much higher than the approx. 460 μm in the 1.5 and 2 mmol experiments) and by vibration effects. The lubricant formulation with the lowest concentration tributyl thiophosphate used indicates an initial failure by vibration effects at a load of approx. 110 kg. Increased loads (10 kg stage) with peak loads of 250 kg do not lead to welding of the four-ball system, but failure for all concentration experiments can be confirmed by comparable WSDs in the range of 3200 μm through vibration effects. One possible explanation, why a decent torque-load curve is measurable after severe vibration effects accompanied by large WSD might be formation of a sufficient contact area between the running ball, capable of sustaining the load, thus no welding is observed. The 20 kg stage led to welding within the starting period in case of the 1.5 mmol P/50g base stock. A possible explanation

for this finding may be insufficient time for build-up of tribolayers. Similar experiments with 2 mmol P/50g base stock lubricant again gave a WSDs over 3000 μm , confirming that no effective tribolayer can be formed.

In conclusion, aliphatic thiophosphates exhibit poor EP properties independent of the concentration. The failure load of thiophosphates lies in the range of 110 kg for 1 mmol P/50g base stock and around 160 kg for 1.5 and 2 mmol P/50g base stock. The failure mechanism is vibration behavior, leading to WSDs in the range over 3000 μm exceed indicating the ISL.

In addition to the aliphatic thiophosphate, industrial TPPT standard substance is investigated.

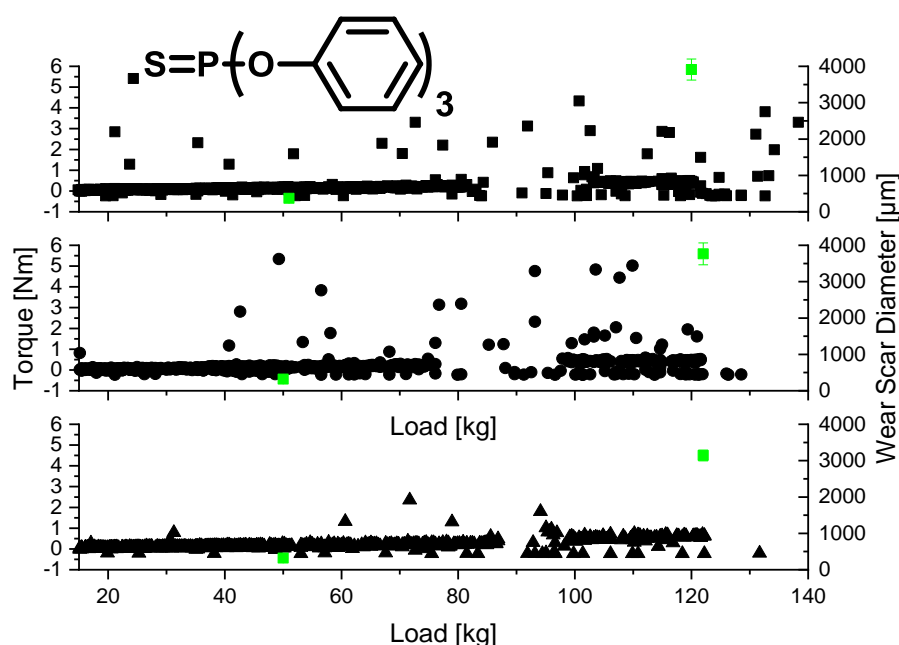


Figure 75. Torque-load curves and the WSDs (green) for triphenyl thiophosphate (TPPT). Concentrations: 1 mmol S/50g base stock (squares), 1.5 mmol S/50g base stock (spheres) 2 mmol S/50g base stock (triangle).

The data obtained are comparable to those obtained for the aliphatic thiophosphate. The failure is clearly indicated by vibration effects accompanied with high WSDs in the range of 3000 to 4000 μm . The failure loads are in the range of 85 kg for the lowest concentration, 75 kg for 1.5 mmol P/50g base stock and 88 kg for the highest concentration. The inferior performance of TPPT over tributyl thiophosphate may perhaps be related to the sterically more hindered triphenyl entities of the thiophosphate, which could render coordination to the metal surface less effective,

and/or the proposed reaction of reduction of the thiophosphate to phosphite may take too long under the EP testing conditions.¹⁰²

5.3.7 Extreme Pressure Performance of Dithiophosphoric Acids

The experiments with thiophosphates revealed poor EP properties, leading to efforts investigating dithiophosphoric acid derivatives in that regard. Dithiophosphoric acids are commonly used as reagents for synthesis of lubricant additives (cf. 2.4 Structure-response Relationship & 2.3 Synthesis of Phosphor Additives).^{90,141,142} It may be assumed, that the acid can coordinate readily to the metal surface and alter the passive layer. Another aspect is the ability of dialkyl dithiophosphoric acids to form coordination compounds with iron and chromium.^{175–177} This behavior was elaborated from the results of the AW experiments. Experiments were again conducted using the same moles of additives to obtain comparable data experiments with compounds containing different amounts of sulfur and phosphor per molecule (Figure 76).

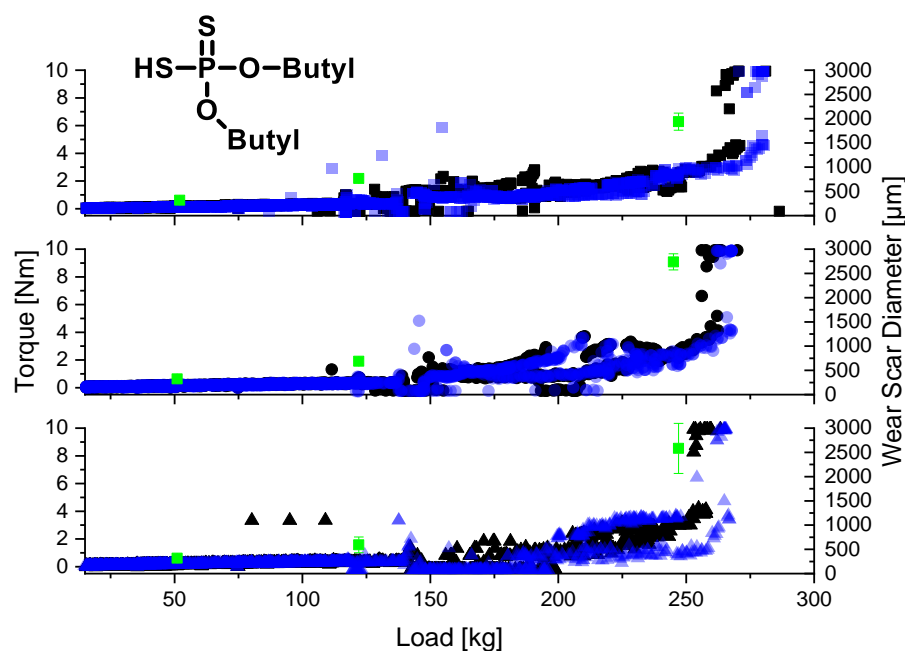


Figure 76. Torque-load curves and the WSDs (green) of dibutyl dithiophosphoric acid. Concentrations: 1 mmol S/50g base stock (squares), 1.5 mmol S/50g base stock (spheres) 2 mmol S/50g base stock (triangles). Duplicates are in blue.

The EP experiments with dibutyl dithiophosphoric acid additive exhibit good reproducibility throughout the examined concentration range. A major influence of the concentration on WSD between 1 and 2 mmol/ 50 g base stock was not obvious, as was found in AW experiments. The lowest load stage giving WSDs in the range of 320 μm, independent of the additive concentration. The WSDs for the second load

stage are 770, 690 respectively 590 μm at 1, 1.5 and 2 mmol, indicating a somewhat smaller WSD at higher concentration. A possible explanation may be the effective build-up of sulfur containing protecting layers induced by tribofragmentation. EP experiments at the 10 kg load stage resulted in an increase in WSD as well as an increase in torque. The obtained WSDs are 1938, 2738 and 2583 μm (at 1-2 mmol/50g base stock). These values are not significantly different, no concentration effects are found again. EP experiments at weld loads in the range of 250 to 275 kg show the same indifference. The results indicate that additives with high sulfur to phosphorus ratio exhibit better EP performance.

5.3.8 Extreme Pressure Performance of Dithiophosphate Acrylate Adducts

Based on the results with the dialkyl dithiophosphoric acids, neutral dithiophosphoric acid derivatives were considered next. Therefore, Irgalube 63® (Figure 77) and dibutyl dithiophosphate acrylate adducts were evaluated for their EP properties.

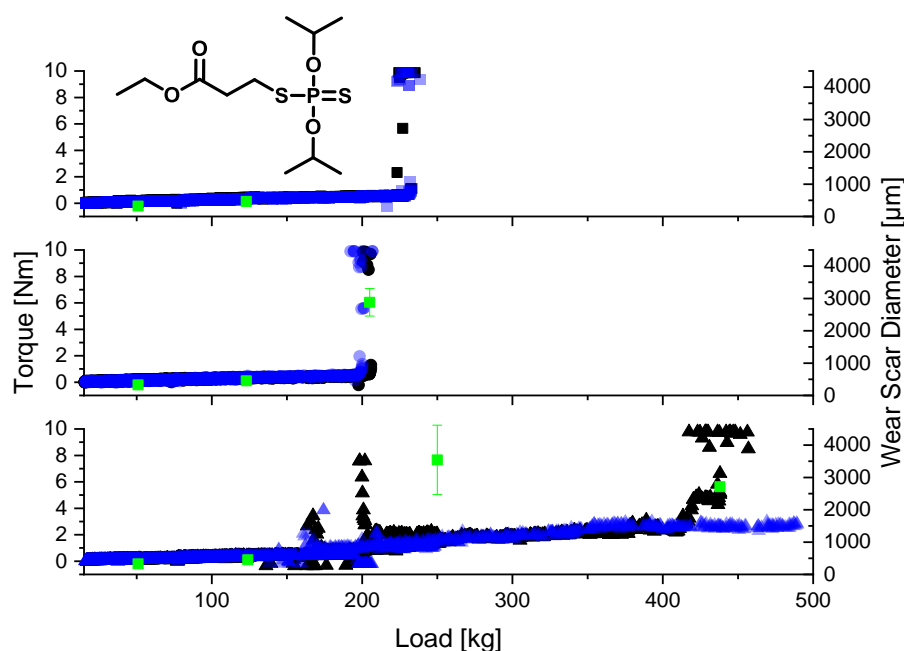


Figure 77. Torque-load curves and the WSDs (green) of Irgalube 63®. Concentrations: 1 mmol P/50g base stock (squares), 1.5 mmol P/50g base stock (spheres) 2 mmol P/50g base stock (triangles). Duplicates in blue.

Irgalube 63® has a comparable performance in EP experiments to the free acid. The first load stage WSDs are 322, 326 and 326 μm . The WSDs at the 10 kg load stage are 463, 453 and 450 μm , significantly lower than those of the free acid. It should be pointed out, that the acrylate adduct is weighted in with regard to phosphorus content,

which is half of the sulfur content. A lower wear thus could be expected. A useful comparison of 2 mmol S of the free acid and 1 mmol P of the acrylate adduct shows that the WSDs are 590 respectively 463 μm , to indicate that the neutral derivative yields significant lower wear at the same load stage. This observation may be accounted for by the different corrosiveness of these derivatives.

The weld loads of the neutralized dithiophosphate were determined in the range of 200 to 225 kg for the 1 and 1.5 mmol P in Irgalube/50g base stock experiments. One friction welded four-ball system broke during the cleaning procedure allowing to investigate the WSDs. The median WSD after welding was 3000 μm . The 2 mmol P/50g base stock probe was analyzed at the 10 kg stage, in which no welding occurred, but the WSD was 3500 μm , indicating a failure to lubricate. The 20 kg stage revealed vibration effects in the starting period and a weld load of approx. 450 kg. Rerunning the 20 kg stage experiment did result in a welding, but the obtained WSD is in the range of failure WSD. It should be mentioned here that experiments with Irgalube 63® were accompanied by the occurrence of an unpleasant smell, which was not observed for the free acid.

Further experiments with dibutyl dithiophosphate acrylate adduct were performed, also with the objective to the phosphor and sulfur equivalent molecular weight (Figure 78, Figure 79). The lowest load stage with peak loads of 51 kg gives a behavior that compares well to dibutyl dithiophosphoric acid or Irgalube 63 ®. The experiments at higher loads indicate poorer EP properties for the neutral alkyl dithiophosphate at equal concentrations. The failure loads range from 100 to 120 kg for the examined concentrations with WSD values ranging from 3000 to 3500 μm .

Higher concentrations of the dibutyl dithiophosphate acrylate adduct gave slightly better EP results with failure loads ranging from 125 to 180 kg and resulting WSDs of 2000 to 3500 μm . Experiments with the highest concentration may come in range of the dibutyl dithiophosphoric acid. The executed experiments gave welding at 180 kg and one negative experiment with WSD of 2000 μm . Nevertheless, duplication of the concentration resulted only in slight increase of EP performance, as stated by the slightly increased failure load. The resulting WSD after failure remains in the range of 3000 to 3500 μm .

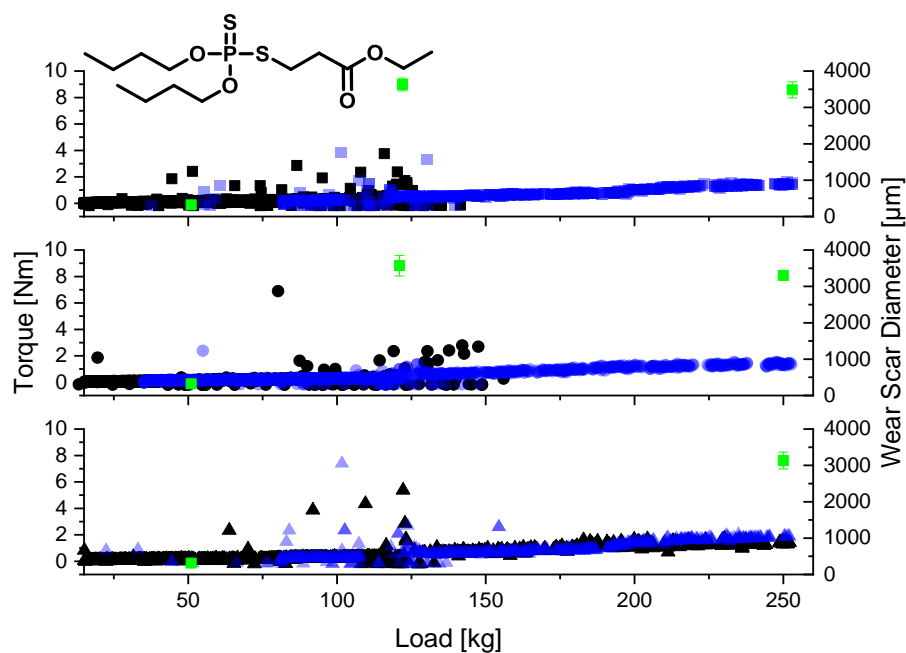


Figure 78. Torque-load curves and the WSDs (green) of dibutyl dithiophosphate ethyl acrylate adduct. Concentrations: 1 mmol S/50g base stock (squares), 1.5 mmol S/50g base stock (spheres) 2 mmol S/50g base stock (triangles). Duplicates in blue.

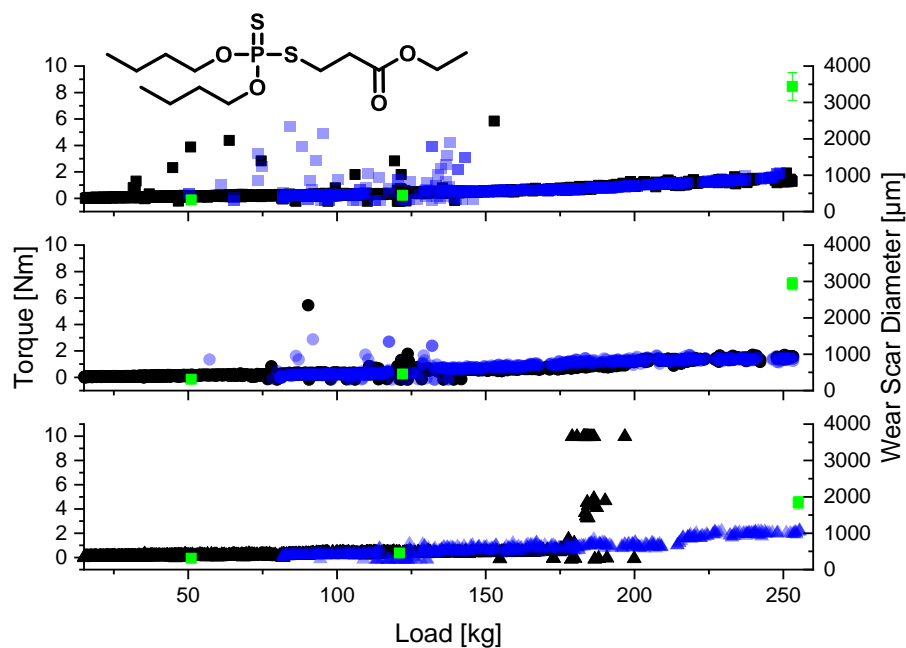


Figure 79. Torque-load curves and the WSDs (green) of dibutyl dithiophosphate ethyl acrylate adduct. Structure shown in graph. Examined concentrations: 1 mmol P/50g base stock (squares), 1.5 mmol P/50g base stock (spheres) 2 mmol P/50g base stock (triangle). Reproduction depicted in blue.

In conclusion, neutral alkyl dithiophosphates exhibit lower failure loads than the dibutyl dithiophosphoric acid. This may be explained by the corrosiveness of the free acid leading to increased wear. The commercial Irgalube 63 ® alkyl dithiophosphate

exhibited failure loads around 200 kg for 1 and 1.5 mmol P/50g base stock and strongly shattered failure loads ranging from 200 to 420 kg at 2 mmol P/50g base stock.

5.3.9 Extreme Pressure Performance of 1,3,4-Thiadiazol-2,5-dithiol Derivatives

The experiments above strengthened the assumption, that the presence of sulfur is important for reaching good EP properties. Thus, further sulfur-containing substances were examined In that regard. DMTD (**d**imercapto **t**hiadiazole) derivatives are commonly used additives as metal deactivators, copper inhibitors and EP additives.^{182–184} One disadvantage is their high corrosivity, indicated by reaction with metallic copper, silver and mercury.¹⁸⁵ A representative DMTD derivative is MC210® a 2,5-bis-tert.-dodecyl disulfanyl thiadiazole.¹⁸² The obtained EP data are given in Figure 80.

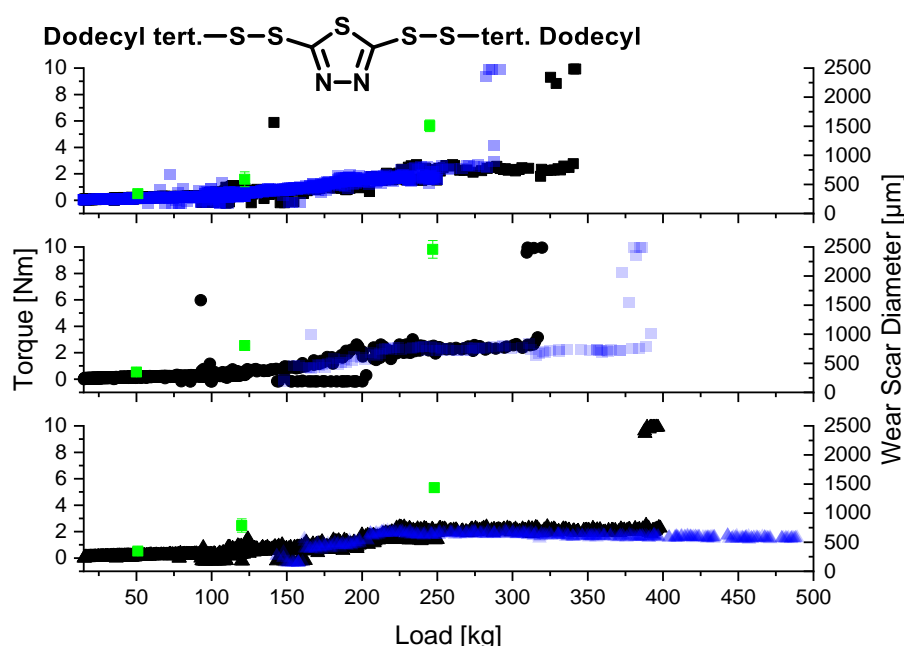


Figure 80. Torque-load curves and the WSDs (green) of MC 210®, structure shown in graph. Concentrations: 1 mmol S/50g base stock (squares), 1.5 mmol S/50g base stock (spheres) 2 mmol S/50g base stock (triangles). Duplicates in blue.

The experiments with MC210® also indicate that sulfur plays a key role in acquiring extreme pressure properties. The first load stage with peak loads of 50 kg gave WSDs in the range from 341 to 349 μm. The second load stage yields WSDs of 589 to 805 μm. Within the third load stage with peak loads of 250 kg the WSDs increase to a range of 1437 to 1508 μm and the torque curve exhibits a step at loads of 225 kg. This step might indicate a consecutive reaction of the additive with the iron surface. The

next higher load stage leads to welding and a concentration dependence is visible. The 1 mmol experiment exhibits weld loads of 285 kg to 340 kg while the 1.5 mmol experiment welds at loads ranging from 317 to 380 kg and the 2 mmol experiment at loads of 393 kg.

5.3.10 Extreme Pressure Performance of Dialkyl Polysulfides

Following the results obtained with MC 210®, next polysulfides were investigated as EP additives. This class of compounds is commonly accepted as superior EP additives in case of heavy duty applications.^{113,114} Their superior properties are related to the formation of iron sulfides, iron sulfites as well as iron sulfates.¹⁰⁶ Those layers effectively separate the metal surfaces from each other due to their mechano-chemical properties (melting points of the resulting layers, low shear forces, low hardness).¹⁸⁶ A commercially offered standard substance is TBPS454® (a product of Chevron Phillips) which is a di tert. butyl polysulfide with a sulfur content of approx. 53.5 wt%.^{187,188} The molecular weight of the (mixture of) component varies with the amount of sulfur in the polysulfide unit. An equivalent sulfur molecular weight can be calculated from the elemental composition. The resulting unit was $\frac{g_{product}}{mole_{sulfur}}$, from which the amount per mole sulfur could be calculated.

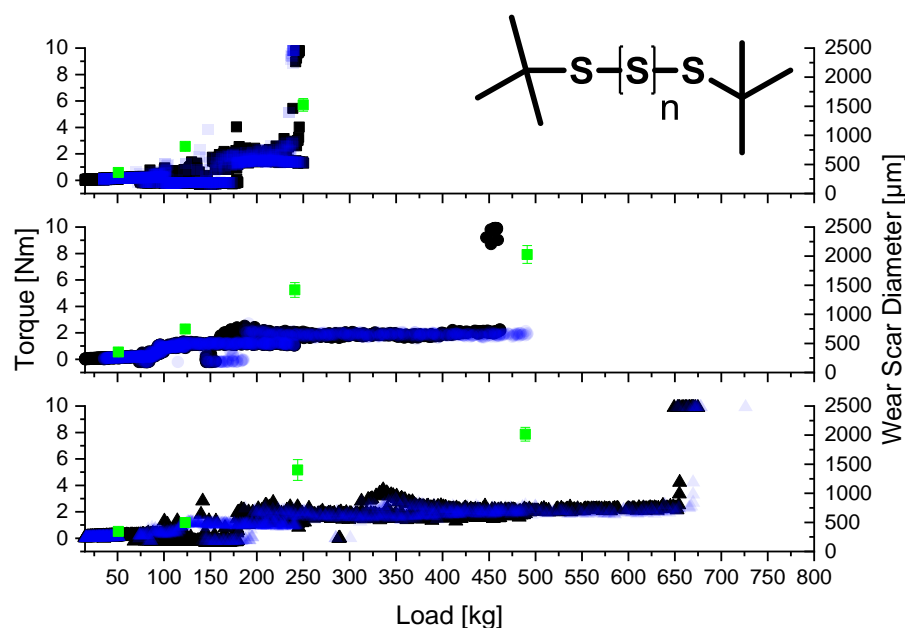


Figure 81. Torque-load curves and the WSDs (green) of di tert. butyl polysulfide. Concentrations: 1 mmol S/50g base stock (squares), 1.5 mmol S/50g base stock (spheres) 2 mmol S/50g base stock (triangles). Duplicates in blue.

The WSDs after the 2 kg load stage in EP experiments are 361, 351 and 345 μm (Figure 81). The 5 kg load stage revealed a significant increase of the torque and gave WSD with values of 809, 748 and 496 μm for sulfur concentrations of 1, 1,5 and 2 mmol/50 g of base stock, indicating a concentration dependent decrease of the wear. The WSDs from the 10 kg load stage are even higher with values of 1524, 1419 and 1401 μm .

The 20 kg load stage led to welding of the 1 mmol S/50g base stock experiment at 238 and 245 kg and 450 kg for the 1.5 mmol S/50g base stock experiment. No welding was observed in a second experiment, but a WSD of 2028 μm was obtained, indicating severe wear. The 2 mmol S/50g base stock experiments gave WSD values of 2015 μm for the 20 kg stage and instant welding within the starting period of the 30 kg and 40 kg stage. This observation is interpreted in terms of an imperfect formation of protecting iron-sulfidic layers in the initial phase. To reveal the true weld load, an advanced test was used, taking 20 kg as running-in conditions, and without unloading of the system the 30 kg respectively the 40 kg stage of increase were applied. Tribolayers were presumed to initially build. The WSDs obtained were 2078 μm for the 30 kg stage and welding at 655 kg respectively 670 kg for the 40 kg stage. Interestingly, the 30 kg load stage did not lead to welding. A possible explanation for this observation is based on

the available amount of additive. During the 40 kg run, exhaustive use of the additive may have occurred, leading to the welding.

The EP experiments with the polysulfide reveal its superior EP performance. Apparently, the quality of the lubrication is higher at higher concentrations, which is probably related to the amount of iron sulfidic species that can form in the time of the experiment. It needs to be mentioned, that all experiments of TBPS454® were accompanied by a pungent smell. It is strongly assumed, that an expected decomposition component in form of tert. butyl mercaptane is causing this. The usage of EP additives giving rise to release of safety relevant alarm substances may thus be reconsidered.¹⁸⁹

D-limonene and balsam turpentine oil (pinene) were next taken as starting materials for the preparation of polysulfides in an attempt to synthesize novel EP additives from renewable feedstocks with superior performance and with more pleasant esthetics. These compounds are naturally occurring terpenes with the empirical formula $C_{10}H_{16}$.¹⁵⁶ The sulfurization of D-limonene was easily performed, whereas the balsam turpentine oil could not be fully converted to the desired product (c.f. 5.1.4 Innovative Polysulfides).

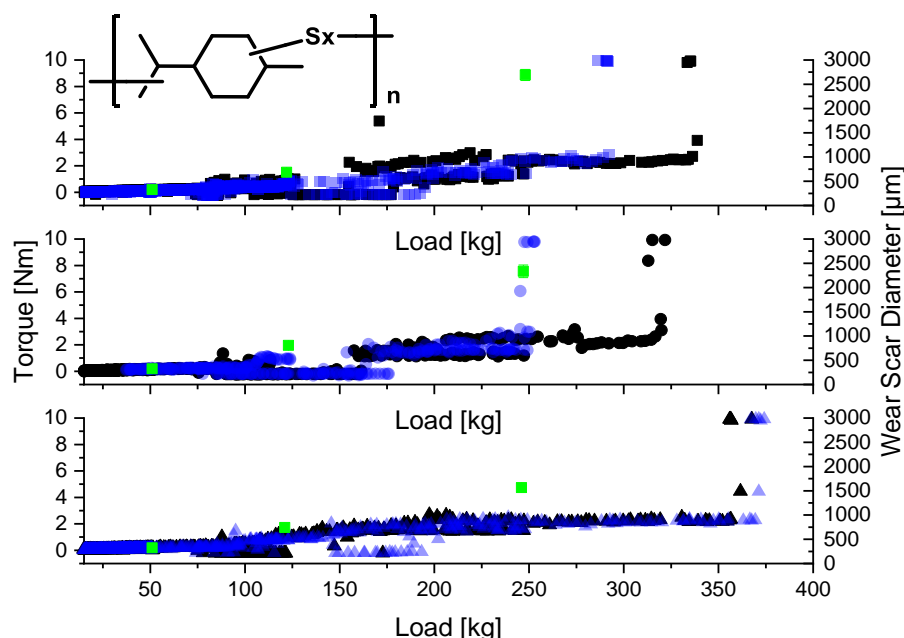


Figure 82. Torque-load curves and the WSDs (green) of D-limonene polysulfide. Examined concentrations: 1 mmol S/50g base stock (squares), 1.5 mmol S/50g base stock (spheres) 2 mmol S/50g base stock (triangle). Reproduction depicted in blue.

The polysulfide from limonene with the empirical formula $C_{10}H_{16}S_{3.2}$ showed good EP behavior as additive in stock oil (Figure 82). Note that the crude product was used. This product contains approx. 24 wt% volatile compounds at heating to 150 °C, p-cymene being the major compound.¹³¹

After the 2 kg load stage the WSDs after the 2 kg load EP experiment are 328, 323 and 324 μm for concentrations of 1, 1.5 and 2 mmol/ 50 g of base stock. These values are lower than the values obtained from the commercial polysulfide TBPS454®. This possibly is related to the better availability of sulfur for reaction with the iron surface.

The WSD values of 686, 808 and 743 μm for the 5 kg load stage are comparable to the values of TBPS454®. The values suggest, that the volatile sulfur containing compounds have limited EP properties at medium to high loads. The 10 kg load stage is characterized by a significant increase of WSDs to 2692, 2335 and 1565 μm at the concentrations of 1, 1.5 and 2 mmol/ 50 g of base stock.

The values indicate a concentration dependence of the resulting wear with lower WSDs at higher concentrations. The WSDs of the 2 mmol S/50g base stock experiment are comparable to the TBPS454® results. Lower concentrations of limonene polysulfide exhibit significantly higher wear. The 20 kg load stage is characterized by welding at all concentrations. The weld loads are in the range of 292 kg to 370 kg with the tendency to higher weld loads with increasing concentration. In conclusion, the novel polysulfides exhibit superior EP properties over the standard commercial product.

The limonene polysulfide however contains volatile components. These volatile components are undesired due to regulatory aspects. Therefore, these volatile compounds were removed by vacuum distillation and the resulting product was examined again with regard to the EP properties (Figure 83).

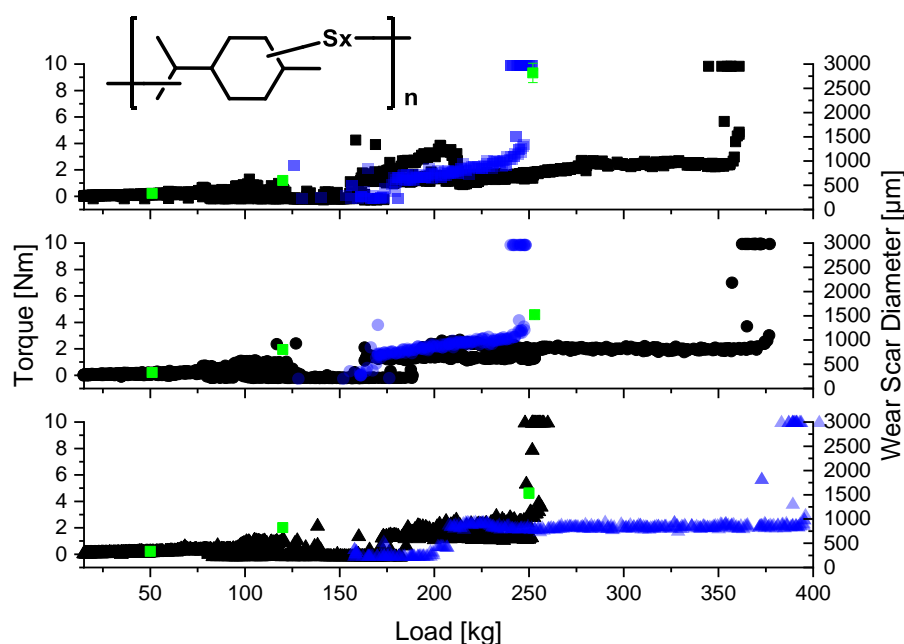


Figure 83. Torque-load curves and the WSDs (green) of vacuum distilled limonene polysulfide. Concentrations: 1 mmol S/50g base stock (squares), 1.5 mmol S/50g base stock (spheres) 2 mmol S/50g base stock (triangles). Duplicates in blue.

The WSDs after the first load stage with peak loads of 50 kg are in the range of 331 μm and comparable to the results of the crude product. A next load stage climaxes at 120 kg, yielding WSDs of 599 to 823 and no difference to the unpurified product is noticed. Based on these results, the assumption that volatile “mercapto” species are effective at lower loads can be negated. The third load stage climaxing at 250 kg yields WSDs of 2818 μm for the 1 mmol experiment and 1523 respectively 1532 μm for the 1.5 and 2 mmol experiments. In comparison to the unpurified product (2692, 2335 and 1565 μm) this may indicate the volatile components to be corrosive, and thus increase the WSD. No difference can be identified for the 2 mmol experiment. The weld loads occurring in the 20 kg load stage range from 250 to 400 kg and are comparable to the unpurified product with weld loads ranging from 250 to 375 kg.

In conclusion, the removal of the volatile by-products has no negative impact on the EP performance of the limonene polysulfide. This is of considerable advantage due to obligatory registration and declaration of small molecule by-products. It needs to be mentioned, that after heating under vacuum, the product turned into a sticky resin, which takes significant longer for complete solvation in mineral oil. This disadvantage can be circumvented by adding base oil or liquid AW additive directly after the thermal deodorization. Compared to reported EP data (wear scar diameter vs. load; 0.5wt% sulfur in the base oil) of monosulfides & disulfides the examined polysulfides yield lower

WSD at comparable loads as well as higher weld loads at lower sulfur contents (1 mmol – 2 mmol equals 0.06wt% to 0.13wt% sulfur). This observation is in good agreement to the postulated trend, that disulfides yield better EP data than monosulfides.⁹³

5.3.11 Extreme Pressure Additives in Comparison

An overview of the determined failure loads extracted from the 2 mmol experiments shows that some additives tested for show concentration dependencies, others do not (Figure 84). The failure loads were determined either by vibration effects of the load lever and significant increase of the WSD or extracted from curves, which exhibited decent weld loads. The failure loads given are the median of two experiments whenever possible. Trends may be discussed along the sulfur content of the molecules.

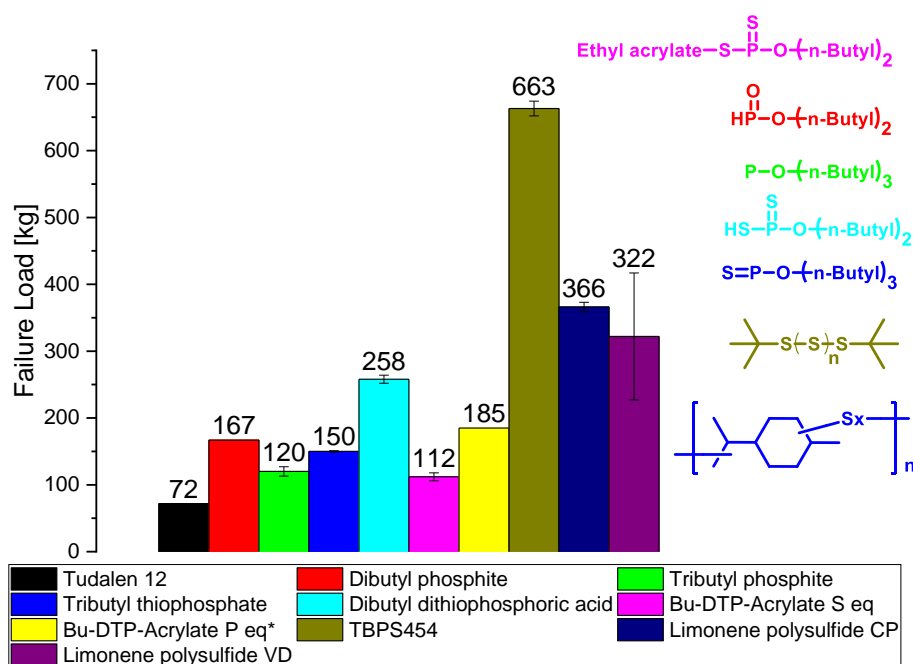


Figure 84. EP values of the butyl benchmark and additional D-limonene polysulfide experiments. Experiments at 2 mmol S/50 g base stock.* 2 mmol P equals 4 mmol S.

The base oil exhibited a failure load in the range of 70 kg in EP experiments. The experiments with phosphor (III) additives in form of dibutyl phosphite or tributyl phosphite are characterized by heavy vibrations and vibration effects. The failure loads ranged from 167 for the dibutyl phosphite to 120 kg for tributyl phosphite. It is assumed that dibutyl phosphite is more reactive towards the metal, leading to (weak) tribolayers.

The EP experiment with tributyl thiophosphate gives failure loads in the range of 150 kg accompanied by severe vibration effects. Experiments with dithiophosphates showed dibutyl dithiophosphoric acid to exhibit acceptable failure loads in the range of 258 kg. The neutral, alkylated derivatives yielded poor failure loads in the range of 112 kg for sulfur equivalent probes respectively 185 kg for the corresponding P equivalent experiment (2 mmol P implies 4 mmol S), nevertheless being significant better than dibutyl dithiophosphoric acid at equal concentrations. The experiment with tert. butyl polysulfide yielded failure loads in the range of 663 kg. It should be mentioned, that di tert. butyl polysulfide gives rise to a pungent smell that becomes worse during the experiment. Polysulfides derived from D-limonene yielded failure loads in the range of 322 to 366 kg in dependence to the work-up procedure. The crude product (CP) delivered median failure loads of 366 kg, while the vacuum distilled (VD) product exhibited failure loads over a broad range with a median failure load of 322 kg (illustrated by the error bars). The odor during the experiments with limonene derivatives was improved compared to the tert. butyl polysulfide.

In conclusion, sulfur carriers were confirmed as superior EP additives. In addition, it needs to be mentioned, that preparation of D-limonene polysulfide was the simplest, thus optimizations with regard to temperature, reaction conditions etc. can be considered. The results confirm, that renewable feedstocks can be used to synthesize highly efficient EP additives with comparable properties to commercial products.

5.3.12 Performance of Combined Anti Wear/Extreme Pressure Additives

Phosphonates could be identified as superior anti wear additives in the carried out experiments, while polysulfides confirmed their outstanding extreme pressure properties and the capability to separate surfaces thus inhibit welding. A patent was filed claiming oleyl-stearyl phosphonates as a superior AW additive and a petty patent for the use of polysulfides derived from natural occurring D-limonene as EP additive.

Based on these findings, it seemed of interest to examine combinations of phosphonates and polysulfides with regard to their AW and their EP performances. Such a potential “lubricants on demand” system could show advantages by varying the relative composition of both additives, depending on the application, e.g heavy load or long life anti-wear. The joint performance could be impeded by a possible reaction

between both additives. Phosphonates can be oxidized to phosphor (V) compounds by sulfur, resulting in poor AW properties.¹⁹⁰ As a consequence, the polysulfide would deplete and poor EP properties are the result.

Therefore, AW and EP experiments were performed with different ratios of AW (phosphonate) to EP (polysulfide) additive. One formulation had equal amounts of phosphonate and polysulfide (molar ratio 1:1), the second one combined 0.1 mmol phosphonate with 6 mmol S polysulfide. The first formulation was designed for long life anti-wear performance, the second for heavy duty applications. The resulting AW data can be seen in Figure 85 and the corresponding EP data in Figure 86.

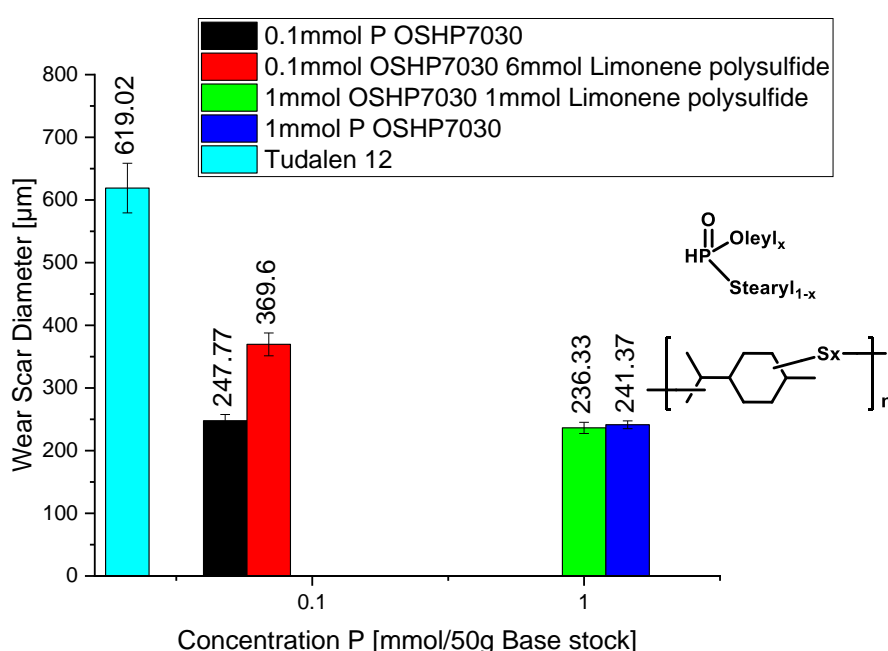


Figure 85. AW performance of a mixture of oleyl stearyl phosphonate and D-limonene polysulfide. 1 mmol P : 1 mmol S /50g base stock and 0.1 mmol P : 6 mmol S/50g base stock. Test conditions: 15 kg, 60 min, 1450 rpm, 25°C, 100Cr6 G10 steel balls.

The AW experiments of the 0.1 mmol P/50g base stock revealed a significant increase in the WSD: The obtained WSDs are 248 μm for the pure phosphonate and 370 μm for the mixture. This may indicate a reaction between both additives, however, The experiment of the mixture with 1 mmol P/50g base stock shows WSDs of 236 μm for the mixture and 241 μm for the pure phosphonate. The mixture exhibits thus comparable AW properties to the pure phosphonate at concentrations ≥ 1 mmol P. A reaction between both additives can thus be negated by these experiments.

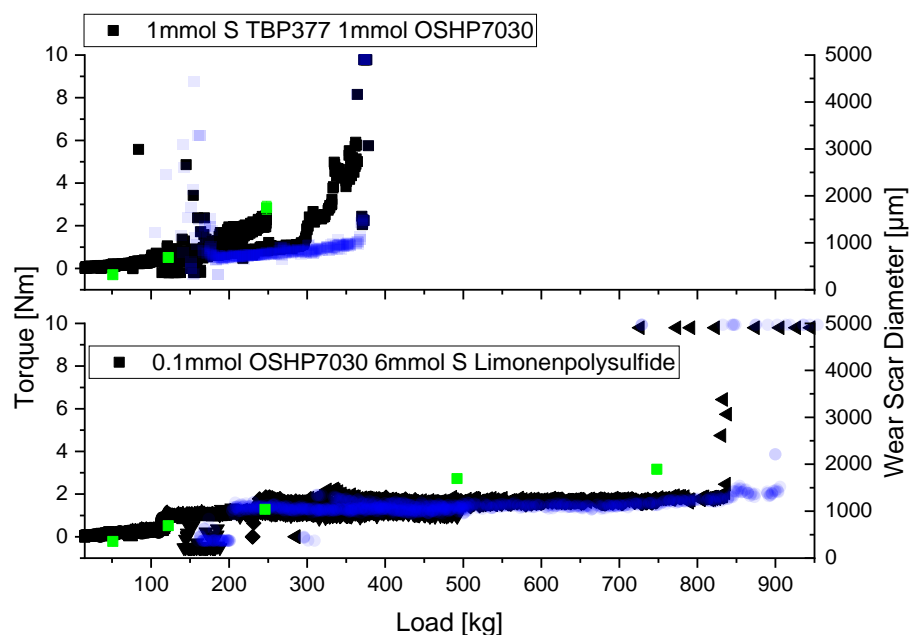


Figure 86. Torque-load curves and the WSDs (green) of the experiments with a mixture of oleyl stearyl phosphonate and limonene polysulfide. Top: 1 mmol P : 1 mmol S /50g base stock (squares), bottom: 0.1 mmol P : 6 mmol S /50g base stock (spheres). Duplicates in blue.

The obtained EP data strengthen the conclusion of absence of a reaction between the additives. The mixture with 1 mmol S/50g base stock exhibit a weld load in the range of 370 kg. This is slightly higher than in experiments of the pure limonene polysulfide with a weld load in the range of 292 to 336 kg, but still in the same order. The experiments with 6 mmol S reveal significantly higher weld loads in the range of 837 to 900 kg. As a result, both additives are compatible in a mixture and show synergistic effects. The concept of “lubricants on demand” with regard to tuneability of the AW/EP properties of the lubricant by variation of the S:P ratio could thus be a useful one. Typically, AW and EP additives are dosed in the range of 0.5 to 2 wt%.¹⁸² The 0.1 mmol P : 6 mmol S/50g base stock experiment corresponds to 0.11 wt% phosphonate and 1.12 wt% polysulfide. For the experiment with 1 mmol P : 1 mmol S/50g base stock weight fractions of 1.16 wt% phosphonate and 0.18 wt% of polysulfide were calculated. The weight fractions for the novel additives are lower than or on a scale with the industrial dosage and exhibit superior anti-wear and extreme-pressure performance.

5.3.13 Energy Dispersive X-Ray Analysis of Extreme Pressure Wear Scars

The resulting wear scars of the EP screening experiments after each stage load were analyzed by EDX to gain information about the correlation between EP performance (failure load) and surface composition as well as distribution of phosphor and if present sulfur. Various elemental distributions were expected in dependence of the load and the region within the wear scar.

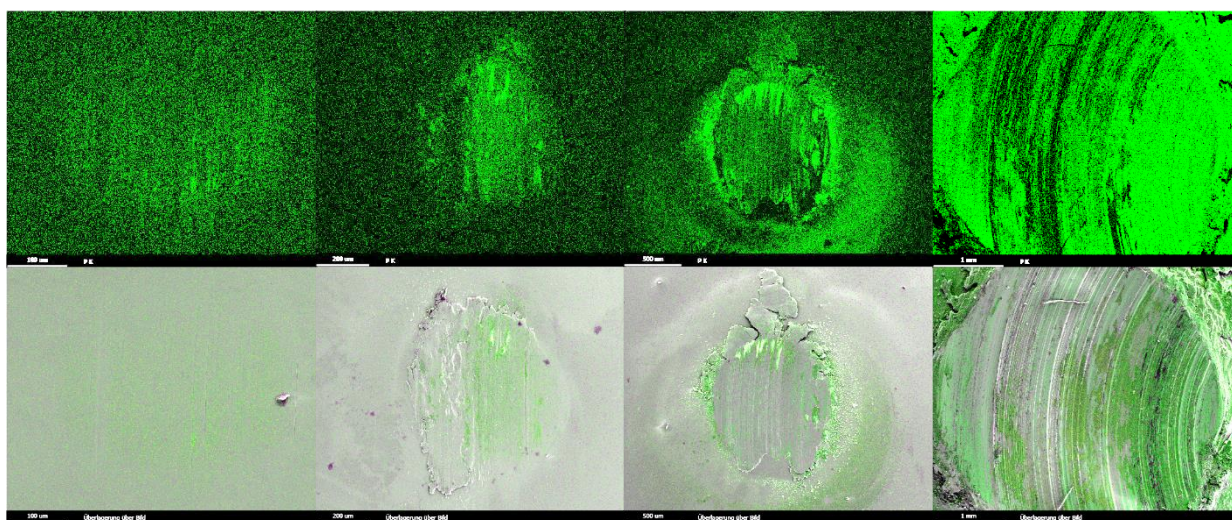


Figure 87. EDX analysis of 2 mmol dibutyl phosphonate. Top row: phosphor, bottom row: phosphor and wear scar image overlay. From left to right: 51 kg, 120 kg, 250 kg stage & 480 kg peak loads.

The EDX analysis of an EP experiment with 2 mmol of dibutyl phosphonate confirmed the presence of phosphor within the wear scar at lower loads up to 120 kg (Figure 87). Phosphor is detected within as well as in the surrounding of the wear scar at higher loads (250 kg). The highest load of 480 kg led to severe wear and phosphor was detectable throughout the wear scar and the close surrounding.

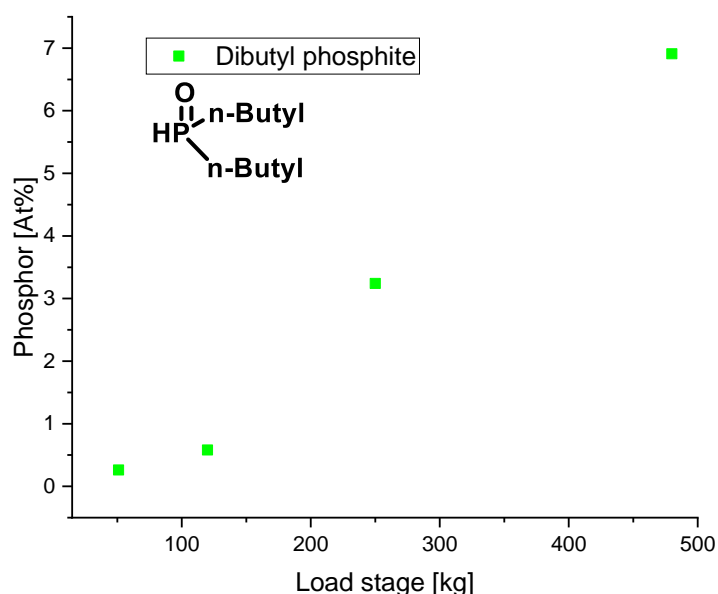


Figure 88. Measured phosphor in at% from the EDX analysis of EP experiments using 2 mmol dibutyl phosphonate in 50 g of base stock.

The phosphor content increases with the applied load with a peak phosphor content of approx. 7 at% in the measured wear scar area (Figure 88). Thus, increased load and wear lead to increased phosphor content of the tribolayer. In addition to phosphor, the presence of oxygen was found. It may be envisioned that also phosphor oxygen species might be formed, possibly in form of phosphates. Further investigations are necessary to clear this.

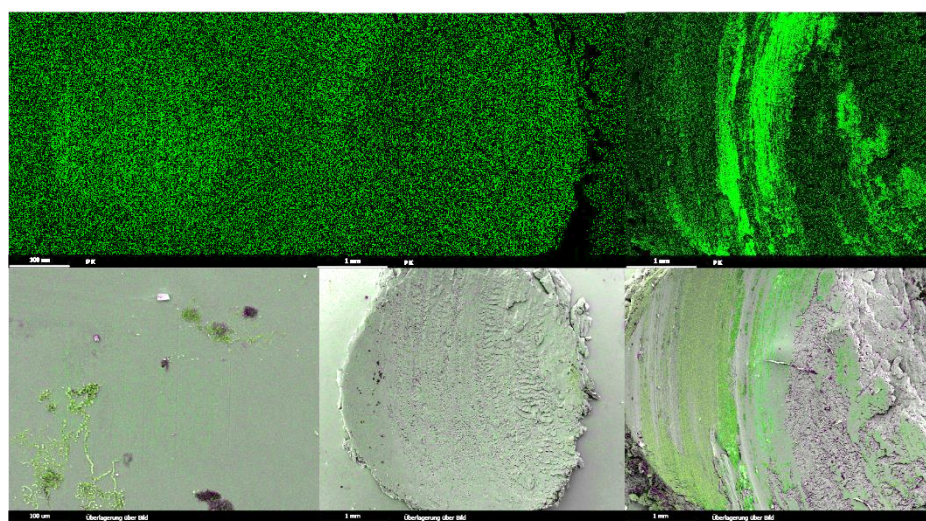


Figure 89. EDX analysis of EP experiments using 2 mmol tributyl phosphite in 50 g of base stock as lubricant. Top row: phosphor, bottom row: phosphor and wear scar image overlay. From left to right: 51 kg, 120 kg, 250 kg peak loads.

The observations for tributyl phosphite as lubricating additive at lower loads (51 and 120 kg) indicate less phosphor in the wear scar. Distinct phosphor signals occur only after application of 250 kg (Figure 89). The phosphor centers are predominantly in the middle of the wear scar. In total, significant less phosphor is detected as for dibutyl phosphonate and the distribution hints that no effective formation of a tribolayer has taken place (Figure 90). Overall very low phosphor contents were measured. At lower loads (51 and 120 kg) the phosphor content is close to zero, while higher loads lead to the incorporation of approx. 1.3 at% phosphor within the tribolayer. This correlates to the poor EP properties, indicating the relevance of generating a phosphorous containing tribolayer.

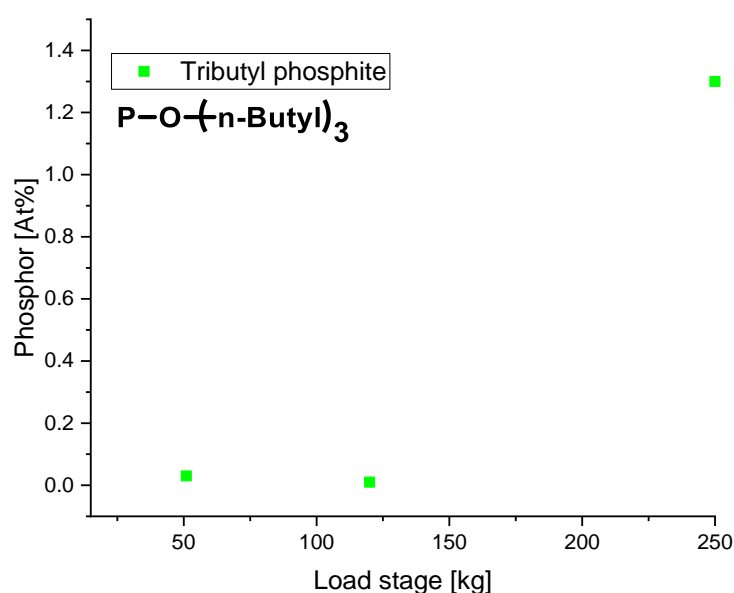


Figure 90. Measured phosphor at% from the EDX analysis EP experiments using of 2 mmol tributyl phosphite in 50 g of base stock.

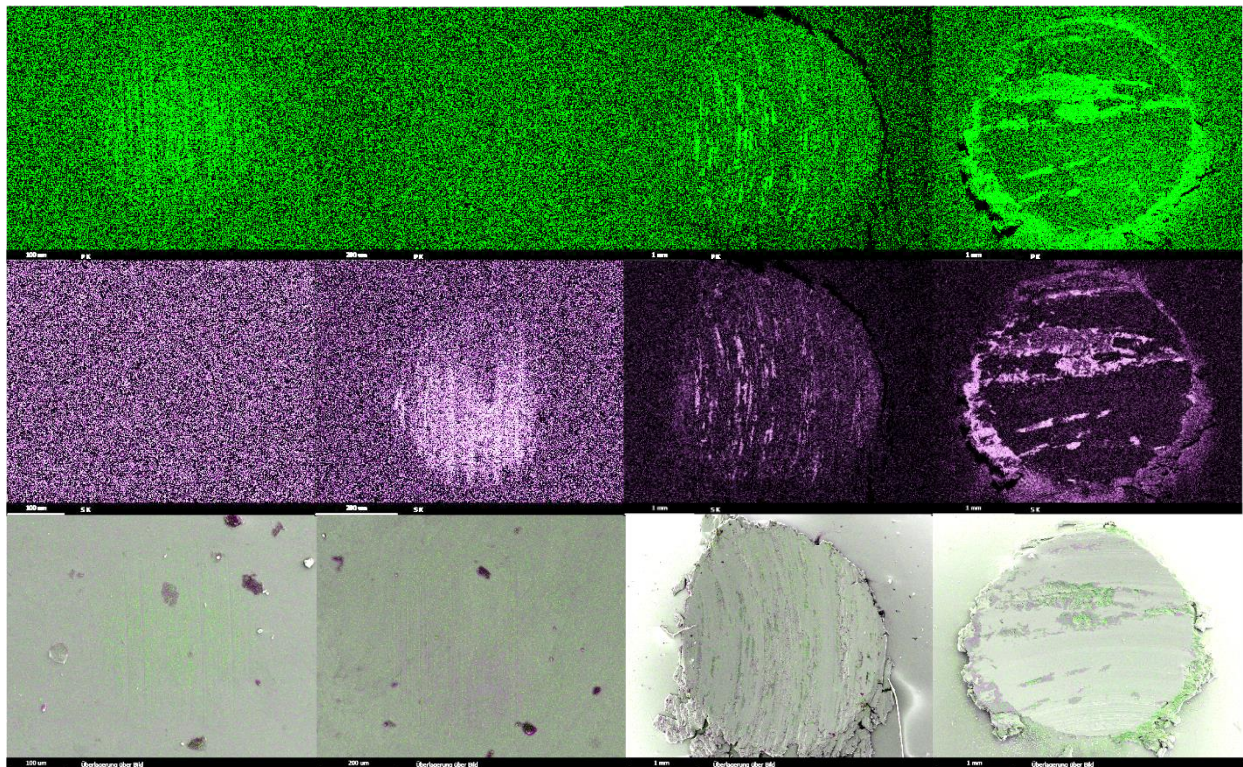


Figure 91. EDX analysis of EP experiments with a lubricant containing 2 mmol tributyl thiophosphate per 50 g of oil. Top row: phosphor, middle row: sulfur, bottom row: phosphor, sulfur and wear scar image overlay. From left to right: 51 kg, 120 kg, 250 kg & 480 kg peak loads.

Tributyl thiophosphate contains equal amounts of phosphor and sulfur. The EDX analysis of the EP screening wear scars of the lowest load indicates presence of phosphor but no sulfur (Figure 91). This fits to the EDX analysis of the wear scars from AW experiments in which no sulfur was detected. At increasing loads the situation inverts and sulfur is detected in the wear scars but no phosphor. This suggests that after extraction of phosphor the resulting sulfur containing compounds need more severe conditions to react with the metal surface. As a consequence, the low load phosphor containing layers are torn apart or covered by sulfur containing layers. Both phosphor and sulfur are detected in the scar at increasing loads of 250 kg. Both elements are detected in regions of intense contact also in EP experiments of still higher loads (Figure 92).

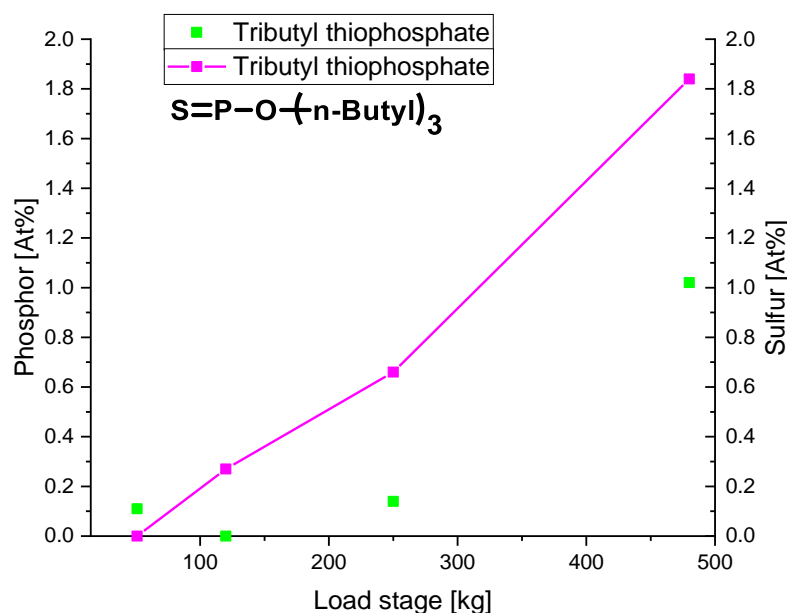


Figure 92: Measured at% phosphorus (green squares) and sulfur (magenta line) resulting from the EDX analysis of 2 mmol tributyl thiophosphate in 50 g of base stock.

The results of the EP experiments are readily interpreted from the images. Low loads (51 kg) favor the build-up of phosphorus containing tribolayers, while sulfur is not actively incorporated. Increasing loads lead to incorporation of sulfur (0.3 at%) and no phosphorus is detectable. Further increased loads (250 to 480 kg) lead to increased incorporation of sulfur and moderate incorporation of phosphorus with at% range between 0.2 at% to 1 at% for phosphorus and from 0.2 to approx. 1.8 at% for sulfur. The distribution of the detected elements can be a hint for the weak EP properties. Especially at higher loads sulfur and phosphorus pile up in the vicinity of the wear scar in sliding direction. Within the wear scar scattered distributions are observed in contrast to the lower load EDX pictures (51 kg & 120 kg peak load), where the elements are more or less evenly distributed throughout the wear scar. The uneven formation of a tribolayer within the wear scar as well as the accumulation of torn tribolayers at the edges of the wear scar in sliding direction might be a hint for the weak EP properties.

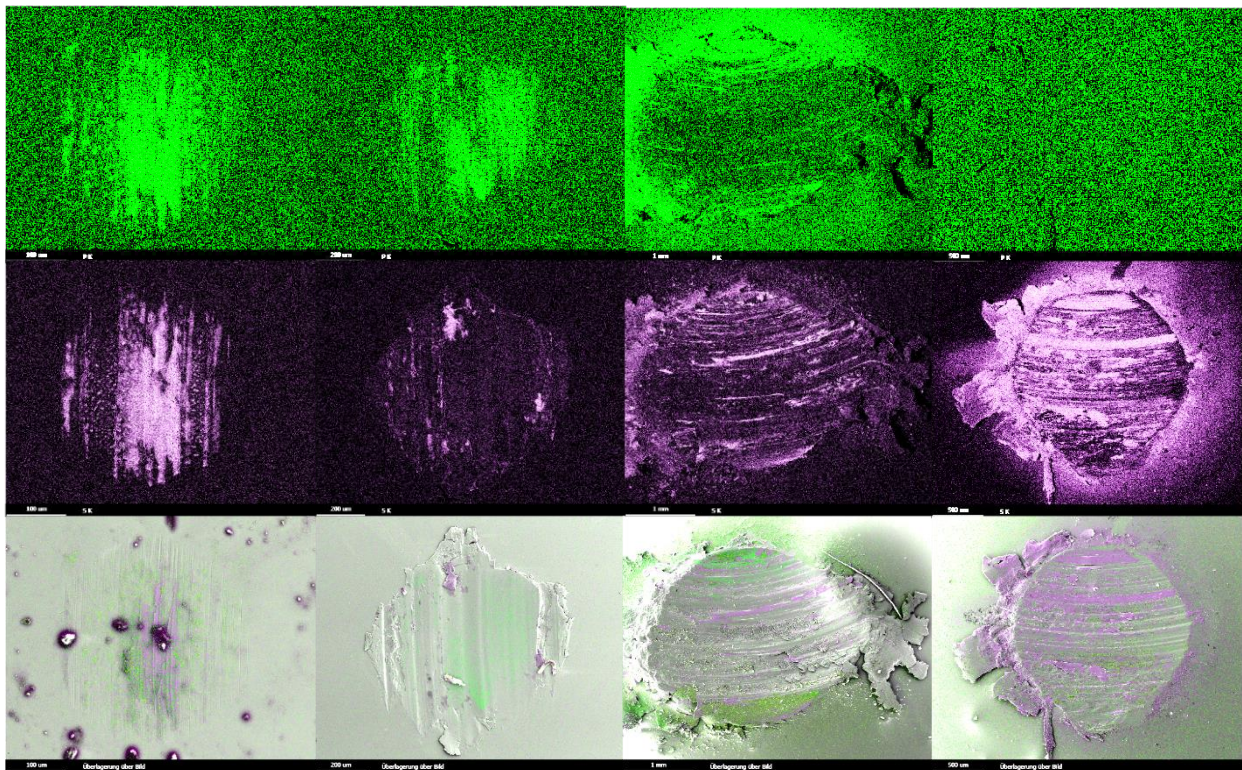


Figure 93. EDX analysis of EP experiments with 2 mmol dibutyl dithiophosphoric acid in 50 g of stock oil. Top row: phosphor, middle row: sulfur, bottom row: phosphor, sulfur and wear scar image overlay. From left to right: 51 kg, 120 kg, 250 kg & 480 kg peak loads.

The wear scar in EP experiments using dibutyl dithiophosphoric acid reveal phosphor and sulfur throughout the wear scar for low loads up to 51 kg (Figure 93, Figure 94). The wear scar after up to 120 kg load show phosphor and only a low sulfur content. Experiments with loads up to 250 kg show phosphor especially in the surrounding area of the wear scar and sulfur within the wear scar and at the edges where debris is piled up. The highest load of 480 kg has a wear scar lacking phosphor but sulfur was detected within and around the wear scar. In addition, sheet like structures are noticed where high sulfur contents are present. This may be due to the formation of iron sulfide and iron sulfate layers, which shear facile from the bulk metal, thus separating the surfaces.^{106,186} In addition, it becomes evident, that phosphor has no significant impact on EP properties.

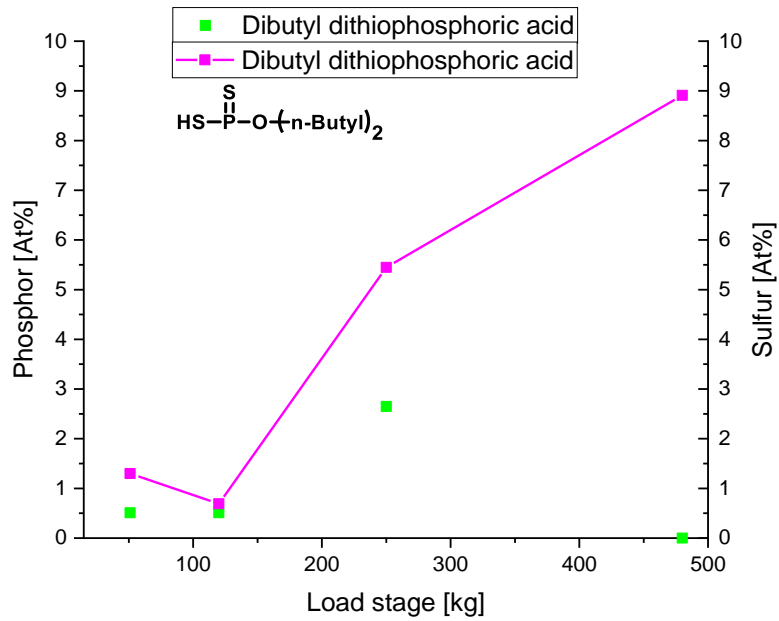


Figure 94. Measured phosphor at% (green squares) and sulfur (magenta line) resulting from the EDX analysis of 2 mmol dibutyl dithiophosphoric acid in 50 g of base stock.

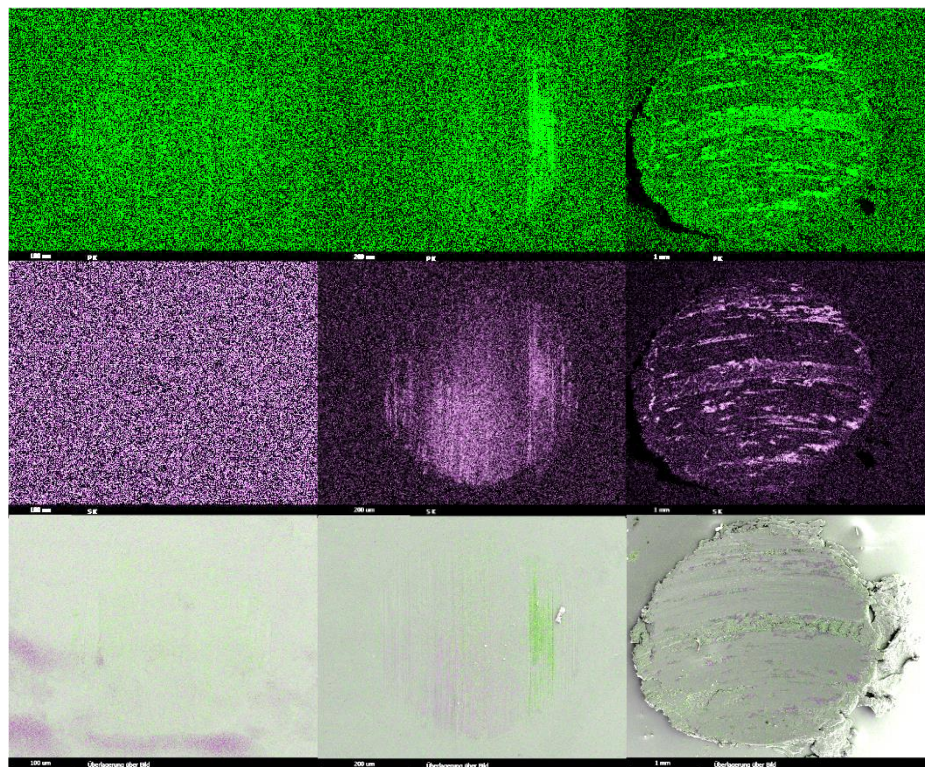


Figure 95. EDX analysis of 2 mmol S dibutyl dithiophosphate acrylate. Top row: phosphor, middle row: sulfur, bottom row: phosphor, sulfur and wear scar image overlay. From left to right: 51 kg, 120 kg & 250 kg peak loads.

The analysis of the wear scars when using dibutyl dithiophosphate acrylate gives a similar picture with minor amounts of phosphor at low loads (Figure 95). The scar from a 120 kg peak load reveals sulfur throughout the wear scar whereas slightly increased

amounts of phosphor were detected in the area next to the deeper scar (Figure 96). With increasing loads, phosphor and sulfur are detected only in the scratches. It is likely, that the neutral dithiophosphate is either not adsorbed at the metal surface in time or that depletion takes significant longer than for the free acid. The EDX values strengthen the poor ability of tribolayer formation within the short period of the EP experiment. The peak load 250 kg yields approx. 0.5 at% of phosphor and 5.5 at% of sulfur. The sulfur content compares well to the values found for the corresponding free acid.

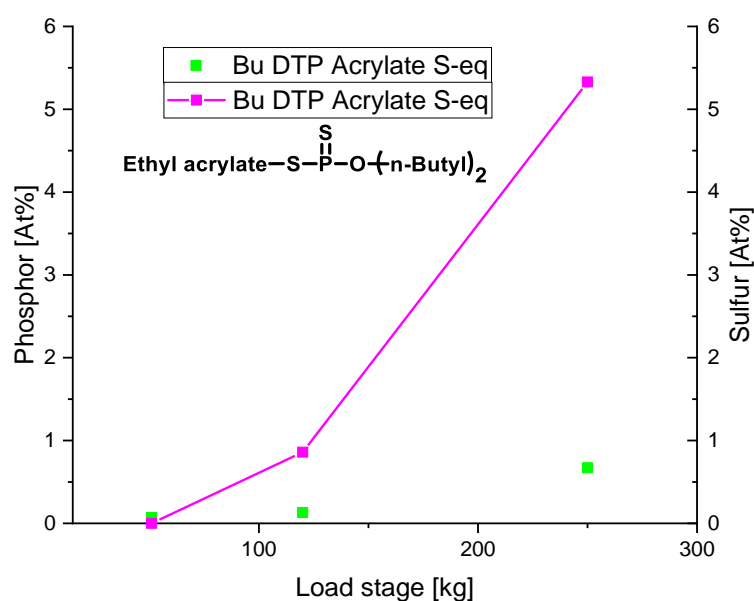


Figure 96. Measured at% phosphor (green squares) and sulfur (magenta line) resulting from the EDX analysis of 2 mmol S dibutyl dithiophosphate acrylate adduct in 50 g of base stock.

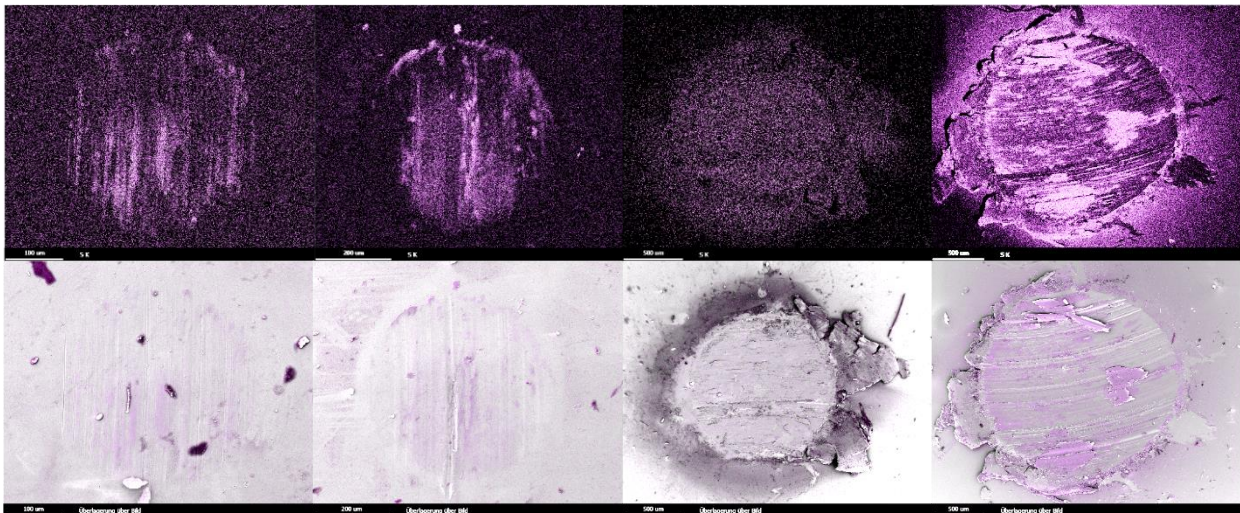


Figure 97: EDX analysis of 2 mmol di tert. butyl polysulfide (TBPS454®). Top row: sulfur, bottom row: sulfur and wear scar image overlay. From left to right: 51 kg, 120 kg, 250 kg & 480 kg peak loads.

The EDX analysis of the wear scars from using di tert. butyl polysulfide (TBPS454®) indicate increasing sulfur content with increasing peak load (Figure 97). At low loads climaxing at 51 and 120 kg minor traces of sulfur are detected within the wear scar. The distribution is even, and only small aggregations are found in deeper scratches. At higher loads climaxing at 250 kg the distribution of sulfur is both within the wear scar and also in the close vicinity, which may result from debris at the edges of the wear scar. The maximum load of 480 kg yielded a similar picture. The formation of debris at the edges of the wear scar in the sliding direction has significant amounts of sulfur. This is comparable to the observations of the dithiophosphoric acid experiment and strengthens the assumption, that shearing off of sulfur-containing tribolayers effectively separates the metal surfaces. In addition flakes can be seen in the overlay image.

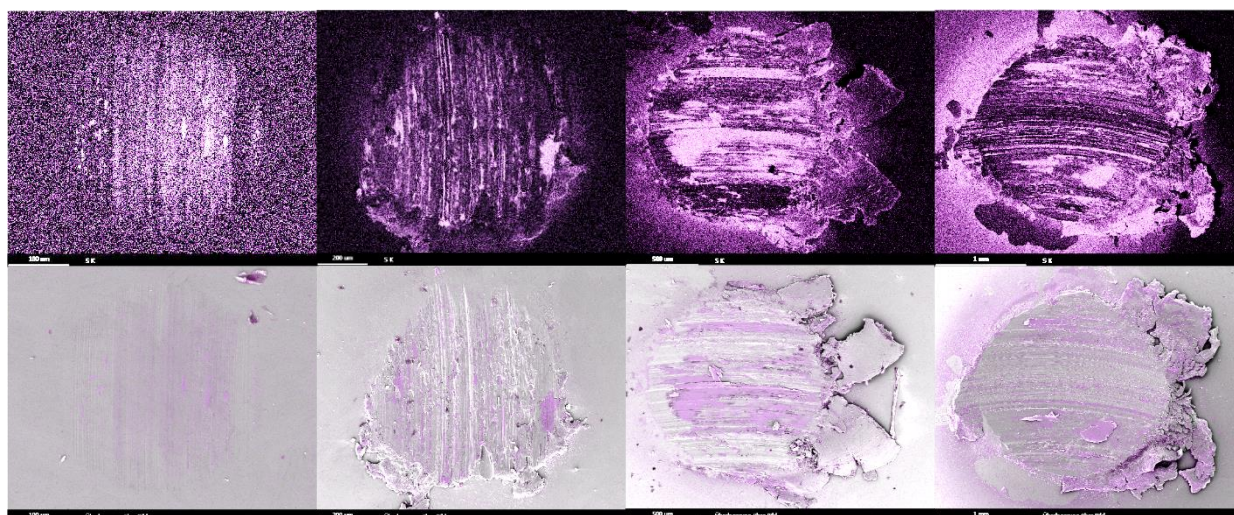


Figure 98. EDX analysis of 2 mmol limonene polysulfide vacuum distilled. Top row: sulfur, bottom row: sulfur and wear scar image overlay. From left to right: 51 kg, 120 kg, 250 kg & 480 kg peak loads.

The EDX of the scars using limonene polysulfide (Figure 98) are quite similar to those of di tert. butyl polysulfide TBPS454®. The sulfur content increases with increasing load, and the formed debris contains significant amounts of sulfur. In addition, flakes of debris indicate the separation of the surfaces by formation of tribolayers with low adhesion to the bulk metal. Polysulfides appear to react according to a similar mechanism of action: the organic residue has minor impact on the EP performance. The wear scars of the heated product of sulfurizing limonene show comparable results.

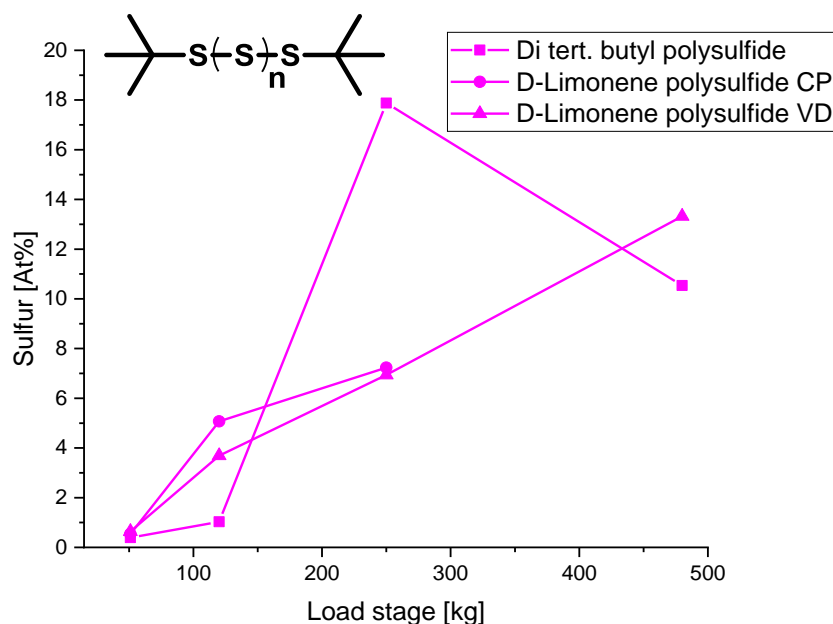


Figure 99. Measured at% sulfur (magenta line) resulting from the EDX analysis of 2 mmol S di tert. butyl polysulfide (squares), limonene polysulfide CP (dots) and limonene polysulfide VD (triangles) in 50 g of base stock.

The EDX data indicate minor differences between the sulfurizing activity of the commercial di tert. butyl polysulfide (TBPS454®) and the limonene polysulfide (Figure 99). In detail, the lowest peak load yields sulfur contents of approx. 0.5 at% for all three polysulfides. After the next load stage with peak loads of 120 kg, the limonene derivatives exhibit sulfur contents ranging from 4 to 5 at%, significantly higher than the values of approx. 1 at% for the commercial product. The commercial product then reveals the highest sulfur content in the scars of 18 at%, which is declared as an outlier due to the significant lower sulfur content at the next higher load stage, while the limonene polysulfide yields values of approx. 7 wt%. The next load stage with peak loads of 480 kg equals the sulfur contents in the range of approx. 14 at% to 11 at% for the commercial product, respectively the D-limonene polysulfide.

In addition, EDX analyses of the experiments with combinations of oleyl-stearyl phosphonate as AW component and limonene polysulfide as EP component were performed (Figure 100).

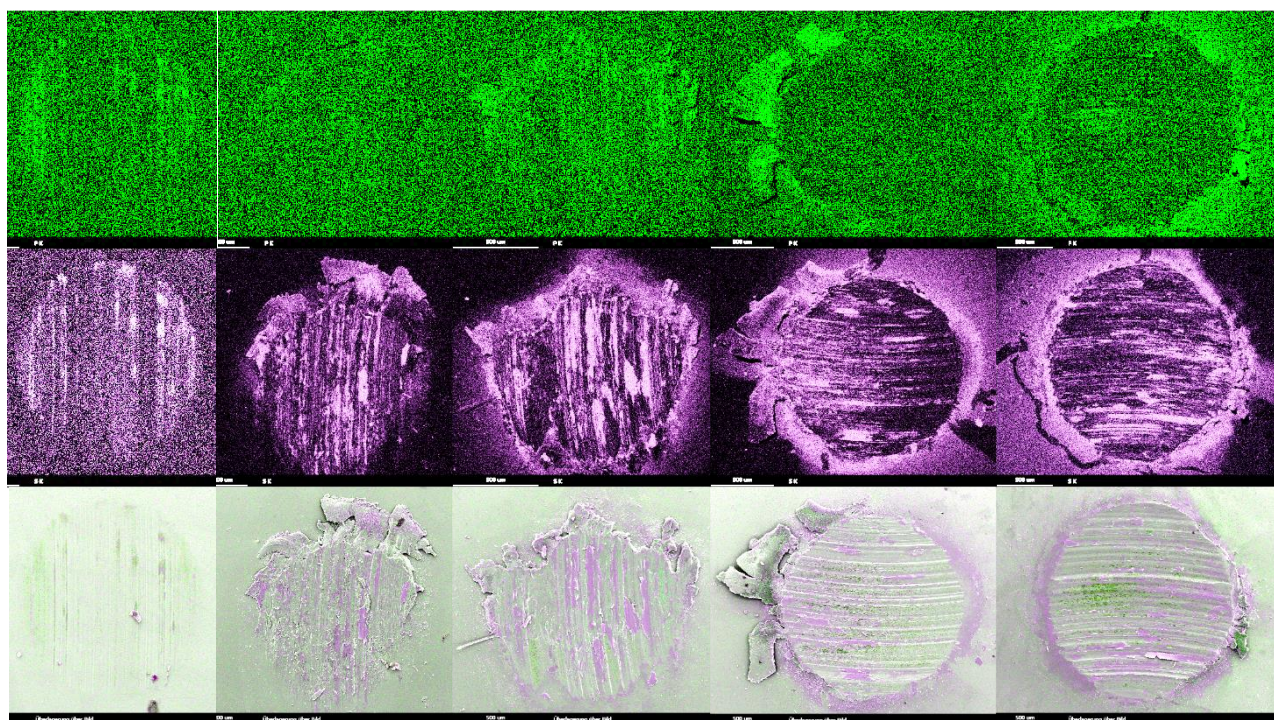


Figure 100. EDX analysis of 0.1 ml P oleyl-stearyl phosphonate and 6 mmol S limonene polysulfide crude product in 50 g of base stock. Top row: phosphor, middle row: sulfur, bottom row: phosphor, sulfur and wear scar image overlay. From left to right: 51 kg, 120 kg, 250 kg, 480 kg & 1000 kg peak loads.

The results from the EDX analysis confirm the AW effect of phosphor at low loads and sulfur for high loads. The wear scar resulting from peak loads of 51 kg contains both elements evenly distributed. The next load stage with peak loads of 120 kg shows significant lower amounts of phosphor and increased sulfur content in the scratches in sliding direction. In addition, the wear scar again shows debris with high sulfur contents. The load stage with 250 kg peak load gives comparable results. The phosphor content is slightly increased and distributed near the edge of the wear scar in sliding direction. The sulfur is detected throughout the wear scar. The wear scars resulting from peak loads of 480 and 1000 kg yield low phosphor contents which are located around the wear scar and high sulfur content. In contrast to the aforementioned wear scar yielded from peak loads up to 250 kg, the sulfur content within the wear scar of peak loads yielded from 480 and 1000 kg peak load is lower and focused on the edges where debris piled up. This is typical for low shear-stable sulfur containing tribolayers and further again strengthens the assumption, that no reaction occurred between both additives.

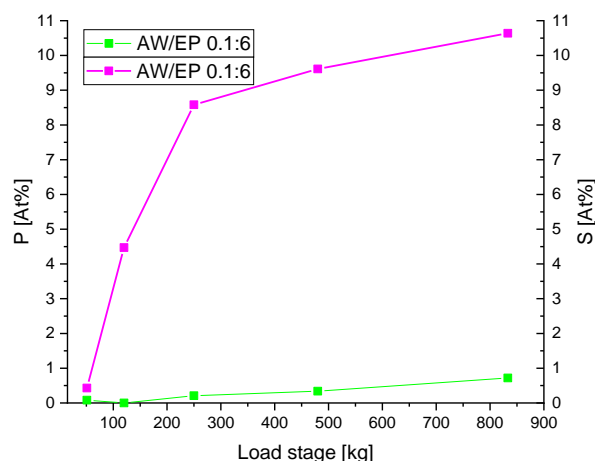


Figure 101. Measured at% phosphorus (green squares) and sulfur (magenta line) resulting from the EDX analysis of 0.1 mmol P oleyl stearyl phosphonate and 6 mmol S limonene polysulfide CP.

The experiments yield increasing sulfur contents ranging from approx. 0.5 at% to approx. 10.5 at% at loads ranging from 51 to approx. 850 kg (Figure 101). Until approx. 250 kg a strong growth of the sulfur content is found, which levels off at even higher loads. The values strengthen the assumption that sulfur contributes significantly to the EP properties and phosphorus has minor impact on the EP properties but yields superior protection at low loads. Comparing the sulfur contents of the commercial product (10 at% after 500kg peak load) and the D-limonene polysulfide it might be possible, that at a certain load (for the examined D-limonene polysulfide above approximately 250 kg) a threshold of sulfur within the tribolayer occurs until welding. As a consequence an equilibrium where growth and shearing-off of excess sulfur takes place, separating the surfaces. This equilibrium is dependent of the sulfur source (e.g. polysulfides, dithiophosphates, etc.) and thus, different weld loads for those additives are observed.

Further investigations on an optimized synthesis of D-limonene polysulfide need to be performed to check if I) even higher sulfur contents in the final product correlate with a higher sulfur content within the tribolayer, respectively higher failure loads or II) the weld load is a function of the available additive, which depletes in the friction zone. Possible approaches for improved synthesis may be the dosage of sulfur containing compounds over a period, addition of catalytic amounts radical initiators or amines.¹¹³

The EDX analysis of the wear scars of different functional groups showed polysulfides to give the highest sulfur content in the wear scars. This goes along with being the best

EP additives. Generally, EP and AW performance can be related to the EDX results. The assumed difference in the reactivity of the sulfur derivatives resulting from depletion of phosphor and sulfur containing additives were strengthened by the EDX analysis of the EP-wear scars. It was observed, that at low loads, phosphor is the dominating element within the wear scar, while higher loads yield higher sulfur contents in the wear scar. It could be suggested, that an equilibrium of growth and shearing-off of the tribolayer separates the surfaces until welding occurs. The detected sulfur amount in the range of 10at% might resemble this equilibrium. The limited growth of (oxide) layers was described by Mott-Cabrera¹⁹¹ and discussed in context of tribolayer growth resulting from disulfide depletion on metal surfaces.¹⁹²

It was further shown, that renewable feedstocks are suitable for the synthesis of ecofriendly EP additives with superior performance and the possibility to combine AW and EP additives. This gives future opportunities to design AW/EP combination suitable for appropriately desired tasks.



6. Experimental










Parts of the following chapters are summarized elsewhere.¹⁻⁵









All chemicals were used as received. Substances prone to oxidation and hydrolysis were stored and handled under argon.











6.1 Chemicals and Safety¹⁹³









Table 2.: Detailed Chemicals and Suppliers


Substance CAS-Nr.	GHS Label	H- Statements	P- Statements	Supplier Purity Art. Nr
Acetone-d6 666-52-4	 	225-319-336	210-240- 305+351+338 -403+233	Deutero 99.80% 00105-100mL

Argon 7440-37-1				Diverse 99.999%
Dibenzothiophene 132-65-0		302-410	273-501	Fishersci 98% 10010800
				
Dibutyl phosphite 1809-19-4		312-315-318- 335-351	201-280- 302+352+312 - 305+351+338 +310- 308+313	TCI >95% D0300
Dimethylphosphite 868-85-9		317-341-351- 412	201-273-280- 302+352- 308+313	Sigma Aldrich 98% D178454- 500G
				
Dipentene dimercaptane 4802-20-4		317-320	264-280- 302+352- 305+351+338 -333+313- 337+313- 363-501	Chevron Phillips 80-100% 1102727
TBPS454® (Di-tert. butyl polysulfide) 68937-96-2		317-410	261-272-273- 280- 302+352- 333+313- 362+364- 391-501	Chevron Phillips 90-100% 1120381
				

2-Ethylhexyl acrylate 103-11-7		315-317-335- 412	273-280- 304+340+312 -333+313	BASF >99.6% BASF 2-EHA
Hexanediol diacrylate 13048-33-4		319-315-317	280- 305+351+338	BASF >90% Laromer HDDA
D-Limonene 5989-27-5		226-315-317- 410	210-273-280- 302+352	Weissmeer Baltische >93% WMB- d'Limonene
				
				
Menthol 89-78-1		315-319	302+352- 305+351+338	Merck >99% 818452
Octanethiol 111-88-6		317-410	273-280- 302+352	Fishersci 98% 11397176
				
Oleyl alcohol Tech. 143-28-2	No hazardous substance according to GHS			Sigma Aldrich 85% Z Isomer 11459156- 500G

Phosphor pentasulfide 1314-80-3	  	228-260-302- 332-400	210-260- 231+232- 273- 370+378-422	Prasol Chemicals PVT.LTD 71.8-72.7 % Sulfur PR/PPS/17/09 -00
Phosphor trichloride 7719-12-2	  	314-330-373- 300	280- 301+330+331 -304+340- 305+351+338 -310- 402+404	Acros 99% 169480010
Phenoxyethyl acrylate 48145-04-6	  	317-361df- 411		BASF 100% Laromer POEA
Sulfur 7704-34-9		315		Sigma Aldrich >99% 84683

Toluol Tech. 108-88-3		225-304-315- 336-361d- 373	210-240- 301+310+330 -302+352- 314-403+233	BCD >99
				
				
Tri-n- butylphosphite 102-85-2		312-315-319	264-280- 337+313- 332+313- 302+352+312 -501	TCI >93% T0362
Triethylamine 121-44-8		225-302- 311+331- 314-335	210-280- 303+361+353 -304+340- 310- 305+351+338 -403+233	Roth >99.5% X875.3
				
				
Tris(2-ethylhexyl) phosphate 78-42-2		315-319	264-280- 302+352+332 +313+362+36 4- 302+351+338 +337+313	TCI >98% P1022
Trilauryl trithiophosphite 1656-63-9	No classification according to GHS			TCI 100% T0460

Trioleyl phosphite 13023-13-7	No classification according to GHS	TCI 98% P0390
Tudalen ® 12	No classification according to GHS	Hansen & Rosenthal KG
Vanillin 121-33-5		319 264-280- 305+351+338 -337+313
		Sigma Aldrich 99% V1104-100G

12.7 mm 100Cr6 steel balls used in VKA anti wear analyses were manufactured by KGM in G10 grade. Extreme pressure data was obtained using 12.7 mm 100Cr6 steel balls in G10 grade purchased from TIS GmbH.

12.7 mm 1.0616 steel balls in G200 grade were purchased from TIS GmbH.

12.7 mm 1.4034 steel balls in G100 grade were purchased from TIS GmbH.

6.1.1 Disposal

Arising substances were disposed according to the rules of action from the University of Hamburg¹⁹⁴ compliant to the DGUV 213-850¹⁹⁵. Liquids were separated into halogenated and non-halogenated substances. Solid materials were collected in plastic bags, glassware was collected in plastic packaging. Syringes were collected in particular syringe containers and disposed with solid waste. CMR substances were collected in the container for halogenated substances. Acidic and basic disposals were each collected in separated containers.

6.2 Scientific Devices

Nuclear Magnetic Resonance

The NMR analyses were performed on 300, 400 or 500 MHz Bruker Avance I, II or III devices at the NMR faculty of the University of Hamburg. NMR solvents were purchased from Deutero GmbH. Spectra were primarily referenced to the solvent signal (preferred CDCl₃), otherwise on the tetramethyl silane signal. Data processing was performed with MestReNova ® 14.

Elemental Analysis

The elemental analyses were performed at the faculty of elemental analysis of the University of Hamburg. The CHNS combustion analyses were performed on EuroEA Elemental analyzer devices and the combustion gases were quantified by GC and thermal conductivity, while phosphor analyses were performed by titration after chemical digestion by a mixture of HNO₃ and sulfuric acid.

Mass Spectroscopy

The MALDI-MS spectra were obtained on a Bruker Ultraflexxtreme Smartbeam II Laser MALDI TOF-TOF device. Dithranol (CAS Nr.: 1143-38-0) was used as matrix and silver trifluormethanesulfonate (CAS Nr.: 2923-28-6) was used as ionizing agent. The samples were solved in an appropriate solvent and mixed with a solution of the matrix as well as the ionizing agent. The combined solutions were dropped on the MALDI sample plate. The obtained signals were assigned to the sodium, ammonium, potassium or silver compounds.

Electron Microscopy

The chemical surface composition of the wear scars was analyzed by energy dispersive x-ray scattering (EDX). The analysis was performed on a Zeiss Leo Gemini 1525 equipped with EDAX software and in-lens as well as SE detector. The coating of the steel balls with carbon was not necessary due to the conductive properties of the steel balls. The EDX analysis was typically performed at 20kV. Element mapping was performed using the K-lines of oxygen, phosphor, carbon and sulfur.

Laser Microscopy

Optical microscopy was performed to collect information about the wear scar diameters. The wear scar diameters were measured with a Keyence® VK-X200 laser scanning microscope. The evaluation was performed with the corresponding Keyence® software. Magnification was chosen so that the wear scar was visible in total.

6.3 Organic Chemical Nomenclature

	$\text{HO}-\text{R}$ Alcohol	$\text{HS}-\text{R}$ Mercaptane	$\text{R}-\text{S}(\text{S})_n\text{S}-\text{R}$ Dialkyl polysulfide		
$\begin{array}{c} \text{O} \\ \parallel \\ \text{R}-\text{O}-\text{P}-\text{H} \\ \\ \text{O} \\ \\ \text{R} \end{array}$	$\begin{array}{c} \text{R}-\text{O}-\text{P}-\text{O}-\text{R} \\ \\ \text{O} \\ \\ \text{R} \end{array}$	$\begin{array}{c} \text{O} \\ \parallel \\ \text{R}-\text{O}-\text{P}-\text{O}-\text{R} \\ \\ \text{O} \\ \\ \text{R} \end{array}$	$\begin{array}{c} \text{S} \\ \parallel \\ \text{R}-\text{O}-\text{P}-\text{O}-\text{R} \\ \\ \text{O} \\ \\ \text{R} \end{array}$	$\begin{array}{c} \text{S} \\ \parallel \\ \text{R}-\text{O}-\text{P}-\text{SH} \\ \\ \text{O} \\ \\ \text{R} \end{array}$	$\begin{array}{c} \text{S} \\ \parallel \\ \text{R}-\text{O}-\text{P}-\text{S}-\text{R}' \\ \\ \text{O} \\ \\ \text{R} \end{array}$
A	B	C	D	E	F
A	Dialkyl phosphites; Dialkyl phosphonates				
B	Trialkyl phosphites				
C	Trialkyl phosphates				
D	Trialkyl thiophosphates				
E	Dialkyl dithiophosphoric acid				
F	Dialkyl dithiophosphates				

6.4 Synthesis of Dialkyl Dithiophosphates

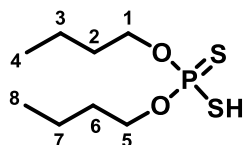
The synthesis of dithiophosphoric acids was performed by alcoholysis of phosphor pentasulfide according to an adapted procedure of Wystrach et al.⁷³

In a typical experiment alcohol (1 mol) was placed in a round bottom flask equipped with a condenser and heated to the desired temperature (see Table 3). Phosphor pentasulfide (0.12 moles) was added stepwise. The evolving H_2S was neutralized with sodium hydroxide solution in two serial connected gas washing flasks. The reaction was stirred over night until phosphor pentasulfide was dissolved completely. Then argon was bubbled through the solution for 0.5 h to degas solved hydrogen sulfide. Vacuum (approx. 10^{-1} mbar) was applied for 1 h to remove excess alcohol.

Table 3. Substance masses for the synthesis of dialkyl dithiophosphoric acid.

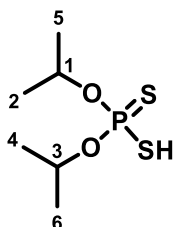
Substance	Alcohol	P_4S_{10}	Temperature / °C
Bu-DTP	n-Butanol/20g (0.27mol)	14.54g (0.033 mol)	65 °C
iPr-DTP	Isopropanol/20 g (0.34 mol)	18.26 g (0.04 mol)	65 °C

Bu-DTP: CHSP for dibutyl dithiophosphoric acid (C₈H₁₉O₂PS₂) found (calc): C 40.75 (39.65), H 7.94 (7.90), S 25.68 (26.46), P 12.88 (12.78).



¹H NMR (400 MHz, Chloroform-d) δ 4.07 (dt, $J_{1,P} = 9.4$, $J_{1,2} = 6.5$ Hz, 4H, **H1&H5**), 3.23 (s, 1H, SH), 1.67 – 1.57 (m, 4H, **H2&H6**), 1.41 – 1.29 (m, 4H, **H3&H7**), 0.87 (t, $J = 7.4$ Hz, 6H, **H4&H8**).

³¹P NMR (162 MHz, Chloroform-d) δ 85.37 .



iPr-DTP: ¹H NMR (400 MHz, Chloroform-d) δ 4.89 (dhept, $J_{1,P} = 12.5$, $J_{1,5} = 6.2$ Hz, 2H, **H1&H3**), 3.12 (s, 1H, SH), 1.37 (d, $J_{5,1} = 6.3$ Hz, 12H, **H2H5H4H6**).

³¹P NMR (162 MHz, Chloroform-d) δ 81.75.

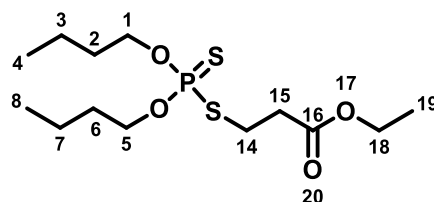
6.5 Synthesis of Dialkyl Dithiophosphoric-Acid-Michael-Adducts

The addition of dialkyl dithiophosphoric acids to activated olefins (e.g. acrylates) was performed according to an adapted procedure of Cassaday et al.⁷⁴ The corresponding dithiophosphate was placed in a round bottom flask and heated to the desired temperature (see Table 4). The acrylate was added dropwise with a syringe over a period of 30 min. After addition of acrylate, the reaction was stirred for 1 h, then vacuum (approx. 10⁻¹ mbar) was applied for 1 h to remove excess acrylate, dithiophosphate and volatile compounds. During the reaction the color changed from violet green to colorless slightly yellow. The weighted samples are given in Table 4.

Table 4. Substance masses for the Dithiophosphate-Michael-Adducts.

Substance	Acrylate	DTP	Temperature / °C
Bu-DTP-EA	Ethyl acrylate/4.54g (0.045mol)	10.00g (0.041 mol)	100 °C
iPr-DTP-EHA	Ethyl hexyl acrylate/10.96 g (0.060 mol)	15.00 g (0.070 mol)	90 °C
iPr-DTP-POEA	Phenoxy ethylacrylate/11.46 g (0.06	15.00 g (0.070 mol)	90 °C
iPr-DTP-HDDA	Hexanediol diacrylate/ 6.73 g (0.030 mol)	15.00 g (0.070 mol)	90 °C

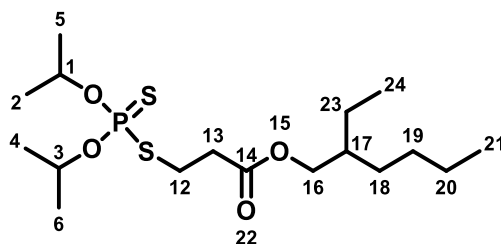
Bu-DTP-EA: **CHSP for Bu-DTP-EA (C₁₃H₂₇O₄PS₂) found (calc):** C 45,41 (45.60), H 7.94 (7.95), S 19.39 (18.72), P 9.88 (9.04).



¹H NMR (400 MHz, Chloroform-*d*) δ 4.17 – 3.93 (m, 6H, **H1&H5, H14**), 3.05 (dt, ⁴*J*_{15,P} = 17.9, *J*_{15,14}=7.1 Hz, 2H, **H15**), 2.66 (t, *J*_{18,19} = 7.1 Hz, 2H, **H18**), 1.64 (quint, ⁴*J*_{2,P} = 8.4, *J*_{2,1}=6.6 Hz, 4H, **H2&H6**), 1.37 (sextett, *J*_{3,2} = 7.4 Hz, 4H, **H3&H7**), 1.22 (t, *J*_{19,18} = 7.2 Hz, 3H, **H19**), 0.89 (t, *J*_{4,3} = 7.4 Hz, 6H, **H4&H8**).

³¹P NMR (162 MHz, Chloroform-*d*) δ 94.55 .

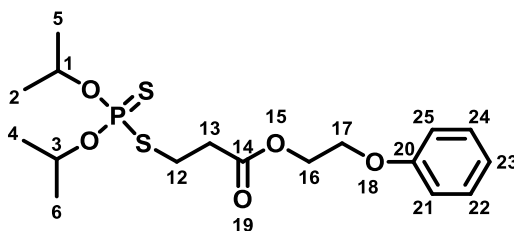
iPr-DTP-EHA: CHSP for iPr-DTP-EHA (C₁₇H₃₅O₄PS₂) found (calc): C 50.78 (50.23), H 8.73 (6.70), S 16.10 (15.77), P 7.90 (7.77).



^1H NMR (400 MHz, Chloroform-*d*) δ 4.83 (dhept, $J_{1,P} = 12.4$, $J_{1,5} = 6.2$ Hz, 2H, **H1&H3**), 4.02 (dd, $J_{16,17} = 5.8$, $J_{16a,16b} = 2.1$ Hz, 2H, **H16**), 3.13 (dt, $J_{12,P} = 17.9$, $J_{12,13} = 7.2$ Hz, 2H, **H12**), 2.75 (t, $J_{13,12} = 7.2$ Hz, 2H, **H13**), 1.57 (m, $J_{17,18} = 5.9$ Hz, 1H, **H17**), 1.35 (dd, $J_{2,1} = 6.2$, $J_{2,P} = 2.3$ Hz, 13H, **H2H4H5H6**), 0.95 – 0.84 (m, 6H, **H24&H21**).

^{31}P NMR (162 MHz, Chloroform-*d*) δ 91.47.

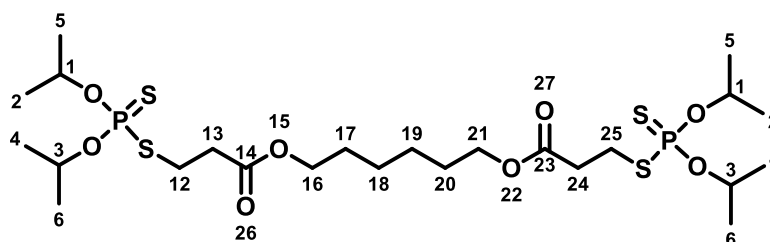
iPr-DTP-POEA: CHSP for iPr-DTP-POEA (C₁₇H₂₇O₅PS₂) found (calc): C 50.13 (50.23), H 8.71 (8.85), S 16.02 (16.09), P 7.63 (7.62).



^1H NMR (400 MHz, Chloroform-*d*) δ 7.33 – 7.24 (m, 2H, **H24&H22**), 6.96 (td, $J = 7.4$, 1.1 Hz, 1H, **H23**), 6.90 (dt, $J = 7.8$, 1.1 Hz, 2H, **H25&H21**), 4.80 (dhept, $J_{1,P} = 12.3$, $J_{1,5} = 6.2$ Hz, 2H, **H1&H3**), 4.50 – 4.41 (m, 2H, **H16**), 4.21 – 4.13 (m, 2H, **H17**), 3.13 (dt, $J_{12,P} = 17.9$, $J_{12,13} = 7.1$ Hz, 2H, **H12**), 2.79 (t, $J_{13,12} = 7.2$ Hz, 2H, **H13**), 1.34 (dd, $J_{5,1} = 6.3$, $J_{5,P} = 3.3$ Hz, 12H, **H5&H2&H4&H6**).

^{31}P NMR (162 MHz, Chloroform-*d*) δ 91.23 .

iPr-DTP-HDDA: CHSP for iPr-DTP-HDDA (C₂₄H₄₈O₈P₂S₄) found (calc): C 44.34 (44.02), H 7.34 (7.39), S 19.54 (19.58), P 9.53 (9.46).



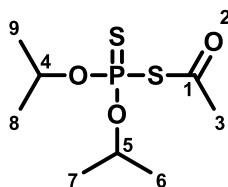
¹H NMR (400 MHz, Chloroform-*d*) δ 4.80 (dhept, $J_{1,P} = 12.4$, $J_{1,5} = 6.2$ Hz, 4H, **H1&H3**), 4.07 (t, $J_{16,17} = 6.7$ Hz, 4H, **H16&H21**), 3.10 (dt, $J_{12,P} = 17.8$, $J_{12,13} = 7.2$ Hz, 4H, **H12**), 2.71 (t, $J_{13,12} = 7.2$ Hz, 4H), 1.62 (m, 4H, **H17&H20**), 1.45 – 1.24 (dd, $J_{5,1} = 6.3$, $J_{5,P} = 2.06$ Hz, 24H).

³¹P NMR (162 MHz, Chloroform-*d*) δ 91.35.

6.6 Synthesis of Acylated Diisopropyl Dithiophosphate

The synthesized dialkyl dithiophosphoric acids were transformed with an excess of acetic anhydride into acylated dithiophosphates. Therefore diisopropyl dithiophosphoric acid (140.85 g, 0.66 mol) were mixed with acetic anhydride (73.82 g, 0.72 mol) and stirred for 2h at 90°C. After 45 min, vacuum (approx. 10⁻¹ mbar) was applied to distill the evolving acetic acid. The product was obtained as a deep green liquid with a vinegar smell.

iPr-DTP-Ac: CHSP for iPr-DTP-Ac (C₈H₁₇O₃PS₂) found (calc): C 37.21 (37.49), H 6.66 (6.69), S 24.92 (25.02), P 12.92 (12.08).

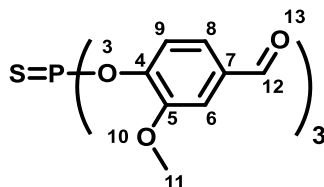


¹H NMR (400 MHz, Chloroform-*d*) δ 4.92 (dhept, $J_{4,P} = 12.6$, $J_{4,9} = 6.3$ Hz, 2H, **H4&H5**), 2.39 (d, $J_{3,P} = 2.8$ Hz, 3H, **H3**), 1.33 (dd, $J_{9,P} = 15.4$, $J_{9,4} = 6.2$ Hz, 13H, **H6H7H8H9**).

³¹P NMR (162 MHz, Chloroform-*d*) δ 75.97.

6.7 Synthesis of Novel Thiophosphates Derived from Phosphor Trichloride

Thiophosphates derived from phosphor trichloride were obtained by adapted reports described in the literature.^{14,15} 1 equivalent of vanillin (25 g), 3.1 equivalents triethyl amine and a proper amount of toluene were added in a three necked round bottom flask equipped with a condenser, a septum and an inert gas inlet. The round bottom flask was placed in an ice bath and 1/3 equivalents of phosphor trichloride was added dropwise via a syringe, keeping the mixture beneath ambient temperature. During addition of phosphor trichloride a white solid precipitated (triethyl ammonium chloride). After complete addition, the solution was stirred for 1 h followed by heating to reflux (ca. 120°C oil bath). Then 1 equivalent of ground elemental sulfur was added to the boiling reaction mixture, and refluxing continued for 6h, then allowed to cool to room temperature. The precipitate was filtered off, washed three times with toluene and the combined toluene fractions washed with water. The organic fraction was filtered, dried with sodium sulfate and the organic solvent evaporated at reduced pressure. The vanillin thiophosphate was obtained as red powder which was washed with toluene and dried in vacuum.



¹H NMR (400 MHz, Acetone) δ 10.02 (s, 3H, **H12**), 7.82 (dd, $J_{9,8} = 8.6$, $J_{9,P} = 1.8$ Hz, 3H, **H9**), 7.72 – 7.64 (m, 6H, **H6&H8**), 4.01 (s, 9H, **H11**).

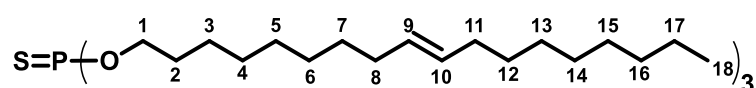
6.8 Synthesis of Thiophosphates Derived from Trialkyl Phosphites P(OR)₃

The synthesis of thiophosphates from phosphites was realized by the oxidation with elemental sulfur according to literature reports.¹⁵ Therefore, 1 equivalent phosphite was placed in a round bottom flask equipped with a magnetic stirring bar and 1 equivalent of ground elemental sulfur was added at ambient temperature. The reaction was accompanied by a temperature increase. After approx. 30 min the major fraction of sulfur was dissolved, after 60 min complete solution of sulfur was observed. The weighted amounts are given in Table 5.

Table 5. Substance masses for the synthesis of thiophosphates derived from phosphites.

Phosphite	Sulfur
Trioleyl phosphite/ 5 g (0.006 mol)	0.19 g (0.006 mol)
Tributyl phosphite/ 8 g (0.032 mol)	1.02 g (0.032 mol)

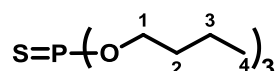
Trioleyl thiophosphate:



^1H NMR (500 MHz, Chloroform-*d*) δ 5.51 – 5.20 (m, 4H, **H9H10**), 4.02 (dt, $J_{1,P} = 9.0$, 6.6 Hz, $J_{1,2} = 6\text{H}$, **H1**), 2.01 (q, $J_{8,7} = 6.5$ Hz, 9H, **H8H11**), 1.66 (quint, $J_{2,3} = 6.6$ Hz, 6H, **H2**), 1.45 – 1.15 (m, 75H, **H3-H7&H12-H17**), 0.88 (t, $J_{18,17} = 6.9$ Hz, 10H, **H18**).

^{31}P NMR (202 MHz, Chloroform-*d*) δ 69.32 .

Tributyl thiophosphate: CHSP for Tributyl thiophosphate ($\text{C}_{12}\text{H}_{27}\text{O}_3\text{PS}$) found (calc): C 50.85 (51.04), H 9.54 (9.64), S 11.56 (11.35), P (9.46).



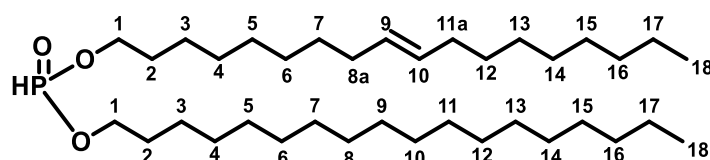
^1H NMR (400 MHz, Chloroform-*d*) δ 3.90 (dt, $J_{1,P} = 8.8$, $J_{1,2} = 6.5$ Hz, 6H, **H1**), 1.59 – 1.45 (m, 6H, **H2**), 1.36 – 1.20 (m, 6H, **H3**), 0.80 (t, $J_{4,3} = 7.4$ Hz, 9H, **H4**).

^{31}P NMR (162 MHz, Chloroform-*d*) δ 68.04 .

6.9 Synthesis of Renewable Phosphonates

Phosphonates were obtained by transesterification of dimethyl phosphonate with the corresponding alcohol or mixture of alcohols.^{71,72} 290.88 g (1.08 mol) of a mixture of 70 mol% oleyl alcohol (203.16 g) and 30 mol% stearyl alcohol (87.7 g) were placed in a round bottom flask equipped with a magnetic stirring bar, inert gas inlet and distillation apparatus. 65.83 g (0.60 mol) dimethyl phosphonate were added and the

reaction mixture heated to 150 °C under argon atmosphere. During the heating period, stearyl alcohol melted and the compounds formed a clear colorless solution. As the temperature increased first distillate drops were observed. After 2 h at 150 °C vacuum was applied to remove excess dimethyl phosphonate. The reaction mixture was allowed to cool to ambient temperature and the product was obtained as a white waxy solid.



Oleyl-stearyl-7030-phosphonate: **CHP** for **oleyl-stearyl-7030-phosphonate (C₃₆H₇₃O₃P)** found (calc. for 50:50 mol% oleyl:stearyl): C 73.6 (73.92), H 12.34 (12.58), P 5.35 (5.30).

¹H NMR (500 MHz, Chloroform-*d*) δ 7.47 (s, 0.5H, POH), 6.09 (s, 0.5H, HPO), 5.39 – 5.25 (m, 2H, **H9&H10**), 4.11 – 3.97 (m, 4H, **H1**), 1.99 (q, *J*_{8a,9} = 6.8 Hz, 5H, **H8a&H11a**), 1.77 – 1.58 (m, 4H, **H2**), 1.49 – 1.07 (m, 47H, **H3-H7&H12-H17**), 0.86 (t, *J* = 6.9 Hz, 6H).

³¹P NMR (202 MHz, Chloroform-*d*) δ 8.99.

6.10 Synthesis of Renewable Terpene Polysulfides

Novel polysulfides were synthesized from natural limonene and pine oil (alpha & beta pinene both MW = 136.24 g/mol) according to a process from Gardner.¹⁵³ The amounts of terpene and sulfur (Table 6) were placed in a round bottom flask equipped with a condenser and a magnetic stirring bar. The flask was placed in an oil bath and heated to the desired temperature. The weighted samples and temperatures are given in Table 6. At approx. 120 °C sulfur melted into a yellow liquid, and vigorous stirring led to a homogenous phase. At increased temperatures of approx. 140 to 150°C, the yellow solution turned blood red. After stirring for 6 h, a drop of the reaction mixture was diluted with chloroform to check for insoluble moieties. If a clear solution was obtained, the mixture was allowed to cool to ambient temperature and was used without further purification. The products were obtained as blood red liquids.

A second approach for the limonene polysulfide included a vacuum distillation at 150°C and 10⁻¹ mbar for 2h (33 wt% S VD) after 6 h reaction time to remove volatile compounds. Therefore, the condenser was replaced by a distillation apparatus. During the distillation, yellow to orange fluids were collected (approx. 25 wt%) and the product was obtained as a deep blood red wax.

Table 6. Substance masses for the synthesis of renewable terpene polysulfides.

Sample	Limonene	Sulfur
33 wt% S	10 g (0.07 mol)	4.94 g (0.15 mol)
41 wt% S	10 g (0.07 mol)	7.06 g (0.22 mol)
50 wt% S	10 g (0.07 mol)	10 g (0.31 mol)
33 wt% S VD	10 g (0.07 mol)	4.94 g (0.15 mol)
Sample	Pine oil (Pinene)	Sulfur
33 wt% S	10 g (0.07 mol)	4.94 g (0.15 mol)
41 wt% S	10 g (0.07 mol)	7.06 g (0.22 mol)
50 wt% S	10 g (0.07 mol)	10 g (0.31 mol)

CHS for 33 wt% S limonene polysulfide found (calc): C 58.58 (59.00), H 7.65 (7.92), S 33.78 (33.07)

CHS for 33 wt% S limonene polysulfide VD found (calc): C 50.24, H 6.59, S 42.92

CHS for 41 wt% S limonene polysulfide found (calc): C 50.98 (51.68), H 6.66 (6.94), S 42.72 (41.38)

CHS for 50 wt% S limonene polysulfide found (calc): C 45.79 (44.08), H 5.95 (5.92), S 48.25 (50.00)

Elemental analysis was not performed for the pine oil derivatives due to incomplete conversion.

6.11 Linear Drive Screening Procedure

The procedure for the novel EP method was as follows: 4 cleaned balls were charged into the ball holder and fixed. A proper amount of lubricant was added, until all resting balls were immersed (approx. 8 mL). The running ball was fixed in a cleaned ball chuck and located in the motor mount. Afterwards, the ball holder was placed in the four-ball

machine and the torque lever was connected to the torque sensor. The desired load stage (2kg, 5kg, 10kg etc.) was applied on the weight lever and attached to the linear drive with a steel cord. The lever weight was pushed as much as possible to the left side, resulting in a tense steel cord and the lowest observable load for the weight. The VKA motor starts with small delay (approx. 2 sec.) after clicking the “Start Test” button, whereas the linear drive starts immediately after clicking the “Start Test” button in the Grib software. Therefore, the VKA test was started, and immediately as the VKA motor began to run, the linear drive was started. After 60 s the test was completed and the set-up was relieved and cleaned. The balls were collected, and the resulting wear scars measured. The wiring of the stepper motor control unit is given in Figure 102.

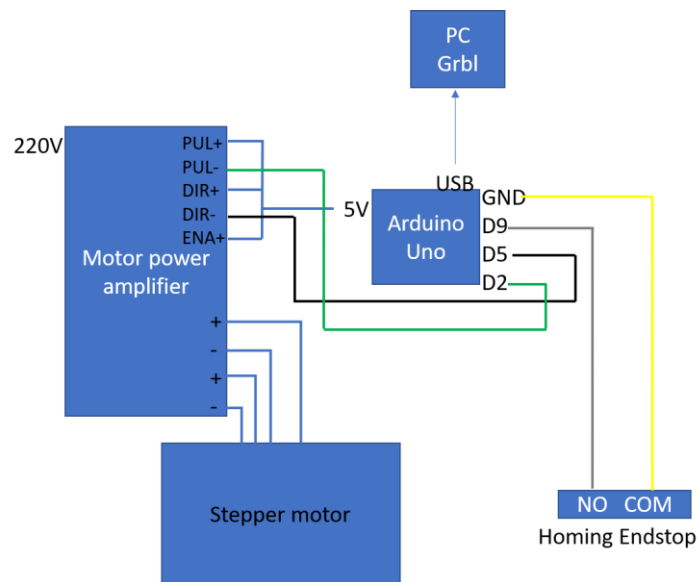


Figure 102. Schematic wiring setup of the stepper motor.

The settings in Grbl are given in Figure 103 and Figure 104.

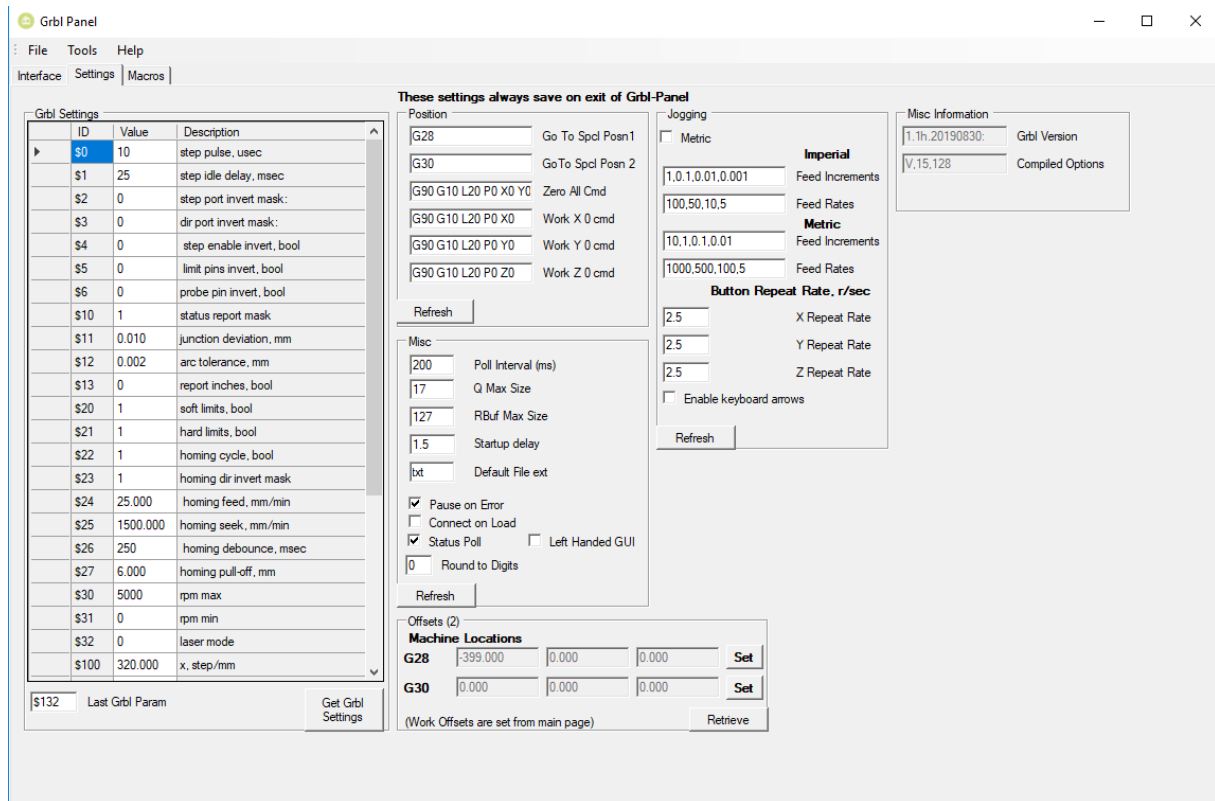


Figure 103. Grbl Settings part I.

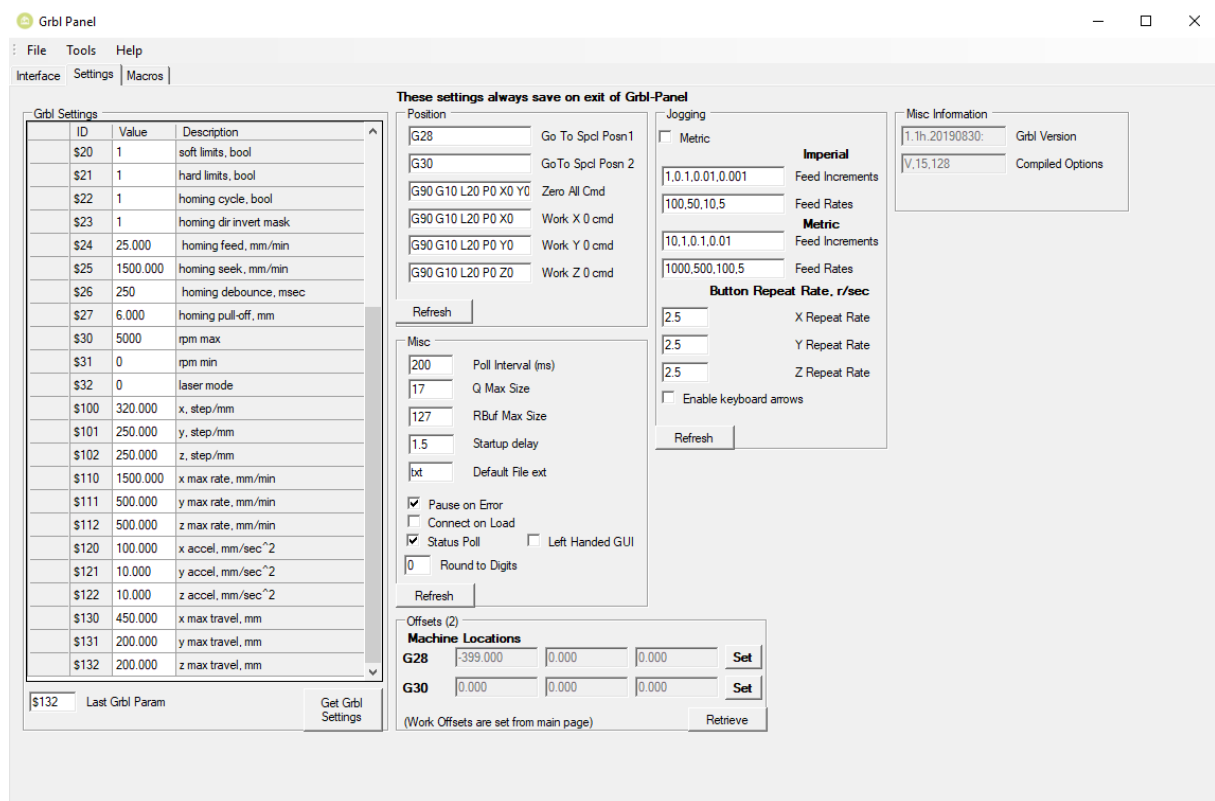


Figure 104. Grbl settings part II.

6.12 DIN 51350-2 Procedure

The procedure for the DIN method was as follows²⁶: 4 cleaned balls were charged into the ball holder and fixed. A proper amount of lubricant was added, until all resting balls were immersed (approx. 8 mL). The running ball was fixed in a cleaned ball chuck and located in the motor mount. Afterwards, the ball holder was placed in the four-ball machine and the torque lever was connected to the torque sensor. The desired load was applied on the four-ball system and the test was started. After 60 s the test was completed and the set-up was relieved and cleaned. The balls were collected, and the resulting wear scars measured.

6.13 DIN 51350-3 Procedure

The procedure for the DIN method was as follows²⁵: In a typical experiment 4 12.7 mm 100Cr6 balls with G10 surface grade were cleaned with ethyl acetate and dried with paper tissue. The three resting balls were put in the ball pot and fixed with the clamp. The resting balls were immersed in the lubricant (approx. 12 ml fluid) and conditioned to 25 °C. The running ball was fixed in the chuck and mounted in the engine spindle. The ball pot was set in the test casing and the load was applied. The AW performance was determined at 150 N for 60 min at 1450 rpm. Every test was performed two times. The balls were cleaned with ethyl acetate after the test load was relieved.

7. References

- (1) Luinstra, G. A.; Kipphardt, H.; Beermann, T. *Verschleißadditive auf Basis von biologischen Alkoholen. Abschlussbericht über ein Entwicklungsprojekt, gefördert unter dem Az : 34486 / 01 von der Deutschen Bundesstiftung Umwelt*; Hamburg, 2021.
- (2) Luinstra, G. A.; Kipphardt, H.; Beermann, T. Deutsches Gebrauchsmuster: AW-Additive. DE20 2020 107 390, 2021.
- (3) Luinstra, G. A.; Kipphardt, H.; Beermann, T. EP-Additive. Deutsches Gebrauchsmuster. DE20 2021 002 910, 2021.
- (4) Luinstra, G. A.; Kipphardt, H.; Beermann, T. Polymere AW-Verbindungen. DE 10 2020 000 344 A1, 2021.
- (5) Luinstra, G. A.; Kipphardt, H.; Beermann, T. Polymer AW Compounds. WO 2021/148385, 2021.
- (6) Bhushan, B. In *Introduction. In Introduction to Tribology.*; Wiley: New York, 2013; pp 1–8.
- (7) Bhushan, B. In *Boundary Lubrication and Lubricants. In Introduction to Tribology.*; Wiley: New York, 2013; pp 501–523.
- (8) Anderson, K. J. *MRS Bull.* **1991**, 16 (10), 69–69.
- (9) Sukmawati; Lestari, P. P. *J. Phys. Conf. Ser.* **2020**, 1428 (1).
- (10) Holmberg, K.; Erdemir, A. *Friction* **2017**, 5 (3), 263–284.
- (11) Pitenis, A. A.; Dowson, D.; Gregory Sawyer, W. *Tribol. Lett.* **2014**, 56 (3), 509–515.
- (12) Benz, C. Fahrzeug mit Gasmotorenbetrieb, 1886.
- (13) Mang, T.; Dresel, W. In *Additives. In Lubricants and Lubrication*; Jürgen Braun, Ed.; Wiley-VCH Verlag GmbH: Weinheim, 2007; pp 43–55.
- (14) Svara, J.-; Weferling, N.; Hofmann, T. In *Phosphorous Compounds, Organic. In Ullmann's Encyclopedia of Industrial Chemistry.*; Wiley-VCH Verlag GmbH: Weinheim, 2012; pp 19–49.

- (15) Angeline Baird Cardis. Use of reaction products of trialkyl phosphites with elemental sulfur and process for making same. EP 0 319 617 B1, 1987.
- (16) Bowden, F. P.; Tabor, D. *Proc. R. Soc. London. Ser. A. Math. Phys. Sci.* **1939**, 169 (938), 391–413.
- (17) Vakis, A. I.; Yastrebov, V. A.; Scheibert, J.; Nicola, L.; Dini, D.; Minfray, C.; Almqvist, A.; Paggi, M.; Lee, S.; Limbert, G.; Molinari, J. F.; Anciaux, G.; Aghababaei, R.; Echeverri Restrepo, S.; Papangelo, A.; Cammarata, A.; Nicolini, P.; Putignano, C.; Carbone, G.; Stupkiewicz, S.; Lengiewicz, J.; Costagliola, G.; Bosia, F.; Guarino, R.; Pugno, N. M.; Müser, M. H.; Ciavarella, M. *Tribol. Int.* **2018**, 125, 169–199.
- (18) Li, H.; Jiang, Z.; Wei, D.; Gao, X. *Tribol. Lett.* **2014**, 53 (2), 383–393.
- (19) Leng, J. A.; Davies, J. E. *Tribol. Int.* **1989**, 22 (2), 137–142.
- (20) Popov, V. L. In *Lubricated Systems. In Contact Mechanics and Friction: Physical Principles and Applications*; Springer: Berlin Heidelberg, 2010; pp 207–229.
- (21) Stribeck, R. *Kugellager für beliebige Belastungen*; Mitteilungen über Forschungsarbeiten auf dem Gebiete des Ingenieurwesens, insbesondere aus den Laboratorien der technischen Hochschulen; Springer, 1901.
- (22) Stribeck, R. *Die wesentlichen Eigenschaften der Gleit- und Rollenlager*; Mitteilungen über Forschungsarbeiten auf dem Gebiete des Ingenieurwesens, insbesondere aus den Laboratorien der technischen Hochschulen; Julius Springer, 1903.
- (23) Bhushan, B. In *Fluid Film Lubrication. In Introduction to Tribology*; Wiley: New York, 2013; pp 399–500.
- (24) Sommer, K.; Heinz, R.; Schöfer, J. *Verschleiß metallischer Werkstoffe*; 2014.
- (25) Deutsches Institut für Normung. *Prüfung von Schmierstoffen- Prüfung im Vierkugel-Apparat- Teil 3: Bestimmung von Verschleißkennwerten flüssiger Schmierstoffe*; DIN 51350-3; Beuth Verlag GmbH: Berlin, 2015.
- (26) Deutsches Institut für Normung. *Prüfung von Schmierstoffen- Prüfung im Vierkugel-Apparat- Teil 2: Bestimmung der Schweißkraft von flüssigen Schmierstoffen*; DIN 51350-2; Beuth Verlag GmbH: Berlin, 2015.

- (27) Piekoszewski, W.; Szczerek, M.; Tuszyński, W. *Wear* **2001**, 249 (3–4), 188–193.
- (28) Hansa Press- und Maschinenbau GmbH. *Hansa Press- und Maschinenbau: Shell-Vierkugelapparat Erläuterungen; available from Hansa Press- und Maschinenbau GmbH*; Hansa Press- und Maschinenbau GmbH: Hamburg.
- (29) Mang, T.; Dresel, W. In 8. *Lubricants for Internal Combustion Engines. In Lubricants and Lubrication*; Manfred Harperscheid, Ed.; Wiley-VCH Verlag GmbH: Weinheim, 2007; pp 62–77.
- (30) Mang, T.; Dresel, W. In 1. *Introduction. In Lubricants and Lubrication*; Mang, T., Ed.; Wiley-VCH Verlag GmbH: Weinheim, 2007; pp 6–7.
- (31) Krafft, F. *Angew. Chemie Int. Ed. English* **1969**, 8 (9), 660–671.
- (32) Louis D. Quin. *Heteroat. Chem.* **2013**, 24 (4), 243–251.
- (33) Schrader, G. *Angew. Chemie* **1950**, 62 (20), 471–490.
- (34) Corbridge, D. E. C. In 1. *Introduction and Historical Background. In Phosphorus Chemistry, Biochemistry and Technology.*; CRC Press: Boca Raton London New York, 2013; pp 1–22.
- (35) Corbridge, D. E. C. In 12. *Application of Phosphorus Compounds. In Phosphorus Chemistry, Biochemistry and Technology.*; CRC Press: Boca Raton London New York, 2013; pp 1021–1244.
- (36) Ashley, K.; Cordell, D.; Mavinic, D. *Chemosphere* **2011**, 84 (6), 737–746.
- (37) Knowles, J. R. *Annu. Rev. Biochem.* **1980**, 49, 877–919.
- (38) Grob, D.; Harvey, J. C. *J. Clin. Invest.* **1958**, 37 (3), 350–368.
- (39) O,O,O-tris(2(or 4)-C9-10-isoalkylphenyl) phosphorothioate. CAS Nr.: 126019-82-7. European Chemicals Agency <https://echa.europa.eu/de/substance-information/-/substanceinfo/100.100.849> (accessed Oct 18, 2020).
- (40) O,O,O-triphenyl phosphorothioate. CAS Nr.: 597-82-0. European Chemicals Agency <https://echa.europa.eu/de/registration-dossier/-/registered-dossier/13644> (accessed Oct 18, 2020).
- (41) Zinc bis[O-(2-ethylhexyl)] bis[O-(isobutyl)] bis(dithiophosphate). CAS Nr.: 26566-95-0. European Chemicals Agency <https://echa.europa.eu/de/substance->

- information/-/substanceinfo/100.043.449 (accessed Oct 18, 2020).
- (42) Zinc bis[O-(6-methylheptyl)] bis[O-(sec-butyl)] bis(dithiophosphate). CAS Nr.:93819-94-4. European Chemicals Agency <https://echa.europa.eu/de/substance-information/-/substanceinfo/100.089.573> (accessed Oct 18, 2020).
- (43) European Chemicals Agency. A mixture of: triphenylthiophosphate and tertiary butylated phenyl derivatives. CAS Nr.: 192268-65-8. European Chemicals Agency <https://echa.europa.eu/de/substance-information/-/substanceinfo/100.102.039> (accessed Oct 18, 2020).
- (44) Phosphorodithioic acid, mixed O,O-bis(1,3-dimethylbutyl and iso-Pr) esters, zinc salts. CAS Nr. 84605-29-8. European Chemicals Agency <https://echa.europa.eu/de/substance-information/-/substanceinfo/100.075.786> (accessed Oct 18, 2020).
- (45) Phosphorodithioic acid, mixed O,O-bis(2-ethylhexyl and iso-Bu and iso-Pr) esters, zinc salts. CAS Nr.: 85940-28-9. European Chemicals Agency <https://echa.europa.eu/de/substance-information/-/substanceinfo/100.080.805> (accessed Oct 18, 2020).
- (46) Phosphorodithioic acid, mixed O,O-bis(2-ethylhexyl and iso-Bu) esters, zinc salts. CAS Nr.: 68442-22-8. European Chemicals Agency <https://echa.europa.eu/de/substance-information/-/substanceinfo/100.064.051> (accessed Oct 18, 2020).
- (47) Phosphorodithioic acid, mixed O,O-bis(iso-Bu and pentyl) esters, zinc salts. CAS Nr.:68457-79-4. European Chemicals Agency <https://echa.europa.eu/de/substance-information/-/substanceinfo/100.064.169> (accessed Oct 18, 2020).
- (48) Phosphorodithioic acid, mixed O,O-bis(sec-Bu and 1,3-dimethylbutyl) esters, zinc salts. CAS Nr.: 68784-31-6. European Chemicals Agency <https://echa.europa.eu/de/substance-information/-/substanceinfo/100.065.651> (accessed Oct 18, 2020).
- (49) Zinc bis(O,O-diisooctyl) bis(dithiophosphate). CAS Nr.: 28629-66-5. European Chemicals Agency <https://echa.europa.eu/de/substance-information/-/substanceinfo/100.064.169>

- /substanceinfo/100.044.630 (accessed Oct 18, 2020).
- (50) Zinc bis[O,O-bis(2-ethylhexyl)] bis(dithiophosphate). CAS Nr.: 4259-15-8. European Chemicals Agency <https://echa.europa.eu/de/substance-information/-/substanceinfo/100.022.032> (accessed Oct 18, 2020).
- (51) Propanoic acid, 3-[[bis(2-methylpropoxy)phosphinothioyl]thio]-2-methyl-. CAS Nr.: 268567-32-4. European Chemicals Agency <https://echa.europa.eu/de/substance-information/-/substanceinfo/100.103.231> (accessed Oct 18, 2020).
- (52) Ethyl 3-[[bis(1-methylethoxy)phosphinothioyl]thio]propionate. CAS Nr.: 71735-74-5. European Chemicals Agency <https://echa.europa.eu/de/substance-information/-/substanceinfo/100.069.038> (accessed Oct 18, 2020).
- (53) Polysulfides, di-tert-dodecyl. CAS Nr.: 68425-15-0. European Chemicals Agency <https://echa.europa.eu/de/substance-information/-/substanceinfo/100.063.922> (accessed Oct 18, 2020).
- (54) Polysulfides, di-tert-nonyl. CAS Nr.: 68425-16-1. European Chemicals Agency <https://echa.europa.eu/de/substance-information/-/substanceinfo/100.063.923> (accessed Oct 18, 2020).
- (55) Polysulfides, di-tert-Bu. CAS Nr.: 68937-96-2. European Chemicals Agency <https://echa.europa.eu/de/substance-information/-/substanceinfo/100.066.438> (accessed Oct 18, 2020).
- (56) European Chemicals Agency. *Justification for the selection of a substance for CoRAP inclusion Substance. O,O,O-triphenyl phosphorothioate* CAS Nr.: 597-82-0; 2015.
- (57) European Chemicals Agency. Environmental fate & pathways. O,O,O-triphenyl phosphorothioate CAS Nr. 597-82-0. Hydrolytical Data <https://echa.europa.eu/de/registration-dossier/-/registered-dossier/13644/5/2/3> (accessed Sep 30, 2020).
- (58) Institut für Arbeitsschutz der Deutschen Gesetzlichen Unfallversicherung. Stoffdatenbankeintrag zu Phenol CAS Nr.: 108-95-2 <https://gestis.dguv.de/data?name=010430> (accessed Sep 11, 2022).

- (59) Institut für Arbeitsschutz der Deutschen Gesetzlichen Unfallversicherung. Stoffdatenbankeintrag zu 4-tert-Butylphenol CAS Nr.: 98-54-4 <https://gestis.dguv.de/data?name=016680> (accessed Sep 11, 2022).
- (60) Willermet, P. A.; Carter, R. O.; Schmitz, P. J.; Everson, M.; Scholl, D. J.; Weber, W. H. *Lubr. Sci.* **1997**, 9 (4), 325–348.
- (61) Spikes, H. *Tribol. Lett.* **2004**, 17 (3), 469–489.
- (62) Williamson, W. B.; Perry, J.; Goss, R. L.; Gandhi, H. S.; Beason, R. E. *SAE Tech. Pap. Ser.* **1984**, 841406, 10.
- (63) Xie, K.; Wang, A.; Woo, J.; Kumar, A.; Kamasamudram, K.; Olsson, L. *Appl. Catal. B Environ.* **2019**, 256 (June), 17.
- (64) Dahlin, S.; Englund, J.; Malm, H.; Feigel, M.; Westerberg, B.; Regali, F.; Skoglundh, M.; Pettersson, L. J. *Catal. Today* **2020**, No. February, 14.
- (65) Dahlin, S.; Lantto, C.; Englund, J.; Westerberg, B.; Regali, F.; Skoglundh, M.; Pettersson, L. J. *Catal. Today* **2018**, No. January, 12.
- (66) Molina, A. *ASLE Trans.* **1986**, 30 (4), 479–485.
- (67) Papay, A. G. *Lubr. Sci.* **1998**, 10 (3), 209–224.
- (68) Luiz, J. F.; Spikes, H. *Tribol. Lett.* **2020**, 68 (3).
- (69) Minami, I.; Mori, S. *J. Synth. Lubr.* **2005**, 22 (2), 105–121.
- (70) Malowan, J. E.; Traise, T. P.; Beck, T. M. *Inorg. Synth.* **1953**, 4, 58–60.
- (71) Dal-Maso, A. D.; Legendre, F.; Blonski, C.; Hoffmann, P. *Synth. Commun.* **2008**, 38 (11), 1688–1693.
- (72) Kolio D. Troev. In *Reactivity of H-Phosphonates. In Chemistry and Application of H-Phosphonates*; Elsevier Science Ltd: Amsterdam, 2006; pp 23–105.
- (73) Wystrach, V. P.; Hook, E. O.; Christopher, G. Basic Zinc Dialkyl Dithiophosphates and Methods of Making the Same. US 2794780, 1957.
- (74) Cassaday, J. T. Addition Product of Diester of Dithiophosphoric Acid and Maleic Acid and its Esters, and Method of Peparation. US 2578652, 1951.
- (75) Miles, P. Acrylate Addition Products of Dialkyl Phosphorodithioic Acids. US 3

784 588, 1974.

- (76) Zinke, H.; Schumacher, R. *Wear* **1994**, 179 (1–2), 45–48.
- (77) Born, M.; Hipeaux, J. C.; Marchand, P.; Parc, G. *Lubr. Sci.* **1992**, 4 (2), 93–116.
- (78) Allum, K. G.; Forbes, E. S. *Proc. Inst. Mech. Eng.* **1968**, 183 (3), 7–14.
- (79) Sieber, I. N. A.; Meyer, K.; Kloss, H. *Wear* **1983**, 85, 43–56.
- (80) Biresaw, G.; Bantchev, G. B.; Harry-O’Kuru, R. E. *J. Am. Oil Chem. Soc.* **2020**, 14.
- (81) Lubricant Performance Additives Italmatch Chemicals Homepage <https://lubperformanceadditives.com/sproducts/?sval=dapraphos&ru=https://lubperformanceadditives.com/elcoline> (accessed Sep 16, 2022).
- (82) Doverchem Chemical Corporation Homepage <https://www.doverchem.com> (accessed Sep 16, 2022).
- (83) Jakupca, M.; Weingart, J.; Rohr, B.; Nussbaumer, J. Polymeric Poly-Phosphorous Additives for: Gear oil, Grease, Engine-Oil, Combustion-Engine Lubricant, Automatic Transmission Fluid, Anti-Wear Agents, Two-Cycle Engine Lubricant, or Marine-Engine Lubricant. US 2020/0231893 A1, 2020.
- (84) Forbes, E. S.; Neustadter, E. L.; Silver, H. B.; Upsdell, N. T. *Wear* **1971**, 18, 269–278.
- (85) Barber, R. I. *Tribol. Trans.* **1976**, 19 (4), 319–328.
- (86) Azelis L&MF US and Azelis Essential Chemicals US. Azelis L&MF US - Azelis Essential Chemicals US Product Page <https://monsonco.com/product/irgalube-349/> (accessed Sep 16, 2022).
- (87) Runze Chemicals Product Info <http://www.runzechem.com/content/?327.html> (accessed Sep 16, 2022).
- (88) Hangzhou Sungate SungateLube 349 https://www.sungatechem.com/product_detail_en/id/133.html (accessed Sep 16, 2022).
- (89) Xu, M.; Li, D. *J. Synth. Lubr.* **2003**, 20 (1), 25–37.

- (90) Farng, L. O. In 8. *Ashless Antiwear and Extreme-Pressure-Additives. In Lubricant Additives Chemistry and Application*; Rudnick, L., Ed.; CRC Press: Boca Raton London New York, 2008; pp 213–249.
- (91) Spikes, H. *Lubr. Sci.* **2008**, 20, 103–136.
- (92) Rounds, F. *ASLE Trans.* **1985**, 28 (4), 475–485.
- (93) Davey, W.; Edwards, E. D. *Wear* **1958**, 1 (4), 291–304.
- (94) European Chemicals Bureau. *Risk Assessment Report: Alkanes C10-13, chloro* CAS Nr.: 85535-84-8; 2008.
- (95) Biresaw, G.; Asadauskas, S. J.; McClure, T. G. *Ind. Eng. Chem. Res.* **2012**, 51 (1), 262–273.
- (96) Rossrucker, T.; Fessenbecker, A. In 9. *Sulfur Carriers. In Lubricant Additives Chemistry and Application*; Rudnick, L. R., Ed.; CRC Press: Boca Raton London New York, 2008; pp 251–279.
- (97) Beeck, O.; Givens, J. W.; Williams, E. C. *Proc. R. Soc. Lond. A. Math. Phys. Sci.* **1940**, 177 (968), 103–118.
- (98) Zinke, H.; Schumacher, R. *Phosphorous, Sulfur, Silicon Relat. Elem.* **1991**, 63 (3–4), 315–322.
- (99) Najman, M. N.; Kasrai, M.; Bancroft, G. M. *Tribol. Lett.* **2004**, 17 (2), 217–229.
- (100) Gao, F.; Furlong, O.; Kotvis, P. V.; Tysoe, W. T. *Langmuir* **2004**, No. 20, 7557–7568.
- (101) Gao, F.; Northwest, P.; Kotvis, P. V.; Stacchiola, D.; Tysoe, W. *Tribol. Lett.* **2005**, 18 (3), 377–384.
- (102) F. Mangolini; Rossi, A.; Spencer, N. D. *J. Phys. Chem.* **2012**, 116, 5614–5627.
- (103) Parsaeian, P.; Ghanbarzadeh, A.; van Eijk, M. C. P.; Nedelcu, I.; Neville, A.; Morina, A. *Appl. Surf. Sci.* **2017**, 403, 472–486.
- (104) Soltanahmadi, S.; Morina, A.; van Eijk, M. C. P.; Nedelcu, I.; Neville, A. *Appl. Surf. Sci.* **2017**, 414, 41–51.
- (105) Dörr, N.; Brenner, J.; Ristić, A.; Ronai, B.; Besser, C.; Pejaković, V.; Frauscher,

- M. *Tribol. Lett.* **2019**, 67 (2), 1–17.
- (106) Zheng, G.; Ding, T.; Pang, S.; Zheng, L.; Ren, T. *Friction* **2020**, 8 (5), 874–881.
- (107) Williams, C. G. *Proc. R. Soc. London. Ser. A. Math. Phys. Sci.* **1952**, 212 (1111), 512–515.
- (108) Ott, E. Terpene Reaction Product and Method of Producing. 2,413,648, 1946.
- (109) Kirshenbaum, A. D.; Boyle, J. M. Sulfurized Additives for Lubricating Compositions. 2,613,183, 1952.
- (110) Waddey, W. E.; Phelan, J. M.; Rogers, D. T. Stabilized sulfur-containing additives for lubricants. 2,703,318, 1955.
- (111) Jayne, G. J. J.; Woods, D. R. Lubricant Additive. 4,188,297, 1980.
- (112) Walsh, R. H. Sulfurized Compositions and Lubricants Containing Them. 4,584,113, 1986.
- (113) Adis, F. W.; Ashjian, H.; Cardis, A. B.; Horodysky, A. G. Sulfurized Olefins. EP0201197 B1, 1986.
- (114) Horodysky, A. G.; Hill, C.; Law, D. A. Sulfurized Olefins As Antiwear/Extreme pressure additives for lubricants and fuels and compositions thereof. 4711736, 1987.
- (115) Fields, E. K. Process of contacting sulfurized dipentene with activated alumina. 2,787,613, 1957.
- (116) Harkin, J. M. *Lignin and its Uses*; 1969.
- (117) van den Bosch, S.; Koelewijn, S. F.; Renders, T.; van den Bossche, G.; Vangeel, T.; Schutyser, W.; Sels, B. F. *Top. Curr. Chem.* **2018**, 376 (36), 1–40.
- (118) Dahl, C. F. Process of manufacturing cellulose from wood, 1884.
- (119) Phillips, M. *J. Chem. Educ.* **1943**, 20 (9), 444–447.
- (120) Calvo-Flores, F. G.; Dobado, J. A. *ChemSusChem* **2010**, 3 (11), 1227–1235.
- (121) Fache, M.; Boutevin, B.; Caillol, S. *ACS Sustain. Chem. Eng.* **2016**, 4 (1), 35–46.

- (122) Luo, H.; Abu-Omar, M. M. *Encycl. Sustain. Technol.* **2017**, No. November, 573–585.
- (123) Sun, Z.; Fridrich, B.; De Santi, A.; Elangovan, S.; Barta, K. *Chem. Rev.* **2018**, *118* (2), 614–678.
- (124) European Chemicals Agency. Menthol CAS Nr.: 89-78-1. European Chemicals Agency <https://echa.europa.eu/de/substance-information/-/substanceinfo/100.001.763> (accessed Sep 25, 2022).
- (125) Schäfer, B. *Chemie Unserer Zeit* **2013**, *47* (3), 174–182.
- (126) Bergner, E. J.; Ebel, K.; Johann, T.; Löber, O. Method for the production of menthol. US7709688 B2, 2010.
- (127) Nissen, D. A.; Rebafka, D. W.; Aquila, D. W. Verfahren zur Herstellung von Citral. 0021074B1, 1982.
- (128) John, I.; Muthukumar, K.; Arunagiri, A. *Int. J. Green Energy* **2017**, *14* (7), 599–612.
- (129) Crockett, M. P.; Evans, A. M.; Worthington, M. J. H.; Albuquerque, I. S.; Slattery, A. D.; Gibson, C. T.; Campbell, J. A.; Lewis, D. A.; Bernardes, G. J. L.; Chalker, J. M. *Angew. Chemie - Int. Ed.* **2016**, *55* (5), 1714–1718.
- (130) Nizamov, I. S.; Nizamov, I. D.; Popovich, Y. E.; Cherkasov, R. A. *Russ. J. Gen. Chem.* **2012**, *82* (1), 27–32.
- (131) Weitkamp, A. W. *J. Am. Chem. Soc.* **1959**, *81* (13), 3430–3434.
- (132) European Chemicals Agency. Chemicals of high concern <https://echa.europa.eu/candidate-list-table> (accessed Mar 23, 2020).
- (133) European Chemicals Agency. *TPPT decision on substance evaluation*; Helsinki, 2019.
- (134) Tarabanko, V. E.; Petukhov, D. V.; Selyutin, G. E. *Kinet. Catal.* **2004**, *45* (4), 569–577.
- (135) Deutsches Institut für Normung. *Prüfung von Schmierstoffen- Prüfung im Vierkugel-Apparat- Teil 1: Allgemeine Arbeitsgrundlagen; DIN 51350-1*; Beuth Verlag GmbH: Berlin, 2015.

- (136) Popov, V. L. In *5. Rigorous Treatment of Contact Problems - Hertzian Contact. In Contact Mechanics and Friction*; Springer: Berlin Heidelberg, 2010; pp 55–70.
- (137) Deutsches Institut für Normung. *Für eine Wärmebehandlung bestimmte Stähle, legierte Stähle und Automatenstähle - Teil 17: Wälzlagerstähle (ISO 683-17:2015)*; *Deutsche Fassung EN ISO 683-17:2015-02*; Beuth Verlag GmbH: Berlin, 2015.
- (138) Deutsches Institut für Normung. *Warmgewalzte Stähle für vergütbare Federn - Technische Lieferbedingungen*; *Deutsche Fassung EN 10089:2003-04*; Beuth Verlag GmbH: Berlin, 2003.
- (139) KGM Kugelfabrik GmbH. Chemische Beständigkeit von Werkstoffen https://www.kgm-kugeln.de/wp-content/uploads/2015/05/Chemische_Beständigkeit.pdf (accessed Nov 1, 2022).
- (140) Deutsches Institut für Normung. *Nichtrostende Stähle - Teil 1: Verzeichnis der nichtrostenden Stähle*; *Deutsche Fassung EN 10088-1:2014*; Beuth Verlag GmbH: Berlin, 2014.
- (141) BASF. Lubricant Additives Selection Guide https://www.btc-europe.com/fileadmin/user_upload/Downloads/Pdf_s/Industries/Brochure_Selection-Guide-Lubricant-Additives.pdf (accessed Nov 1, 2022).
- (142) Fletschinger, M.; Rohrbach, P.; Hamblin, P. C.; Clark, D.; Ribeaud, M. Schmierstoffzusammensetzungen mit Thiophosphorsäureestern und Dithiophosphorsäureestern. EP 0 903 399 B1, 1998.
- (143) Kühl, O. In *The Range of Chemical Shifts, Coupling Constants, and What Influences Each. In Phosphorus-31 NMR Spectroscopy: A Concise Introduction for the Synthetic Organic and Organometallic Chemist*; Kühl, O., Ed.; Springer Berlin Heidelberg: Berlin, Heidelberg, 2008; pp 7–23.
- (144) Zimmerling, R.; Dimmig, T.; Jäger, G.; Ströhl, D. *Z. Chem.* **1990**, 30 (10), 372–373.
- (145) Janesko, B. G.; Fisher, H. C.; Bridle, Ma. J.; Montchamp, J.-L. *J. Org. Chem.* **2015**, 80 (20), 10025–10032.

- (146) Zimin, M. G.; Kamalov, R. M.; Cherkasov, R. A.; Pudovik, A. N. *Phosphorus Sulfur Relat. Elem.* **1982**, 13 (3), 371–378.
- (147) ChemicalBook. ChemicalBook 1H-NMR Spectra of Ethylacrylate. https://www.chemicalbook.com/SpectrumEN_140-88-5_1HNMR.htm (accessed Nov 1, 2022).
- (148) O. Kühl. In λ 3-Phosphanes. In *Phosphorus-31 NMR Spectroscopy: A Concise Introduction for the Synthetic Organic and Organometallic Chemist*; Kühl, O., Ed.; Springer Berlin Heidelberg: Berlin, Heidelberg, 2008; pp 37–70.
- (149) Kühl, O. In λ 5-Phosphanes. In *Phosphorus-31 NMR Spectroscopy: A Concise Introduction for the Synthetic Organic and Organometallic Chemist*; Kühl, O., Ed.; Springer Berlin Heidelberg: Berlin, Heidelberg, 2008; pp 31–35.
- (150) Clément, J. L.; Fréjaville, C.; Tordo, P. *Res. Chem. Intermed.* **2002**, 28 (2–3), 175–190.
- (151) Fakhraian, H.; Mirzaei, A. *Org. Process Res. Dev.* **2004**, 8 (3), 401–404.
- (152) Sabol, A. R. Method of Preparing Non-Corrosive Sulfurized Terpenes and Compositions Containing the Same. 2,910,462, 1959.
- (153) Gardner, H. A.; Hart, L. P. SULPHUR TERPENE COMPOUNDS AND PROCESS OF PRODUCING THE SAME. 1,963,084, 1934.
- (154) Lyle R. Kallenbach; Senn, D. R.; Johnson, M. M. Catalytic cracking process. EP 0 754 747 A1, 1996.
- (155) Loya, Y.; Rinkevich, B. *Mar. Ecol. Prog. Ser.* **1980**, 3 (3), 167–180.
- (156) Tümen, I.; Reunanen, M. *Rec. Nat. Prod.* **2010**, 4 (4), 224–229.
- (157) Santos, M. G.; Morgado, A. F. *Mercosur Congr. Chem. Eng.* **2005**.
- (158) Akiba, M.; Hashim, A. S. *Prog. Polym. Sci.* **1997**, 22, 475–521.
- (159) Farmer, E. . H.; Shipley, F. W. *J. Polym. Sci.* **1946**, 1 (4), 293–304.
- (160) Jones, S. O.; Reid, E. E. *J. Am. Chem. Soc.* **1938**, 60 (10), 2452–2455.
- (161) Mahon, A.; Kemp, T. J.; Varney, J. E.; Derrick, P. J. *Polymer (Guildf)*. **1998**, 39 (25), 6213–6217.

- (162) Chalker, J. M.; Crockett, M. P.; Evans, A. M.; Worthington, M. Sulfur Limonene Polysulfide. WO2016/064615 A1, 2016.
- (163) Smith, W. B. *Magn. Reson. Chem.* **1994**, 32 (5), 316–319.
- (164) Lee, S. G. *Magn. Reson. Chem.* **2002**, 40 (4), 311–312.
- (165) Klaus Noweck; Grafahrend, W. In *Fatty alcohols. In Ullman's Encyclopedia of Industrial Chemistry*; Wiley-VCH Verlag GmbH: Weinheim, 2012; pp 117–139.
- (166) Chen, W.; Viljoen, A. M. *South African J. Bot.* **2010**, 76 (4), 643–651.
- (167) Santhanam, A. T. In *Application of transition metal carbides and nitrides in industrial tools. In The Chemistry of Transition Metal Carbides and Nitrides*; Oyama, S. T., Ed.; Springer Netherlands: Dordrecht, 1996; pp 28–52.
- (168) Riedel, E.; Janiak, C. In *Die Chemische Bindung. In Anorganische Chemie.*; De Gruyter: Berlin, Boston, 2008; pp 69–244.
- (169) Tsuchida, R. *Bull. Chem. Soc. Jpn.* **1938**, 13 (5), 388–400.
- (170) Metall-Chemie Fine Chemicals. *MC TPPT Technical Data Sheet.*; Hamburg, 2014.
- (171) Azelis L&MF US and Azelis Essential Chemicals US. Irgalube TPPT Product Description. <https://monsonco.com/product/irgalube-tppt/> (accessed Oct 31, 2022).
- (172) Metall-Chemie Fine Chemicals. *MC TPPT plus Technical Data Sheet.*; Hamburg, 2015.
- (173) Azelis L&MF US and Azelis Essential Chemicals US. Irgalube 63 Product Description. <https://monsonco.com/product/irgalube-63/> (accessed Nov 2, 2022).
- (174) Institut für Arbeitsschutz der Deutschen Gesetzlichen Unfallversicherung. Stoffdatenbankeintrag zu Ethylacrylat. CAS Nr.: 140-88-5. <https://gestis.dguv.de/data?name=014350> (accessed Oct 17, 2022).
- (175) Drew, M. G. B.; Hopkins, W. A.; Mitchell, P. C. H.; Colclough, T. *J. Chem. Soc.* **1986**, No. Iii, 0–3.
- (176) Zhang, S.; Li, X.; Wang, J.; Jiao, K. *Chem. Res. Chinese U.* **2004**, 20 (2), 146–152

- (177) Coldberry, D. E.; Fernelius, W. C.; Shamma, M. *Inorg. Synth.* **1960**, VI, 142–143.
- (178) Ruf, E.; Naundorf, T.; Seddig, T.; Kipphardt, H.; Maison, W. *Molecules* **2022**, 27 (6), 1–17.
- (179) Ruf, E.; Naundorf, T.; Kipphardt, H.; Maison, W. Naturstoffbasierte Phosphonsäuren als saure Korrosionsinhibitoren. DE102020104085A1, 2021.
- (180) Deutsches Institut für Normung. *Bezeichnungssysteme für Stähle - Teil 2: Nummernsystem; Deutsche Fassung EN 10027-2:2015*; Beuth Verlag GmbH: Berlin, 2015.
- (181) Pagkalis, K.; Spikes, H.; Jelita Rydel, J.; Ingram, M.; Kadiric, A. *Tribol. Lett.* **2021**, 69 (2), 1–20.
- (182) Metall-Chemie Fine Chemicals. *MC 210 Technical Data Sheet*; Hamburg, Germany, 2014.
- (183) William Y. Lam. Metal Deactivator as a Lubricant Additive. US 4,487,706, 1984.
- (184) Metall Chemie Fine Chemicals Produktdetails MC 210 <https://www.mc-chemie.com/produkte/produktdetail/metalldesaktivatoren/mc-210> (accessed Oct 27, 2022).
- (185) Huang, L.; Tang, F.; Hu, B.; Shen, J.; Yu, T.; Meng, Q. *J. Phys. Chem. B* **2001**, 105 (33), 7984–7989.
- (186) Coy, R. C.; Quinn, T. F. J. *ASLE Trans.* **1975**, 18 (3), 163–174.
- (187) Chevron Phillips Chemical. *TBPS 454 Technical Data Sheet*; The Woodlands, Texas, United States of America, 2022.
- (188) Chevron Phillips Chemical Product Details. Di-tert-butyl Polysulfide (TBPS 454) <https://www.cpchem.com/what-we-do/solutions/specialty-chemicals/products/di-tert-butyl-polysulfide-tbps-454> (accessed Oct 27, 2022).
- (189) Chevron Phillips Chemical. Chevron Phillips Chemical tert-Butyl Mercaptan Product Description. <https://www.cpchem.com/what-we-do/solutions/specialty-chemicals/products/tert-butyl-mercaptan> (accessed Oct 31, 2022).
- (190) Wallin, R.; Kalek, M.; Bartoszewicz, A.; Thelin, M.; Stawinski, J. *Phosphorus*,

- Sulfur Silicon Relat. Elem.* **2009**, 184 (4), 908–916.
- (191) Cabrera, N.; Mott, N. F. *Reports Prog. Phys.* **1949**, 12 (1), 163–184.
- (192) Furlong, O.; Miller, B.; Kotvis, P.; Adams, H.; Tysoe, W. T. *RSC Adv.* **2014**, 4 (46), 24059–24066.
- (193) Institut für Arbeitsschutz der Deutschen Gesetzlichen Unfallversicherung. Homepage Gestis Stoffdatenbank. <https://gestis.dguv.de/> (accessed Oct 31, 2022).
- (194) Health Safety and Environment Division. Abfallhandbuch Universität Hamburg (ohne UKE) <https://www.chemie.uni-hamburg.de/service/sicherheit-und-entsorgung/entsorgung.html> (accessed Oct 31, 2022).
- (195) Deutsche Gesetzliche Unfallversicherung. *Sicheres Arbeiten in Laboratorien Grundlagen und Handlungshilfen GBI 850-0*; Jedermann Verlag: Heidelberg, 2008.

8. Declaration on Oath

Hiermit versichere ich an Eides statt, die vorliegende Dissertation selbst verfasst und keine anderen als die angegebenen Hilfsmittel benutzt zu haben. Die eingereichte schriftliche Fassung entspricht der auf dem elektronischen Speichermedium. Ich versichere, dass diese Dissertation nicht in einem früheren Promotionsverfahren eingereicht wurde.

13.02.2023, Hamburg

Datum, Ort, Unterschrift